STUDY OF CO_2 MOBILITY CONTROL IN HETEROGENEOUS MEDIA USING CO_2 THICKENING AGENTS

A Thesis

by

ZUHAIR ALI A AL YOUSEF

Submitted to the Office of Graduate Studies of
Texas A&M University
in partial fulfillment of the requirements for the degree of

MASTER OF SCIENCE

August 2012

Major Subject: Petroleum Engineering

Study of CO_2 Mobility Control in Heterogeneous Media Using

CO_2 Thickening Agents

STUDY OF CO_2 MOBILITY CONTROL IN HETEROGENEOUS MEDIA USING CO_2 THICKENING AGENTS

A Thesis

by

ZUHAIR ALI A AL YOUSEF

Submitted to the Office of Graduate Studies of
Texas A&M University
in partial fulfillment of the requirements for the degree of

MASTER OF SCIENCE

Approved by:

Chair of Committee,	David S. Schechter
Committee Members,	Robert H. Lane
	Yuefeng Sun
Head of Department,	Daniel Hill

August 2012

Major Subject: Petroleum Engineering

ABSTRACT

Study of CO_2 Mobility Control in Heterogeneous Media Using CO_2 Thickening Agents.

(August 2012)

Zuhair Ali A Al Yousef, B.S., King Fahd University of Petroleum and Minerals

Chair of Advisory Committee: Dr. David S. Schechter

CO_2 injection is an effective method for performing enhanced oil recovery (EOR). There are several factors that make CO_2 useful for EOR, including promoting swelling, reducing oil viscosity, decreasing oil density, and vaporizing and extracting portions of crude oil. Moreover, the ease with which CO_2 becomes soluble in oil makes it an ideal gas for EOR operations.

However, there are several problems associated with CO_2 flooding, especially when reservoir heterogeneity exists. The efficiency of CO_2 is hindered by mobility problems, which result from the unfavorable mobility ratio. In such cases, the injected CO_2 leads to an early breakthrough, which means fingering through the target zone occurs while leaving most of the residual and/or trapped oil untouched. Furthermore, an increase in the CO_2 to oil ratio makes the EOR project uneconomical. However, if there are techniques available to control the injected CO_2 volume, the problems just mentioned can be resolved.

Nowadays, several methods are applied to control the CO_2 flooding in heterogeneous porous media. In the present study, the CO_2 coreflood system was

integrated with a computed tomography (CT) scanner and obtained real-time coreflood images of the CO_2 saturation distribution in the core sample. Throughout this study, two polymers, Polydimethylsiloxane (PDMS) and Poly (vinyl ethyl ether) (PVEE), were tested to assess their ability to increase the CO_2 viscosity and therefore improve sweep efficiency. A drop-in pressure test was first conducted to evaluate the viscosifier's ability to increase CO_2 viscosity; therefore, reduce its mobility. The results showed that the PDMS polymer has the greatest influence on increasing the CO_2 viscosity and reducing its mobility. Also, the PVEE polymer has lower mobility than that of neat CO_2. Based on the coreflood experiments, injection of viscosified CO_2 using the PDMS polymer resulted in the highest oil recovery among the other injection tests have been conducted. Also, the laboratory tests show that injecting the viscosified CO_2 using the PVEE polymer led to higher oil recovery than from the neat CO_2 injection. This research serves as a preliminary study in understanding advanced CO_2 mobility control using the thickening agents technique and will provide an insight into the future studies on the topic.

DEDICATION

I dedicate this thesis to my father who is my first teacher after Allah. I also dedicate this work to my unforgettable mother; may Allah rest her soul in peace. Also, I dedicate this work to my loving brothers and sisters who encouraged me to continue working hard. I would also like to express my appreciation to everyone who supported me and encouraged me to reach my goals.

ACKNOWLEDGEMENTS

I would like to thank everyone who helped and supported me in making this work possible.

First, I would like to thank my advisor, Dr. David S. Schechter, and my committee members, Dr. Robert H. Lane and Dr. Yuefeng Sun, for all the guidance, help, and support throughout the research work.

I must thank my employer and sponsor company Saudi Aramco and its management, especially Dr. Abdulaziz AlKaabi and Dr. Mazen Kanj, for trust in me and giving me the opportunity to learn, expand my knowledge, and sharpen my skills.

I would like also to acknowledge my great friends Hussain Al Jeshi, Ali AlAli, and Abdullah Al Qassem for their support.

Also, I would like to thank all the faculty, students, and staff in the Texas A&M University Petroleum Engineering Department who helped and supported me during my study.

Finally, I will always be proud to have been a student at Texas A&M University.

NOMENCLATURE

A	Cross-sectional area
^{o}API	Gravity
C	Constant related to the core sample size
$CT_{100\% Oil}$	CT number for 100% saturated with oil sample
$CT_{100\% CO2}$	CT number for 100% saturated with CO_2
$CT_{Injection}$	CT number when the CO_2 injection started
dt	Change of time
dx_f	Change of frontal displacement
EOR	Enhanced Oil Recovery
EOS	Equation of State
fra	Percentage of intermediate (C2-C6) in the oil
GAGD	Gas Assisted Gravity Displacement
IOR	Improved Oil Recovery
k_i	Permeability
L	Length of the core sample
M	Mobility Ratio
M_{Oil}	Oil molecular weight
MMP	Minimum Miscibility Pressure
MOC	Method of Characteristics
MSP	Minimum Solubility Pressure

μ	Viscosity
μ_{sol}	Viscosity of mixture
OOIP	Original Oil in Place
P_{CP}	Cloud point pressure
P_{INLET}	Inlet Pressure
P_{OUTLET}	Outlet Pressure
PV	Pore volume
Q	Flow rate unit of volume per unit of time
S_{CO2}	Saturation of the CO_2 phase
SG	Specific Gravity
T	Temperature
WAG	Water Alternating Gas
x_{int}	Intermediate oil fraction (C_2 to C_4, H_2S and CO_2)
χ_{sol}	Mass fraction of solvent
x_{vol}	Volatile oil fraction (CH_4 and N_2)

TABLE OF CONTENTS

Page

CHAPTER Page

CHAPTER Page

LIST OF FIGURES

Page

Page

Page

Page

Page

LIST OF TABLES

Page

CHAPTER I

INTRODUCTION

1.1 General Introduction

A significant amount of the oil produced nowadays comes from mature oil fields and the oil produced from new discoveries has been declining steadily over the last decades. To solve the problem of decreased oil production and to meet the growing need for energy throughout the world, the techniques to improve oil recovery (IOR) and enhanced oil recovery (EOR) (Manrique et al. 2010) should be applied.

EOR is considered to be one of the most important areas of technology in the petroleum industry. Primary and secondary drive oil-production mechanisms are coming up short in meeting the ever increasing global oil demand due to the high amount of residual oil saturation remaining in the reservoir following completion of these two mechanisms. Typical recovery factor after the primary and secondary oil recovery mechanisms is in range between 45 and 50% of the original oil in place (OOIP) (Sandrea and Sandrea 2007).

Over the last decade, numerous projects were conducted to solve the problem of oil recovery. One of these projects used CO_2 as a tertiary method for EOR.

This thesis follows the style of *SPE International.*

Because CO_2 has the ability to prolong the production life of fields and increase the oil recovery by 15 to 25% of the OOIP, CO_2 injection has become one of the important methods for enhancing oil recovery. The successful results that have been reported from global CO_2 EOR projects demonstrate that the CO_2 injection method is a leading EOR technique in the petroleum industry (Dong et al. 2000). In spite of the successful CO_2 injection operations, there are several problems associated with the application of CO_2 flooding that may result in making the overall project unstable and somehow unfavorable. These problems include the presence of heterogeneity and the interaction of several forces inside the reservoir, namely viscous forces driven by adverse mobility ratios, capillary forces from interfacial forces between immiscible fluids, gravity forces driven by fluid density gradients, and dispersive forces caused by concentration gradients between the fluids (Gharbi et al. 1997).

Reservoir heterogeneity has long been recognized as an important factor in governing reservoir performance. In the petroleum industry, heterogeneity means the variety of permeability, porosity, thickness, saturation, faults and fractures, rock facies, and rock characteristics (Ahmed 2010). In the case of fractures, channels, and super-permeability formations, the injected CO_2 may lead to early breakthrough, which means that fingering might occur through the target zone while leaving most of the residual / trapped oil untouched, and increase the CO_2 to oil ratio, which makes the overall project uneconomical.

Several studies have been conducted to solve the problem of CO_2 mobility in heterogeneous porous media. These studies have been classified into two groups: direct and indirect methods. Indirect methods means decreasing CO_2 mobility by injecting fluids (water, polymers, foams, and gels) inside the reservoir to block the high-permeability zones followed by injecting the CO_2. On the other hand, the direct method involves decreasing CO_2 mobility by increasing its viscosity using polymers that thicken the CO_2 gas (Bae 1995).

1.2 Objectives

In this research project, the study will focus on using CO_2 thickener (viscosifiers) to improve CO_2 mobility in heterogeneous systems. The objective of this study is to increase the CO_2 viscosity by dissolving some polymers in it; hence, reducing its relative permeability and mobility, which results in delaying the CO_2 breakthrough and increasing the oil recovery.

The study will present comparisons of several CO_2 flooding experiments with and without using the CO_2 viscosifiers to demonstrate the importance of using the viscosifiers when the heterogeneities such as high-permeability zones or fractures exist.

1.3 Background

1.3.1 CO_2 Flood Theoretical Background

The use of the CO_2 as an EOR method first appeared in the 1930s and has had significant development as recently as the 1970s (Yongmao et al. 2004). Through use and additional development, CO_2 flooding has become a leading EOR technique for light and medium types of oil (Grigg and Schechter 1997). Currently, the United States produces a significant amount of its oil using EOR processes. As reported by *The Oil and Gas Journal* in 2010, 663,431 barrels per day of oil are produced from 193 EOR projects. Of these projects, there are 109 projects producing 272,109 barrels per day using CO_2 EOR processes. **Figure 1** shows the evolution of the CO_2 EOR projects and U.S. oil prices for the past 28 years.

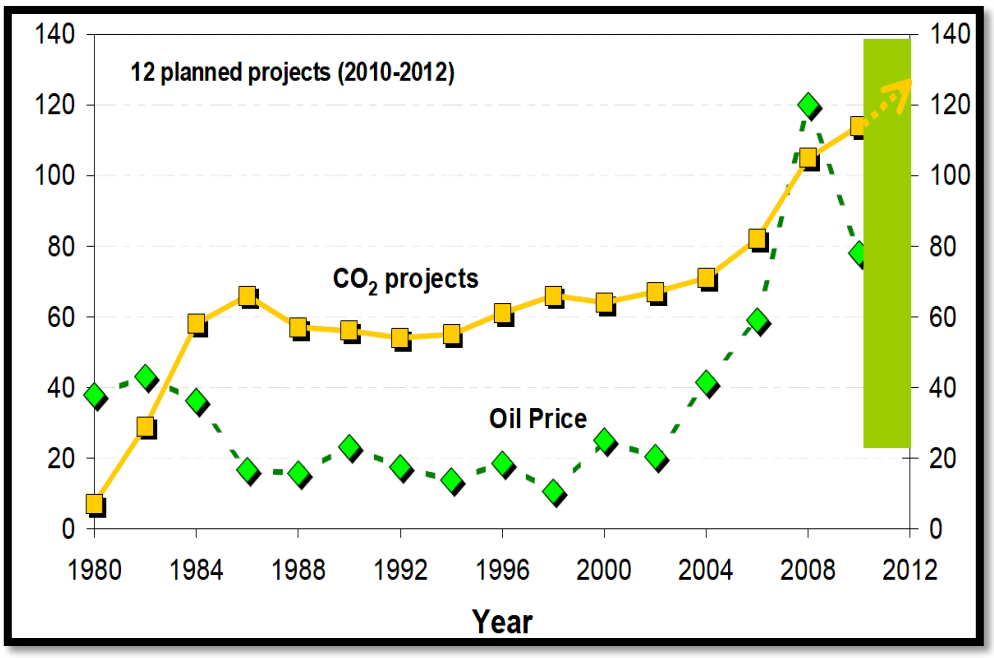

Figure 1. CO_2 EOR projects and oil prices in the U.S (Alvarado and Manrique 2010)

CO_2 has numerous characteristics that make it a favorable oil-displacement agent. These characteristics include the ability of the CO_2 to swell oil, reduce its viscosity, lower the interfacial tension, and change the oil density. Compared with the other gases used for the purpose of EOR, CO_2 has a minimum miscibility pressure (MMP) in oil at reservoir conditions and it is less expensive. In addition, at high pressures, CO_2 density and viscosity increase. **Figures 2 and Figure 3** show a comparison of the density and the viscosity of the three gases used in EOR process; CO_2, N_2, and CH_4. Moreover, CO_2 has minimum problems of gas overriding. Another advantage of CO_2 injection is releasing the produced hydrocarbon gases for other applications and alternative uses. One of the most important factors or drivers that call

for further design and development of CO_2 EOR projects is that of reducing its emission to the atmosphere to avoid damaging the environment (Espie 2005). As reported in the literature, the recovery factor after the primary and secondary recoveries processes is typically in the range of 30 to 50% from OOIP. With the injection of CO_2, any additional oil in the range of 15 to 25% of the OOIP, depending on the reservoir characteristics, can be produced (Yongmao et al. 2004) .

The success of EOR projects depends on several parameters, including the reservoir fluid characteristics, confining zone conditions, injection and production well capabilities, injection rates, and reservoir temperature and pressure (Rao et al. 2004). Even though CO_2 EOR projects worldwide have shown successful results, a major technical challenge, namely mobility control, continues to exist with CO_2 injection. Several methods have been used in hopes of solving this problem. These methods include the water alternating gas (WAG) process, injection of water-CO_2 mixture, generation of a CO_2 foam, and increasing the viscosity of CO_2 by the adding polymer thickening agents (Wu et al. 2004).

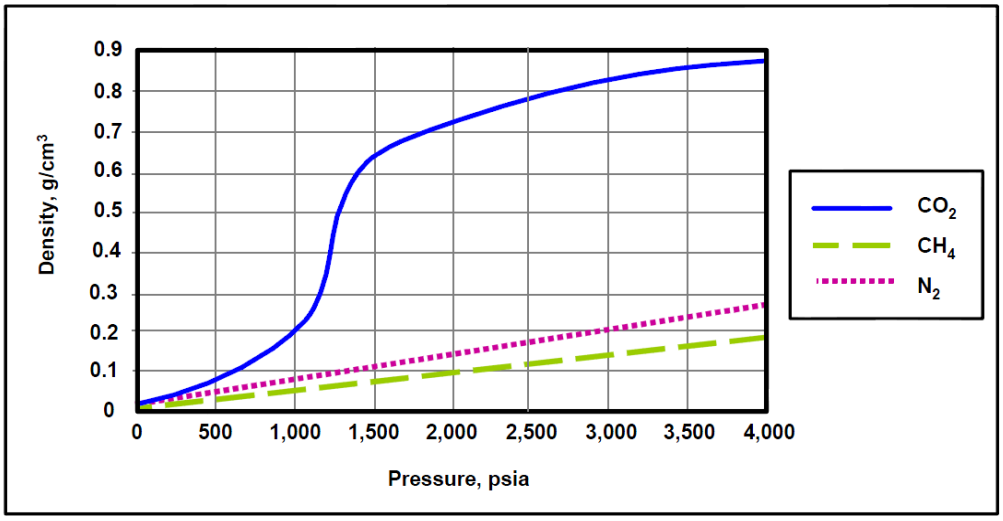

Figure 2. Density of CO_2, N_2, and CH_4 at 105°F (Bank et al. 2007)

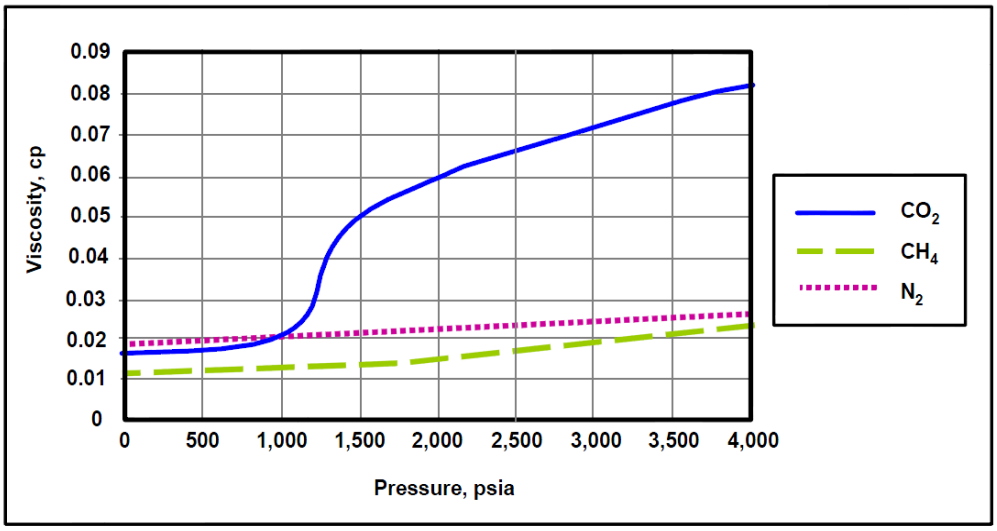

Figure 3. Viscosity of CO_2, N_2, and CH_4 at 105°F (Bank et al. 2007)

1.3.2 CO_2 Displacement Mechanisms

The miscibility or the lack of miscibility of CO_2 in oil can greatly affect the overall EOR performance. Two CO_2 displacement mechanisms for use in oil can be applied in the reservoir; i.e., miscible and immiscible displacements. Miscible or multicontact miscible displacements can be achieved when the reservoir pressure is greater than the MMP, in which there is more interchange and contact between the CO_2 and the reservoir fluid. On the other hand, immiscible displacement occurs when the reservoir pressure is below the MMP, in this case, the interchange or contact between the CO_2 and the oil in the reservoir is less than that of above MMP. The mechanism supporting the miscible displacement can be described as being three processes; i.e., CO_2 contacts, mixes, and dissolve in the oil, forming one phase. Then, CO_2 expands and swells the reservoir oil, making it easy for the oil to flow. Finally, with the assistance of the injection flow pressure, CO_2 pushes the oil to the producer. **Figure 4** shows the miscible displacement mechanism in the EOR process. However, in the case of immiscible displacement, the CO_2 floats above the targeted oil zone due to the difference in density between CO_2 and oil. In such a scenario, the CO_2 supports the gas assisted gravity displacement (GAGD) of the oil at greater depths. This mechanism is very effective when a horizontal well is combined with the GAGD process in which the CO_2 will push the oil down to the producing depth in the lower zone of the reservoir through the support of the gas injection flow pressure (Sweatman et al. 2011). **Figure 5** shows the CO_2 immiscible displacement behavior when it is targeting a horizontal well. Based on previously conducted experiments, the most efficient use of CO_2 in EOR operations

is when CO_2 miscible displacement exists (Holm and Josendal 1974). It has also been reported that to approach a comparable recovery, fewer cycles at miscible displacement process are required compared with that required at immiscible displacement (Ghedan 2009).

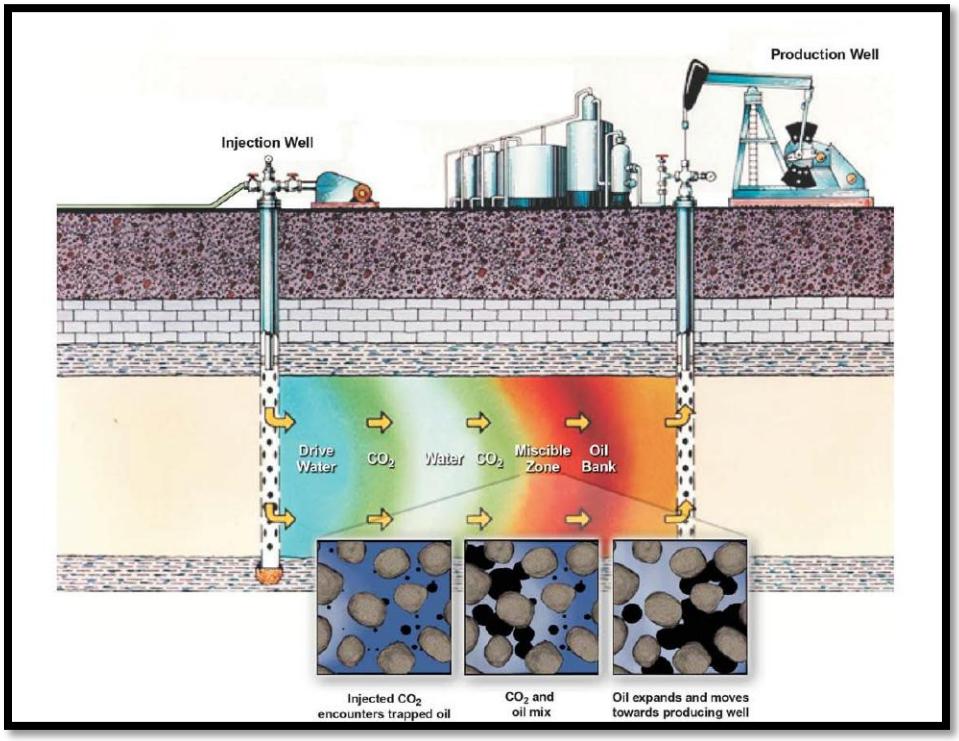

Figure 4. Miscible and immiscible CO_2 EOR processes (NETL 2010)

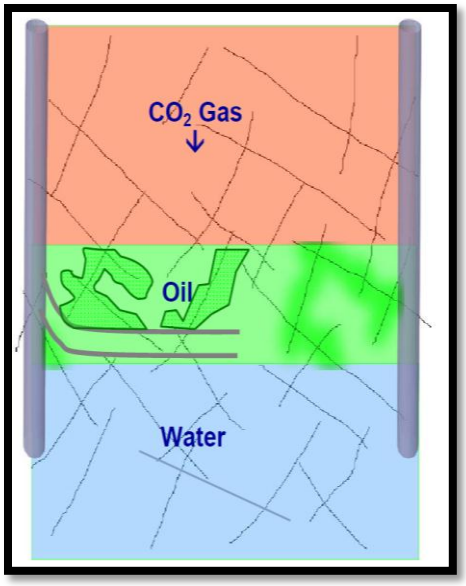

Figure 5. CO_2 immiscible displacement (GAGD). Showing the optimum oil drainage for a horizontal well (Sweatman et al. 2011)

1.3.3 Predicting CO_2 MMP

When CO_2 comes into contact with oil in the reservoir, it might be mixed together to form a single-phase fluid. This mixing is mainly due to three mass transfer mechanisms; i.e., solubility, diffusion, and dispersion. Among the three mass transfer mechanisms, solubility has the most effect on the mixing process. When two fluids are mixed, there is a varying interfacial tension force between them, which depends on several parameters and properties. The MMP is defined as the pressure at which the interfacial tension between the two fluids is equal to zero (Stalkup Jr. 1983). At this pressure, one fluid is dissolving in the other fluid and forms a single-phase fluid. As mentioned previously, the most efficient use of CO_2 as an EOR method is when the CO_2

miscible displacement exists, which means the CO_2 dissolves in the oil phase at reservoir conditions.

There are several parameters affecting the MMP value. These parameters include reservoir pressure, temperature, oil properties, gases injected properties, and the total C2-C6 content of the reservoir fluid.

In practice, there are two methods for estimating the MMP; either conducting a laboratory test or using the correlations. The laboratory test provides a better and a more accurate estimation of MMP compared with that from correlations, although the correlations are based on experimental data. There are several methods used to estimate the MMP, including a slim-tube displacement test, Method of Characteristics (MOC), and mixing-cell methods. The slim-tube displacement test is the best method available to estimate the MMP. During this test, a representative oil sample from a specific field is used to estimate the MMP at different pressures and temperatures. Although this method is considered to be the best technique for estimating the MMP, a limited number of MMPs can be determined this way in practice. This limitation is attributed to the high cost and the time required to run the laboratory test (Stalkup 1984).

The MOC method relies on accurate fluid characterization using a cubic equation of state (EOS). Due to the fast estimate of MMP, this method might be used widely in the industry. Because the correct and unique set of key tie lines can be difficult to locate, this may make it unreliable for use in some cases. The third popular method for estimating the MMP is the mixing-cell test. Like the MOC, the MMP depends on the accuracy of the equation-of-state (EOS) fluid characterization (Yuan and Johns 2005).

Even though the mixing-cell test method requires more time to run than the MOC, it provides a better estimation of MMP than that with MOC (Johns et al. 2009).

As mentioned previously, correlations may be used to estimate the MMP. Several correlations have been developed to estimate the MMP from a regression of experimental data. Although correlations are less accurate than experimental data, correlations are quick, easy to use, and require limited input to estimate the MMP. Moreover, correlations are very useful when there are missing fluid properties or difficulty exists in finding them. **Table 1** summarizes some of the correlations used to estimate the MMP with independent variables along with each correlation. The independent variables are oil C5+ molecular weight (MC5+), temperature (T), volatile oil fraction (xvol) (CH_4 and N_2), intermediate oil fraction (xint) (C_2 to C_4, H_2S, and CO_2), gravity (^oAPI) ,oil molecular weight (M_{Oil}), and percentage of intermediate (fra) (C2-C6) in the oil (Ahmed 2000) .

Table 1. MMP correlations with independent variables

Correlation	Independent Variables
Yellig e Metcalfe	T
Alston et al.	T, MC_5^+, xvol, xint
Enick et al.	T, MC_5^+, xvol, xint
NPC	T, ^oAPI
Glaso	T, MC_7^+, fra
Cronquist	T, MC_5^+, xvol

1.3.4 CO_2 Mobility Control

1.3.4.1 Viscous Fingering

During miscible CO_2 flooding, several factors affect the instability of the floodfront shape of the displacing fluid. These factors include rock-fluid properties, fluid saturation distribution, viscous forces, rock wettability, interfacial tension, and miscibility. Applying all or some of these factors during CO_2 flooding may cause fluid crossflow and mixing of the miscible slug with chase gas, resulting in front instabilities that reduce the displacement efficiency.

Fingering of an interface can be defined as a hydrodynamic instability that occurs when fluid with higher mobility (CO_2) displaces another fluid with lower

mobility (oil). Mobility variations are usually related to differences in viscosity or density of the two fluids being considered.

For both miscible and immiscible conditions, propagation of viscous fingering is directed by different mechanisms of shielding, spreading, and splitting. An unfavorable mobility ratio and the level of heterogeneity of porous media significantly affect flood-front shape and viscous instability (Sahimi 1995). In this portion of the project, mobility, mobility ratio, and factors affecting the gas fingering will be discussed.

The mobility, λi, of a fluid i is defined as the ratio of the effective permeability, ki, of the porous medium, experienced by fluid i, and the fluid's viscosity μi (Cheek and Menzie 1955),

$$\lambda i = ki/\mu i \quad \text{.....(1)}$$

When one fluid displaces another, the mobility ratio M, is defined as the ratio of the mobilities of the displacing and displaced fluids. The mobility radio M is considered to be one of the most important parameters influencing any displacement process. Typically, the mobility ratio is not constant because during mixing of the reservoir fluids, the effective viscosity of each fluid will be changing. In addition, the viscosity of the mixed zone also depends on concentrations of the displacing and displaced fluids.

In the case of CO_2 injection, the mobility ratio of the displacing fluid (λ_{CO2}) to the displaced fluid (λ_{Oil}) is as follows (Cheek and Menzie 1955) :

$$M = \frac{\lambda_{CO2}}{\lambda_{Oil}} \quad \text{.....(2)}$$

According to the mobility ratio equation, there are three possible results; the mobility ratio can be less than one, equal to one, or greater than one. When the injected

gas with the fluid displaced in the porous medium are the first miscible contact and when the mobility ratio is less than one ($M < 1$), the displacement process is very simple and said to be efficient. In this case, the displaced fluids move ahead of the displacing fluid, and the displacement front is stable. In addition, a mixed zone, which has a small effect on the displacement process, may exist between the regions of pure displacing and displaced fluids.

However, in practice a miscible displacement process is not so simple because typically, the mobility ratio is greater than one ($M > 1$). In this case, the front is unstable and many fingers of the gas and the displaced fluid mixture develop, leaving behind large amounts of oil untouched. The formation of the fingers, which have very irregular shapes, reduces strongly the efficiency of the miscible displacements and can lead to early breakthrough of the gas. **Figure 6** shows the effect of the mobility ratio M on the formation and shape of the fingers.

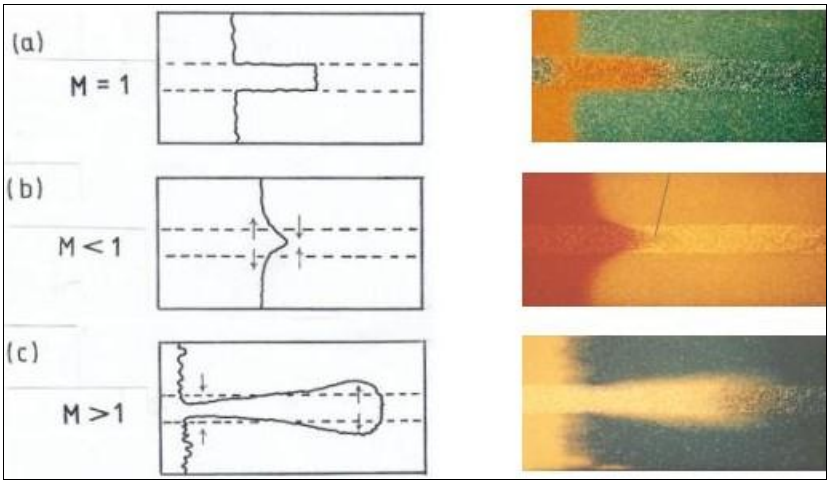

Figure 6. The effect of mobility ratio on the relative frontal advance. (a) M = 1—equal mobility ratio case, (b) M<1—favorable mobility ratio case. (c) M>1—unfavorable mobility ratio case. (Dawe 2004)

In general, the finger patterns that occur during miscible or immiscible displacement processes in porous mediums are caused by two main parameters; the heterogeneity of the porous medium and the fluids' characteristics.

One of the important parameters that plays a major role in the shape and distance of the finger front is the permeability, which is mainly part of the heterogeneity. Suppose that the displacing fluid encounters a high-permeability zone. Then, the front of the displacing fluid will travel faster in that zone compared with the lower permeability zones and produces a bump that is at a distance ahead of the remainder of the front. Darcy's law can be rearranged to account for the change in the flood-front position in a porous medium (Sahimi 1995). The equation can be written as follows:

$$\frac{dx_f}{dt} = \frac{k\Delta P}{\mu_s \phi [ML+(1-M)x_f]} \quad \text{.....(3)}$$

where k, ϕ, ΔP, xf, L, and M are permeability, porosity, pressure difference along the medium, position of the front, length of the medium, and the mobility ratio of displacing and displaced fluid, respectively (Sahimi 1995).

Also, the fluid's characteristics have an important effect in developing the viscous fingers. Mainly viscosity and the density of the displacing and displaced fluids have the greatest effect in developing the viscous fingers and therefore propagation of the floodfront.

1.3.4.2 Previous Attempts to Decrease the CO_2 Mobility

As mentioned previously, the greatest challenge with the CO_2 flooding as an EOR method is the ability to reduce the CO_2 mobility. Several methods have been tried in attempting to solve this problem. The most commonly used methods for approaching this problem are (1) water- alternating gas (WAG) process, (2) generation of a CO_2 foam, and (3) increasing the CO_2 viscosity by adding polymer thickening agents.

1) WAG Process

The WAG process is a reduction of CO_2 relative permeability in the reservoir via co-injection with water. This method was the first attempt to diminish the CO_2 mobility in the reservoir. Even though it reduces the relative permeability and the mobility of the CO_2, it has two main disadvantages, namely severe gravity segregation (i.e., water underlying and CO_2 overriding) and water blocking or shielding (Wu et al.

2004). As a result, oil will be trapped/ untouched; hence, oil recovery will be reduced and the residual oil saturation will be high.

2) Generation of CO_2 Foam

There are numerous projects conducted to test the ability of injecting the CO_2 foam to reduce the CO_2 relative permeability. The main principle of this method is injecting a surfactant solution (an aqueous surfactant solution) into the reservoir to block the high-permeability zones, which result in a reduction of the CO_2 relative permeability and therefore the CO_2 mobility (foam). Theoretically, this method seems to solve the problem of the CO_2 mobility and enhances the CO_2 displacement process. However, in practice, there are two problems associated with this method. The first problem is determining how to properly generate the foam, and the second problem is solving how to control the propagation of the foam inside the oil formation under reservoir conditions. These two problems make the foam method unfavorable and undesired for CO_2 mobility control (Farajzadeh et al. 2009).

Both methods are considered as indirect methods to solve the problem of the CO_2 mobility. This means that they are focused on reducing the relative permeability of the CO_2 rather than increasing its viscosity. The next method will deal with changing the CO_2 viscosity in solving the CO_2 mobility problem.

3) CO_2 Thickening Agents

In this method, a polymer or a viscosifier is added to the pure CO_2 to increase its viscosity by orders of magnitude. Thickening CO_2 by using a polymer as a direct thickener offers several distinct advantages compared with the other two methods mentioned previously. In comparison with the WAG method and because there is no water injection with the CO_2 thickening method, the water-blocking or shielding effect will be eliminated. Another factor that makes the CO_2 thickening method better than the other methods is the stability of the CO_2 and polymer mixture under the actual reservoir conditions (Bae 1995). Moreover, this method can considerably improve the CO_2 sweep efficiency due to the reduction in the mobility and therefore delay the CO_2 breakthrough. As a result, the ultimate oil recovery can be increased, and some of the field operational problems such as excessive water production and treatment and severe CO_2 corrosion will be minimized (Zhang et al. 2011). Generally speaking, this method will lead to an efficient oil recovery and a successful project.

1.3.4.3 CO_2 Viscosifiers Background

As mentioned previously, CO_2 is considered to be one of the most popular EOR methods. Overall, CO_2 reduces the oil viscosity, density, and interfacial tension between phases and makes the oil flow more easily and therefore increases oil recovery (Murray et al. 2001). However, the foremost disadvantage of CO_2 as an oil displacement is its low viscosity. Compared with brine and oil at reservoir conditions, which have viscosity values of 1 and 0.1-50 cp, respectively, CO_2 has very low-viscosity values that range

between 0.03 and 0.10 cp as shown in **Figure 7**. If there is a way to increase the CO_2 viscosity to a level comparable to the oil it is displacing, typically a one to two order of magnitude increase, considerable improvements in sweep efficiency and oil recovery could result and be achieved (Enick 1998).

There are several chemicals made for this purpose. More than 53 chemicals were tested to solve the CO_2 viscosity problem. All the previous attempts focused on identifying the appropriate polymer that can be used for the purpose of thickening the CO_2. Heller and coworkers tested the solubility of these chemicals and they found that only 17 polymers are soluble in CO_2 (Heller et al. 1985) As a main condition, the polymers must be suitable and favorable for application at reservoir conditions. The polymers were tested based on several specifications and conditions in accomplishing the goal of achieving CO_2 thickening agents. These specifications should confirm the ability of the chemical to increase the CO_2 viscosity, while being inexpensive, safe, and stable at reservoir conditions. Moreover, it would have a tendency to remain in the CO_2 -rich phase rather than partitioning into the brine or oil or adsorbing onto the porous media. In addition, the level of viscosity increase should be easily controlled by the concentration and amount of the polymer, and it should not be necessary to inject water or add any chemicals with the thickened CO_2 as is frequently performed with foams. As a result, CO_2 saturation would therefore be higher, resulting in a higher CO_2 sweep efficiency and a higher displacement efficiency of the oil (Enick 1998).

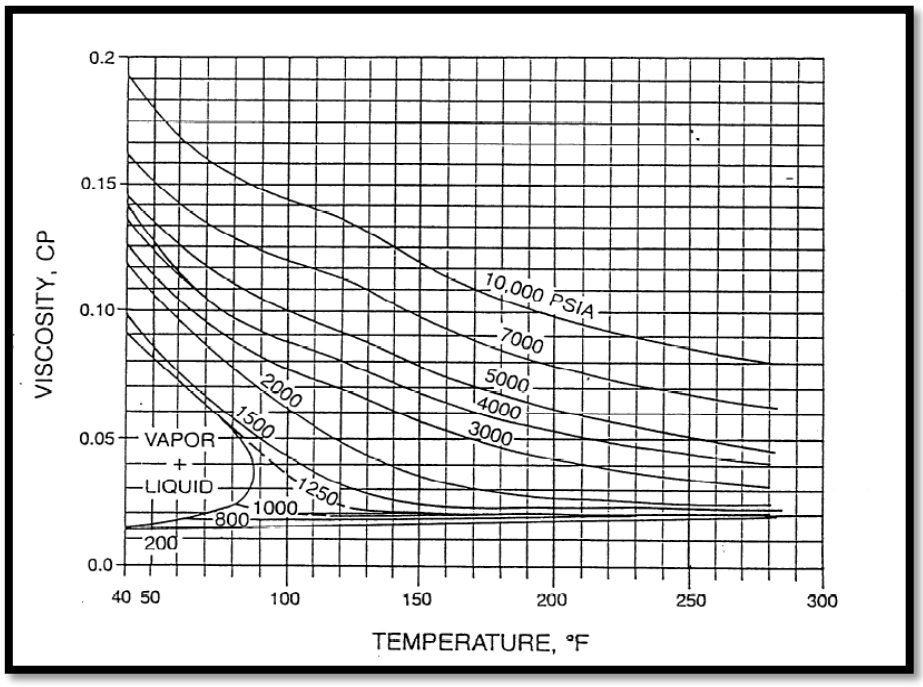

Figure 7. Viscosity of CO_2 as a function of temperature and pressure (Enick 1998)

1.3.4.4 Previous Attempts to Develop CO_2 Viscosifiers

In this section, the most important attempts to identify the appropriate CO_2 thickeners that have been tried will be illustrated and discussed. The major tests that have been conducted since the 1980s until today will be discussed in terms of their advantages or disadvantage with regard to being used and applied for the purpose of increasing the CO_2 viscosity and therefor reducing its mobility in a petroleum reservoir.

Heller and coworkers at New Mexico Institute of Mining Technology (NMIMT) went through several attempts to identify the right polymer for increasing CO_2 viscosity. Approximately 53 chemicals were tested to evaluate their solubility in CO_2, and only 17

were found to be soluble (Heller et al. 1985). In 1995, Heller and coworkers presented the results of their tests on gel organic fluids and carbon dioxide with 12-hydroxystearic acid HSA. As a first test, this HAS polymer was found to be insoluble with the dense CO_2; however, if a significant amount of the cosolvent such as ethanol was added to the polymer, HSA was found to be soluble in dense CO_2. Also, they found that the degree of solubility of the compound is a function of three parameters, temperature, HSA concentration, and the amount of cosolvent added to the polymer. Two disadvantages that make this polymer unsuitable for thickening CO_2 are that the increase of the CO_2 viscosity is very small and a large amount of the cosolvent is required to achieve solubility (Gullapalli et al. 1995). Even though identifying the CO_2 thickening polymer was unsuccessful, Heller and his team came up with some conclusions to develop future CO_2 thickeners. They suggested that the CO_2 soluble polymer should be amorphous and atactic. Also, they found that the polymers soluble in water are not highly soluble in CO_2 (Heller et al. 1985).

Terry and coworkers at the University of Wyoming tried to develop a new CO_2 thickening polymer using in-situ polymerization of CO_2 soluble monomers. Hydrocarbon polymers can be achieved at high pressures using common types of initiators. Rather than dissolving in CO_2, the polymer converted to a solid phase when mixed with the liquid CO_2. As a final result, Terry and his team concluded that the resulting polymer is insoluble in CO_2 (Terry et al. 1987).

In 1990, Llave and his coworkers evaluated the use of entrainers to increase the viscosity of the CO_2. Entrainers can be defined as a low-molecular weight compound

that is found to be CO_2 soluble. Examples of entrainers are isooctane, 2-ethylhexanol, and ethoxylated alcohol. Although the viscosity of CO_2 after the addition of the entrainers has been found to increase by 243% with isooctane, the concentration needed to achieve this viscosity is very high. For example, 44 mole % of 2-ethylhexanol is needed to increase the viscosity of CO_2 by 1565% (Liave et al. 1990).

Irani and his coworkers tested a silicone polymer for the purpose of improving the CO_2 viscosity. The silicone polymer had a minimum solubility parameter of 6.85 or less with a molecular weight of 197,000. Irani reported that at 130^oF and 2500 psia, when 4 wt% of this polymer combined with 20 wt% cosolvent (Bae 1995) and 76% of CO_2, the mixture had a viscosity of 1.2 cp. Several experimental tests were conducted using the above criteria. The result proved that the silicone polymer accelerated the oil recovery and delayed the CO_2 breakthrough (Bae and Irani 1993). After this approach, Chevron developed several polymers similar to the silicone polymer with guidelines to select the appropriate cosolvent to enhance the polymer solubility in CO_2.

DeSimone and coworkers (Desimone et al. 1994) at the University of North Carolina conducted several polymerizations in supercritical CO_2. After numerous tests, they found that the silicones and fluoropolymers exhibited a higher level of solubility in CO_2 compared with other nonfluorous polymers. As a result of this research, Poly(1,1-dihydroperfluorooctyl acrylate), PFOA, with a molecular weight of 1.4 *106 g/mol, was formed by applying a homogeneous polymerization of the fluorinated monomer in CO_2. This polymer proved its ability by increasing the viscosity of the CO_2 by several orders of magnitude. As an example, 3.7 wt% of the PFOA can increase the viscosity of CO_2

from 0.08 cp to 0.2-0.25 cp at 4060– 5220 psia and 122^{o}F. The most important advantages of PFOA are its ability to be soluble with the CO_2 without adding any cosolvent and its high degree of solubility in CO_2 (Desimone et al. 1994). However, due to some environmental constrains and the amount of pressure required to achieve solubility, this polymer is not commercially used.

McHugh and coworkers (Rindfleisch et al. 1996) conducted a study to evaluate a series of poly methyl acrylate (PMA) and poly (vinyl acetate) (PVAc). The main target of this study was to define the minimum solubility pressure of these polymers with the CO_2. At a concentration of 5 wt% of both polymers, PVAc even with higher molecular weight was found to be much more soluble than PMA. The minimum solubility pressure for PVAc and PMA responded differently with temperature change; i.e., the minimum solubility pressure of PMA decreased as the temperature increased. On the other hand, as the temperature increased, the minimum solubility pressure of PVAc increased. Even so, the minimum solubility pressure of PVAc is much lower than PMA's minimum solubility pressure. For the time being, PVAc is the one polymer with high-molecular weight found to be soluble in CO_2 and inexpensive. For instance, 5 wt% of PVAc with a molecular weight of 600,000 could dissolve in CO_2. However, the pressure required to achieve the minimum solubility pressure is very high (6300– 10,000 psia) compared with the MMP

At the University of Pittsburgh, several attempts were made to identify the appropriate polymer to enhance the viscosity of CO_2. Since 1989, Enick and coworkers conducted several experiments to design the best polymer to enhance the viscosity of the

CO_2. After several attempts, the team reported the first CO_2 thickener, poly (fluoriacrylate-styrene) or polyFAST (Huang et al. 2000). Even though this polymer can improve the CO_2 viscosity, it was not practical to be used in the petroleum fields. The reasons for not being practical are attributed to the cost of the polymer and the availability difficulty in large quantity. Moreover, and due to the high content of fluorine, this polymer was biologically and environmentally persistent.

Overall, each polymer has advantages and disadvantages. Occasionally, a polymer was found to be the right one to be applied for the purpose of increasing the CO_2 viscosity. However, due to some environmental, reservoir, and cost constraints and limitations, the particular polymer was not recommended to be used. Generally speaking, the high-molecular weight polymers that have been developed and identified as CO_2 soluble (listed in order of most CO_2 soluble to less one) are: poly(fluoroacrylat) (PFA), poly(dimethylsiloxane) (PDMS), poly(vinyl acetate) (PVAc), poly(1-O-(vinyloxy)ethyl-2,3,4,6-tetra-O-acetyl-β-D-glucopyyranoside) (PAcGIcVE), amorphous poly(lactic acid) (PLA) and poly(methyl acrylate) (PMA). Another group, which are called oligomers, can also be used for the purpose of decreasing the CO_2 viscosity. These polymers include poly(propyleneoxide)(PPO), poly(vinyl ethyl ether)(PVEE), poly(vinyl methoxymethyl ether)(PVMME), cellulose triacetate oligomers oligoo(CTA), peracetylated cyclodextrins (PACD), poly(acetoxy oxetane)(PAO), and poly(vinyl methoxy ethyl ether)(PVMEE) (Enick et al. 2010).

1.4 Methodology

Throughout this project, we will conduct our study on investigating the ability of the viscosifier to increase the CO_2 viscosity and therefore reduce its mobility in three stages. The first stage will focus on the literature review of previous work conducted in the CO_2 mobility control using the viscosifiers. Based on this review, the most effective and practical polymer (viscosifier) will be selected for our study. The second stage will focus on testing the ability of the polymers to guarantee its solubility in CO_2 at the desired Minimum Solubility Pressure (MSP). The last stage will be related to running several coreflood experiments to verify the viscosifier's ability to improve the CO_2 sweep efficiency and increase the oil recovery. At this stage, a specially designed coreflood system is integrated with the fourth generation of an X-ray CT scanner and will be used to obtain quantitative phase saturation information and real-time core images of the samples that will be tested.

CHAPTER II

EXPERIMENTAL SETUP

The experimental setup consists of three systems: CT-scanner system, coreflood system, and heating system. In this section, we will present a brief description of each system with the main parts needed to build each system. Moreover, the core samples and the chemical used in all of the experiments will be described.

2.1 Instrument Setup

The instruments used in our research were selected carefully to achieve the goals and objectives of this research. The overall setup of the instruments was prepared to enable testing the injection of CO_2 similar to that at reservoir conditions. The major parts of the instrumental setup are the vacuum system, injection system, coreflood cell, heating system, X-ray CT scanner system, production system, and the data acquisition system. **Figure 8** illustrates the instrumental setup of our experiments with each instrument identified. All of the tubing, fittings, and valves used in the experiment were ordered from Swagelok and made of stainless steel to withstand the high pressures and temperatures.

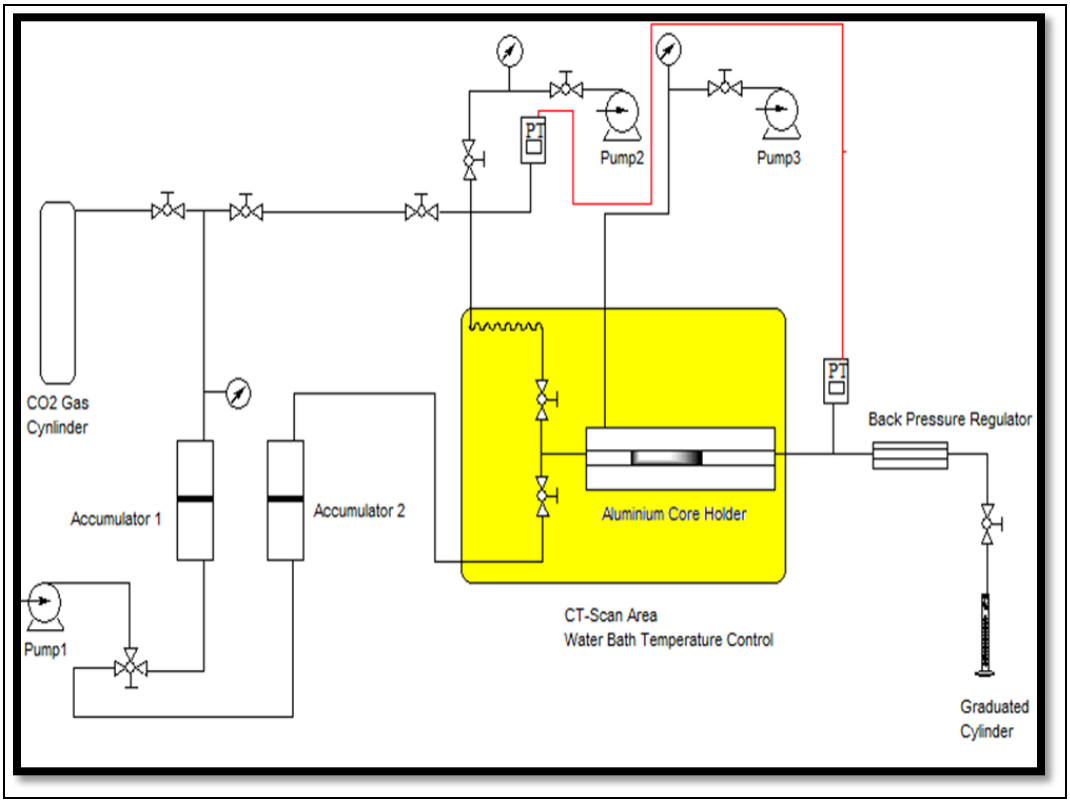

Figure 8. Schematic of the experimental setup

2.1.1 Vacuum Pump

The vacuum system consists of two parts: vacuum pump and desiccator. This system was used to saturate the core samples and remove all of the gas bubbles that might be inside the core. The purpose of this step is to make sure that we have only one phase (100% water saturation) before conducting the test. We go through this step to measure the pore volume (PV) of the core samples and the porosity.

2.1.2 Injection System

The injection system consists of two parts: the accumulator and the pump. The accumulator was used to contain the fluids that will be injected into the coreflood system. The accumulator was filled either with water, oil, pressurized CO_2, or viscosified CO_2. The volume of the accumulator is 2 liters. The other part of the injection system is the pump, which was used to pump the fluid from the accumulator to the coreflood cell. The pump used is a 5000 D syringe pump and it contains a controller to pump at a constant flow rate or constant pressure.

2.1.3 Coreflood Cell

An X-ray can penetrate through a few types of metals, and for this reason, the core holder used in this study was made of aluminum. It is capable of holding cores up to 1 ft in length and 1-in. diameter. The core sample is surrounded by a rubber Hassler sleeve in which a hydraulic pump is used to apply the overburden pressure on the core sample through the rubber sleeve. The overburden pressure can range from 0 to 7000 psi and is controlled easily.

2.1.4 Heating System

A heating system was built to enable running the experiment at the desired temperature. The heating system consists of three parts: the heating bath, pump, and the container. The heating bath is filled with water and it is heated to the desired

temperature. The maximum temperature that the bath can reach is 212ºF. Using the electrical pump, the heated water then circulated through the core holder cell.

2.1.5 X-ray CT Scanner

The X-ray CT scanner is a fourth generation Universal system HD 200 system with a resolution of 0.3 mm x 0.3 mm. The scanner can go up to 4 seconds per scan and is able to scan samples to 48 cm in diameter. The scanned images can be made at any desired number and at regular intervals.

2.1.6 Production System

The production system consists of two parts: the back-pressure regulator and the graduated cylinder. The back-pressure regulator can go up to 2500 psi and be used to control the injected fluid pressure and to increase the system pressure. The graduated cylinder is used to collect the fluid produced and measure its volume.

2.2 Core Samples

Indiana limestone and buff Berea sandstone rock samples were used in this study. The samples were 1 in. in diameter and 5 in. in length. The samples were divided into three categories: Indiana unfractured low-permeability rock samples, Indiana fractured high-permeability rock samples, and buff Berea fractured high-permeability rock samples.

2.3 Chemicals

2.3.1 XIAMETER ® PMX-200 SILICONE FLUID 600,000 CS

Super high-viscosity pure silicone fluids are high-viscosity linear 100% polydimethylsiloxane (PDMS) fluids that range in viscosity from 300,000 cSt to 20,000,000 cSt (centistokes). These fluids are clear, colorless, and odorless. The PDMS fluids belong to a group of polymeric organosilicon compounds that are commonly referred to as silicones. Among the silicone-based organic polymers, PDMS is the most widely used and is particularly known for its unusual rheological properties. PDMS is optically clear, and in general, is considered to be inert, nontoxic, and nonflammable. **Figure 9** shows the repeating unit of PDMS. The most significant advantage of this polymer is its ability to dissolve in the CO_2 and increase its viscosity. To achieve high solubility in the CO_2, toluene as a cosolvent is added to the PDMS. Table 2 summarizes all of the properties and specifications of this polymer.

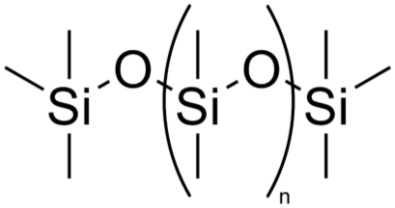

Figure 9. Repeating unit of PDMS

Table 2. Properties and specifications of PDMS

Chemical Name	Polydimethylsiloxane
INCI Name	Dimethicone
Producer	Dow Coring
Appearance	Clear liquid, odorless, and tasteless
Nonflammable	Yes
Thermal Stable	Yes
Specific Gravity	0.978
Viscosity	600,000 cSt
Molecular Weight	260,000 $g.mol^{-1}$

2.3.2 Poly (Vinyl Ethyl Ether)

Poly (vinyl ethyl ether) (PVEE) belongs to a group called oligomers. As mentioned previously, this group of chemicals is used for the purpose of increasing the CO_2 viscosity, especially at the supercritical phase. PVEE is considered to be oxygen-containing polymer with CO_2 philic compounds. PVEE has an average molecular weight of 3800 $g.mol^{-1}$ with a density of 0.968 g/Ml at 25^oC. One of the most important advantages of this polymer is its ability to dissolve in the CO_2 without the need of a cosolvent. **Figure 10** shows the repeating unit of the PVEE. All the main properties and specifications of this polymer are summarized in **Table 3**.

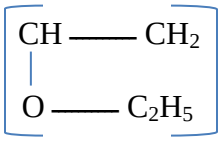

Figure 10. Repeating unit of PVEE

Table 3. Properties and specifications of PVEE

Chemical Name	Poly (vinyl ethyl ether)
Chemical Formula	$[CH_2CH(OC_2H_5)]_n$
Producer	SIGM-ALDRICH
Appearance	liquid
Nonflammable	Yes
Thermal Stable	Yes
Specific Gravity	0.968 g/mL at 25^oC
Molecular Weight	3800 $g.mol^{-1}$

Where P_{cp} and χ_{sol} ($0.0067 \leq \chi_{sol} \leq 0.0080$) are the cloud point pressure and the mass fraction of solvent, respectively, the following correlation was found to estimate the minimum solubility pressure when PVEE is added to the CO_2 (Zhang et al. 2011).

$$P_{CP} = 3590.75\ \chi_{sol} - 9.124 \quad \text{.....(4)}$$

The viscosity of the mixture (μ_{sol}) PVEE and the CO_2 can be found using the correlation proposed by (Zhang et al. 2011):

$$\mu_{sol} = 0.052 P_{CP} - 0.070 \quad \text{.....(5)}$$

Where $(14.6 \leq P_{CP}\ (\text{mPa.s}) \leq 19.7)$

2.3.3 Dopant

A dopant, also called a doping agent, is a trace impurity element that is inserted into a substance (in very low concentrations) to change the electrical properties or the optical properties of the substance. To enhance the CT- image contrasts between different phases in our experiments, a dopant will be mixed with oil in some cases. The dopant that will be used is1-iodohexadecane, 98%. The CAS number of this product is 544-77-4 and it is available at Alfa Aesar Company. **Table 4** summarizes all the specifications and the properties of the 1-iodohexadecane.

Table 4. Properties and specifications of 1- iodohexadecane.

Chemical Name	1-iodohexadecane
Chemical Formula	$[CH3(CH_2)_{15}I$
CAS#	544-77-4
Producer	Alfa Aesar
Appearance	Liquid
Sensitivity	Light Sensitive
Specific Gravity	1.121 g/mL

2.3.4 Refined Oil

The oil used in the experiment is Soltrol oil from Chevron Phillips. It is also called SOLTROL® 130 Isoparaffin Solvent. All of the important properties and specification are reported in **Table 5**.

Table 5. Properties and specifications of SOLTROL® 130 Isoparaffin solvent

Chemical Name	C10-C13 Isoalkanes
CAS#	68551-17-7
Producer	Chevron Phillips Chemical Company
Appearance	Clear liquid, colorless
Odor	Mild, Hydrocarbon
Nonflammable	Yes
Flash Point	61^{o}C (142^{O}F)
Viscosity	1.5 cSt at 38^{o}C (100^{O}F)
pH	7

2.3.5 Toluene

Toluene is an aromatic hydrocarbon that is widely used as an industrial feedstock and as a solvent. Toluene will be used to enhance the solubility of PDMS in CO_2. Because the PDMS solubility in CO_2 can be achieved at high pressures, toluene as a cosolvent will be used to facilitate the overall solubility of the mixture.

CHAPTER III

EXPERIMENTAL CONDITIONS AND PROCEDURE

3.1 Background

The coreflood experiments were designed to test the effect of viscosified CO_2 in improving the CO_2 sweep efficiency in a heterogeneous reservoir. Different Indiana limestone and buff Berea sandstone samples with high permeability will be tested with the neat CO_2 and the viscosified CO_2. In some samples, fractures will be introduced to examine the effect of the viscosified CO_2 in such a case of heterogeneity. Throughout this project, two types of CO_2 thickeners will be evaluated to achieve the goals of this project.

3.2 CO_2 Viscosifier Preparation, Introduction and Dissolution

As mentioned previously, two thickeners will be used in our project, PDMS and PVEE. In this section, the method of preparation, introduction, and dissolution of the two polymers will be illustrated.

3.2.1 Preparation of PDMS

As stated previously, toluene must be added to this polymer to make it soluble in CO_2. Based on the ratios needed of CO_2 and the viscosifier, 4 grams of liquid PDMS will be mixed with 20 grams of toluene as a cosolvent. The mixture must be stirred

overnight to obtain a homogeneous solution. This mixture should form a viscosified polymer to prepare it for being added to the CO_2.

3.2.2 Preparation of PVEE

An advantage of this PVEE polymer over the PDMS is that there is no need to add any cosolvent to make it soluble with the CO_2. PVEE requires only adding 0.8 grams of this polymer to the CO_2. This quantity of polymer was selected based on the size of the accumulator that we have in our laboratory and the CO_2 quantity that will be mixed with the polymer. More details about the ratio selection of both CO_2 and the polymer will be discussed later.

3.2.3 Introduction of PDMS into CO_2

The viscosified polymer is now ready to be added to the CO_2. First, the viscous solution should be poured into the accumulator; then the accumulator is sealed and 310 psi of CO_2 is injected into the accumulator. In this case, the weight of the CO_2 has been calculated to confirm that the overall mixture contains 4 wt% of PDMS, 20 wt% oft, and 76 wt% of CO_2.

3.2.4 Introduction of PVEE into CO_2

Similar to the PDMS procedure, the PVEE polymer was poured into the accumulator; then the accumulator was sealed and 350 psi of CO_2 was injected into the accumulator. Compared with the PDMS, PVEE has much larger volume of CO_2 in its

mixture. The weight of the CO_2 was calculated to make sure the mixture has 0.8 wt% of PVEE and 99.2 wt% of CO_2.

3.2.5 Dissolution of PDMS in CO_2

To evaluate the PDMS solubility in CO_2, the mixture was pressurized by pumping to 2500 psi. With the shrinkage of the CO_2 volume due to the increase in pressure, some heat was generated from the solution of the viscosified mixture. The mixture was left for an hour to equilibrize before being injected into the core sample.

3.2.6 Dissolution of PVEE in CO_2

Initially, the accumulator was pressurized up to 2843 psi to achieve the PVEE solubility in CO_2. Then, the mixture was left for an hour to make sure it reached a homogeneous state.

3.3 MMP Estimation

As mentioned previously, there are two ways to estimate the MMP, either conducting a laboratory test or using the correlations. The laboratory test gives a better and more accurate estimation compared with that from correlations, although the correlations are based on the experimental data. However, due to a technical issue with the MMP apparatus, a correlation will be used to estimate the MMP. Because of the lack of information available regarding the properties of the Soltrol 130 Isoparaffin, Cronquist correlation will be used to predict the MMP. The correlation is (Cronquist 1978):

$$\mathrm{MMP} = 15.988\ \mathrm{T}^{(0.744206+0.0011038\ \mathrm{MW\ C5+})} \quad \text{……………………..…(6)}$$

where T is the temperature in Fahrenheit and MW C5+ is the molecular weight of hydrocarbons containing at least five carbon atoms in a single chain. To estimate the MW C5+, Cronquist proposed the following correlation:

$$\mathrm{MW\ C5+} = 4247.98641\ \mathrm{API}^{(-0.87022)} \quad \text{…………………………..(7)}$$

The API is the API gravity of the oil, which equals:

$$\mathrm{API} = \frac{141.5}{\mathrm{SG}} - 131.5 \quad \text{…………………………………...…….(8)}$$

SG is the specific gravity of the oil being used in the test. After evaluating all of these correlations, the MMP was estimated to be 1200 psi at 130°F. **Table 6** summarizes all of the values that we obtained from previous calculations.

Table 6. Summary of MMP calculations

Parameter	Value
Specific Gravity	0.758
T	130^{o}F
API	55.2
MW C5+	129.6
MMP	1200 psi

3.4 Data Processing

It is good to compare the images from the CT scan with the phase-saturation graph. The phase-saturation graph provides an indication of the flow of the CO_2 in a graphical manner based on the CT numbers taken after the injection of CO_2 and at different injection volumes. The correlation used to estimate the phase saturation from the CT scan result is:

$$S_{CO2} = \frac{CT_{100\%\ Oil} - CT_{Injection}}{CT_{100\%\ Oil} - CT_{100\%\ CO2}} \quad \text{.....(9)}$$

where,

S_{CO2} = the saturation of the CO_2 phase

$CT_{100\%\ Oil}$ = the CT number when the sample is 100% saturated with oil

$CT_{Injection}$ = the CT number when the CO_2 injection started

$CT_{100\%\ CO2}$ = the CT number when the sample is 100% saturated with CO_2

3.5 Typical Experimental Procedure

The experiments were conducted in three scenarios; injection of neat CO_2 above the MMP, injection of viscosified CO_2 using PDMS, and injection of viscosified CO_2 using PVEE. The procedure used for each of the three scenarios will be described.

3.5.1 Neat CO_2 above the MMP

1) Heat and weigh the sample
2) Saturate the sample in brine and weigh
3) Calculate the sample's pore volume and porosity
4) Heat the sample again.
5) Place the dry sample in the core holder and apply 3000 psi of confining pressure
6) Inject oil into sample at the rate of 2cc/min at a minimum of 10 PV.
7) Keep the sample pressurized at 1600 psi overnight and then inject 5PV of oil and record the pressure drop.
8) Take scan images when the sample is 100% saturated with oil.
9) Inject 150 psi of CO_2 in the accumulator and pressurize it up to 2000 psi.
10) Inject the pressurized CO_2 into the core. At a low rate (2.5 cc/min), inject 0.5, 1, 2 and 3 PV of pressurized CO_2.
11) Collect the produced oil and the decrease in pressure at each step. Also, take scan images at each PV injected.

3.5.2 Viscosified CO_2 Using (PDMS) above the MMP

1) Heat and weigh the sample
2) Saturate the sample in brine and weigh
3) Calculate the sample's pore volume and porosity
4) Heat the sample again.
5) Place the dry sample in the core holder and apply 3000 psi of confining pressure
6) Inject oil into sample at a rate of 2cc/min at a minimum of 10 PV.
7) Keep the sample pressurized at 1600 psi overnight and then inject 5PV of oil and record the pressure drop.
8) Take scan images when the sample is 100% saturated with oil.
9) Place the polymer in the accumulator and then inject 310 psi of CO_2 and pressurize the mixture up to 2500 psi.
10) Inject the viscosified CO_2 in to the core at a low rate (2.5cc/min), and inject 0.5, 1, 2 and 3 PV of pressurized CO_2.
11) Collect the produced oil and the decrease in pressure at each step. Also, take scan images at each PV injected.

3.5.3 Viscosified CO_2 Using (PVEE) above the MMP

1) Heat and weigh the sample
2) Saturate the sample in brine and weigh
3) Calculate the sample's pore volume and porosity
4) Heat the sample again.
5) Place the dry sample in the core holder and apply 3000 psi of confining pressure
6) Inject oil into sample at a rate of 2cc/min at a minimum of 10 PV.
7) Keep the sample pressurized at 1600 psi overnight and then inject 5PV of oil and record the pressure drop.
8) Take scan images when the sample is 100% saturated with oil.
9) Place the polymer in the accumulator and then inject 350 psi of CO_2 and pressurize the mixture up to 2843 psi.
10) Inject the viscosified CO_2 in to the core sample at a low rate (2.5 cc/min), and inject 0.5, 1, 2 and 3 PV of pressurized CO_2.
11) Collect the produced oil and the decrease in pressure at each step. Also, take scan images at each PV injected.

CHAPTER IV

EXPERIMENTAL RESULTS

This section will present the results of the experiments that have been conducted. In most tests conducted in this study, CT scan images will be taken. Two types of figures will be presented with each CT scanner run. Initially, one image will show the flood of CO_2 through the rock sample within two planes. As is shown in **Figure 11**, this figure consists of two sections: the vertical cross section and the horizontal cross section. The vertical cross section presents the average CT number across the vertical side of the rock sample. In contrast, the horizontal cross section shows the average CT number of the rock sample across the horizontal plane. This type of curves will have great value if it is run with the fractured rock samples where the flow of CO_2 can be seen within the fracture plane vertically and across the fracture plane horizontally. A second figure that will be presented with the CT scanner run is the vertical slice images. The purpose of this figure is to observe the flow of CO_2 in each slice taken during the CT scan imaging. This figure will provide more precise information about where most of the CO_2 has been flooded and where the residual oil saturation exists within the rock sample.

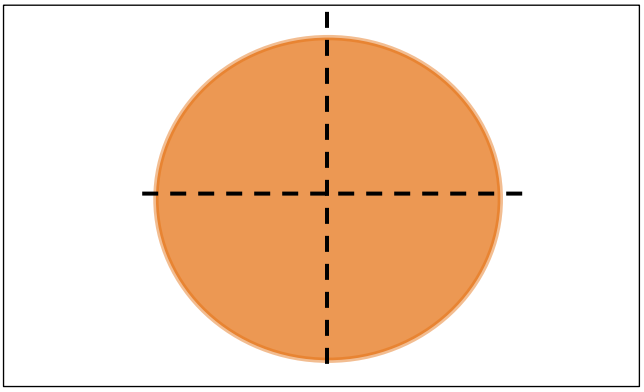

Figure 11. Vertical and horizontal cross sections

4.1 Test 1: Drop in Pressure Test

In our tests, two types of viscosifiers have been tested. Each of these polymers has it effect on increasing the CO_2 viscosity and decreasing its mobility. For comparison purposes, the drop in pressure test should be conducted to evaluate the effectiveness of each viscosifier in increasing the CO_2 viscosity and decreasing its mobility and compare it with the neat CO_2 injection.

According to Darcy's law, the flow rate across a porous medium can be calculated as:

$$Q = -\frac{kA}{\mu}\frac{(P_{OUTLET} - P_{INLET})}{L} \quad \text{.....(10)}$$

Q = flow rate unit of volume per unit of time

K = permeability

A = cross-sectional area of core sample

μ = viscosity

P_{OUTLET} = outlet pressure

P_{INLET} = inlet pressure

L = length of the core sample

Rearranging Equation (10) is as follows:

$$\frac{C}{M} = \frac{C\mu}{k} = \frac{(P_{OUTLET} - P_{INLET})}{Q} = \frac{\Delta P}{Q} \quad \text{.....(11)}$$

$$C = \frac{L}{A} \quad \text{.....(12)}$$

M = mobility ratio

C = constant related to the size of the core sample

As it shown in Equation (11), the mobility (M) consists of the two parameters, permeability and the viscosity of the fluid. The constant parameter (C) as it is stated in Equation (12) is related to the size of the core sample that we have been using. The target of the drop in pressure test is to obtain the ratio of C/M, which is a measure of how the fluid moves inside of the core sample. The fluid here is either neat CO_2 or viscosified CO_2 with PDMS or PVEE.

As mentioned previously, there are specific methods to prepare the viscosifiers for all of the tests that have been conducted. The PDMS is used together with the toluene as a cosolvent. This mixture needs to be added to the CO_2 and pressurize the mixture to the minimum solubility pressure. The minimum solubility pressure of the mixture, which consists of 4 wt% PDMS, 20 wt% toluene and 76 wt% CO_2, is 2500 psi. As stated in the preparation section of the PVEE, the main advantage of the PVEE over the PDMS is that the former has to be added to the CO_2 without the need of adding toluene as a cosolvent. The mixture of the PVEE with the CO_2 can be described as being

almost pure CO_2. This is attributed to the low concentration of the PVEE compared with the CO_2 in the mixture. The mixture is 0.8 wt% PVEE and 99.2 wt% CO_2. Both mixtures after being added to the CO_2were left for an hour to equilibrize and achieve the highest possible solubility that can be obtained.

For the pressure drop test, unfractured 1-in. Indiana limestone cores 5 in. in length were used to obtain a more significant pressure drop difference for both neat CO_2 and viscosified CO_2. The procedure for running the drop in pressure test is similar to that presented in the coreflood test mentioned in the procedure section. The sample was placed in the oven and heated overnight. Then, the sample was placed in the core holder and 3000 psi overburden pressure has been applied. The injection pressure of both CO_2 and viscosified CO_2 was held at approximately 2000 psi. The fluids were injected and left to flow until a relatively constant fluid flow rate was achieved. At this stage, the inlet pressure, outlet pressure, and the flow rate were recorded. Because all of the samples have the same dimensions, the comparison can be made without the need to account for each sample. As stated in Equation (11), only the ratio of $\Delta P/Q$ can be used to evaluate the mobility of the fluids tested. The experimental results are listed in **Table 7**.

Table 7. Results of drop-in pressure test

Run#	Viscosifier Type	Inlet Pressure (psi)	Outlet Pressure (psi)	Flow rate (cc/min)	C/M
1	None	1949	1850	4.89	20.25
2	None	1947	1870	4.38	17.58
3	PDMS	1951	1823	3.66	34.97
4	PDMS	1946	1870	2.92	26.03
5	PVEE	1961	1850	4.82	23.04
6	PVEE	1961	1890	3.49	20.34

Based on the results presented in **Table 7**, PDMS shows the highest drop in pressure and C/M ratio, which means that the highest increase in the viscosity of the CO_2can be achieved when it is mixed with the PDMS. The ratios of C/M as shown in Table 1 prove that the PDMS has the highest drop in pressure across the core sample, which reflects the increase in the viscosity and therefore reduces the mobility of the CO_2. However, the PVEE shows almost the same results as that from the neat CO_2. This means that the PVEE may not be able to increase the viscosity of the CO_2 and improve the overall sweep efficiency. As mentioned earlier, the goal of adding the viscosifiers is to increase the viscosity of the CO_2 and therefore reduce its mobility. Based on the results of the drop in pressure tests, the PDMAS proves its ability to approach these objectives. Even though the PDMS shows higher ratio of C/M, PVEE is also considered to be a good polymer to increase the CO_2 viscosity. Coreflood experiments with CT scan images can show more details on the effectiveness of PDMS and PVEE to improve the sweep efficiency of the CO_2 and increase oil recovery.

4.2 Test 2: Injection of CO_2 and Viscosified CO_2 (PDMS) (1)

High-permeability buff Berea sandstone rock samples with 19.73% and 20.12% porosity were 100% saturated with refined oil (Soltrol 130 Isoparaffin). The refined oil had been injected into the sample at rate of 2 cc/min. The drop in pressure across the core samples was found to be 4 psi.

The objective of this test was to assess the ability of the viscosified CO_2 to improve the oil recovery compared with that produced by the neat CO_2 at a pressure above the MMP using buff Berea sandstone. First, we will inject the neat CO_2 and then to the viscosified CO_2 using PDMS. The injection of CO_2, as mentioned in the procedure of this study, will be conducted at 1400 psi, which is above the MMP. Three PVs of pure CO_2 will be injected. At each injection, the produced oil will be collected to determine if any improvement of oil recovery occurred.

The result of this test shows that after the injection of 0.41PV of neat CO_2, the CO_2 breakthrough has been detected. This behavior of CO_2 early breakthrough is attributed to the high mobility of CO_2 that is a function of its viscosity and relative permeability. One important parameter that is worth mentioning here is that the buff Berea sandstone used in this test has a high permeability, 350 md. This high permeability and heterogeneity of the sample play major factors in developing non-uniform sweep efficiency, which leads to early CO_2 breakthrough. The oil recovery after injection of 0.41 PV was 20.88%.

The next step is to inject another 1.14 PV of neat CO_2 at the same pressure, which is 1400 psi. The test was conducted and more oil was recovered. At this stage, an

increase of 36.04% of the original oil in core was recovered. The total recovery at this level reached 56.04%. More oil has been recovered, but there is still a significant amount of oil untouched inside the core sample. With this recovery, it can be concluded that the CO_2 displaces about 56% of the oil in the pores after 1.55PV injected of CO_2. With 1.55 PV injection of CO_2, the oil recovery expected to be higher than what had been recovered. Due to the poor sweep efficiency, which is caused by the high mobility of CO_2, we produced only this volume of oil. Also, the injection rate of the CO_2, which was 2.5 cc/min, has a huge effect in the displacement and the sweep efficiency. Lowering the rate may result in better displacement and improvement in sweep efficiency.

After the first and second injection, approximately 44% of the original oil in the rock sample needs to be recovered. More CO_2 is needed to recover the remaining oil. Another 0.47 PV was injected at the intended pressure. Throughout this stage, some oil has been produced. The total oil recovery after this injection reached 65.95%, which is a 9.03% increase after the second injection. Still, there is a lot of oil unproduced and not communicating with CO_2 at all.

The residual oil saturation is about 34% of OOIP. Higher oil recovery may be collected with more injection of CO_2. Due to that, another 0.33 PV of neat CO_2 was injected. The result of this injection showed a little oil was produced. The cumulative oil recovery after a total of 2.35 PV of neat CO_2 injected was 67.76%. As stated before, this moderate oil recovery is attributed to the poor sweep efficiency of the CO_2 caused by the high CO_2 mobility and heterogeneity of the core sample. **Table 8** summarizes the results of the oil recovery that was collected during this test.

Table 8.Test 2 oil recovery after injecting neat CO_2

PV Injected	Oil Recovery %	Cumulative Oil Recovery %
0.41	20.88	20.88
1.55	36.04	56.92
2.02	9.03	65.95
2.35	1.81	67.76
Total Oil Recovery	**67.76**	

Overall, after injecting 2.35 PV of the neat CO_2 at a pressure of 1400 psi and 130^{o}F, which is above the MMP of oil, the recovery factor is 67.76%.

Generally speaking, better controlling of the CO_2flood may result in better sweep efficiency. The next step will be injection of viscosified CO_2 to observe the improvement in the oil recovery and sweep efficiency. In this test, the PDMS polymer was mixed with CO_2 to increase the viscosity of the CO_2. As illustrated in the procedure of this test, 4 wt% of this polymer and 20 wt% of toluene as a cosolvent were added to CO_2 and pressurized to 2500 psi. The same steps followed with the neat CO_2 were applied here. To ensure that the core is fully saturated with oil, 10 PV of oil was injected into the core sample. The same procedure was followed; i.e., 0.33, 1.46, and 2.55 PV of viscosified CO_2 will be injected at 1400 psi and 130^{o}F.

The main points here are to investigate for oil recovery and CO_2 breakthrough. After the injection of 0.33 PV of the viscosified CO_2, the oil recovery was found to be 27.53% of the OOIP. This is an indication that we have better sweep efficiency through which the CO_2 contacts most of the oil in the core sample. Compared with 0.41 PV of neat CO_2, viscosified CO_2 shows higher oil recovery during this injection. This result gives an indication of the improvement in sweep efficiency and displacement of large volume of oil by viscosified CO_2.

Approximately 73% of the oil was not produced with the first 0.33 PV injection of the viscosified CO_2. Because of that, an additional 1.13 PV was injected to make sure we achieved the maximum oil recovery that can be obtained. The results show that an additional 31.92% of the original oil in the core sample has been produced. The total oil recovery at this level reached 59.45%. The higher oil recovery produced with viscosified CO_2 compared with neat CO_2 injection is attributed to the good sweep efficiency that has been achieved, which recovered a large volume of the oil in the core sample.

It might be possible to produce more oil with more injection of the viscosified CO_2. An additional 1.05 PV of viscosified CO_2 was injected into the core sample, which contains about 40% of the residual oil saturation. The result showed that about 14.19% of the oil was recovered, making the total oil recovery roughly 73.64%. Table 3 reported the oil recovery at each volume injected. **Table 9** summarizes the oil recovery during the viscosified CO_2 injection. The final results of test 2 are summarized in **Table 10**.

Table 9.Test 2 oil recovery after injecting viscosified CO_2

PV Injected	Oil Recovery %	Cumulative Oil Recovery %
0.33	27.53	27.53
1.46	31.92	59.45
2.51	14.19	73.64
Total Oil Recovery	**73.64**	

Table 10.Test 2 summary of the results

Parameter	Neat CO_2	Viscosified CO_2
Sample	Fractured buff Berea sandstone	Fractured buff Berea sandstone
Injection Status	Above MMP	Above MMP
Porosity	19.73%	20.12%
Oil Recovery	67.76%	73.64 %

The overall results show that the viscosified CO_2 has higher oil recovery compared with the neat CO_2 injection. This result is attributed to the lower mobility of the CO_2 in the former case. As a result, better sweep efficiency has been achieved using

the viscosified CO_2. The late breakthrough of CO_2 and the higher oil recovery with the viscosified CO_2 prove the ability of the viscosifier to increase the CO_2 viscosity and therefore reduce its mobility. **Figure 12** shows a comparison of the oil recovery versus the pore volume injected for both neat and viscosified CO_2 using PDMS.

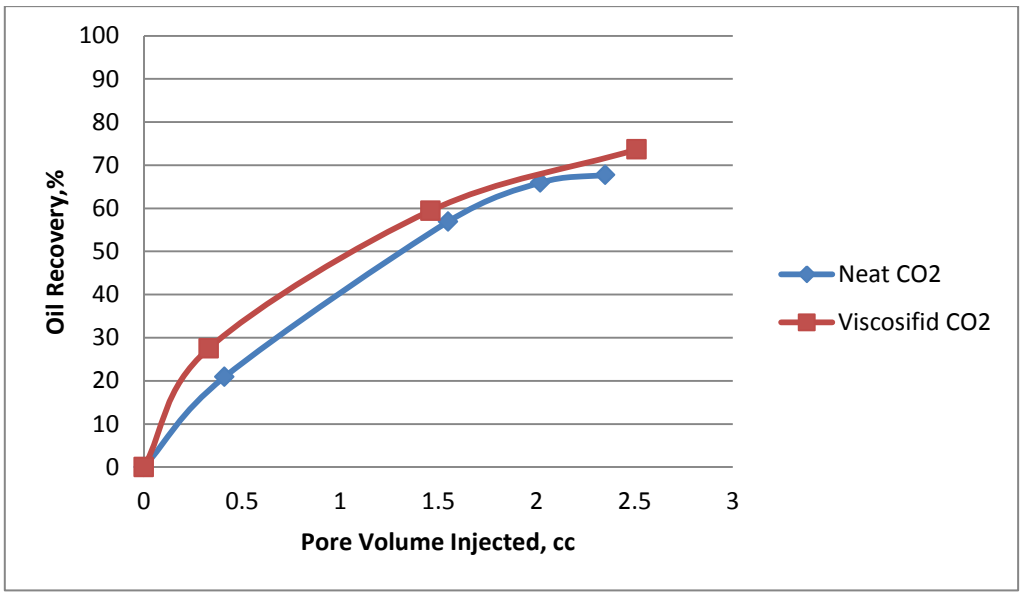

Figure 12.Test 2 oil recovery with PV injected for both neat and viscosified CO_2

4.3 Test 3: Injection of CO_2 and Viscosified CO_2 (PDMS) (2)

High-permeability fractured Indiana limestone with 18.03% porosity was used in this test. **Figure 13** presents the schematic showing how the fracture was created. CO_2 was injected to the sample at the supercritical phase. The objective of this test is to evaluate the ability of the viscosified CO_2 with PDMS to increase the CO_2 viscosity and reduce its mobility and therefore improve the sweep efficiency and enhance the oil recovery in a fractured reservoir. Throughout the description of all of the results in this study, the left side in the CT scan images represents the inlet and the right side represents the outlet. For this test, the scale of the CT number is shown in **Figure 14**. The red color represents the high-CT number, which indicates to the presence of oil in this study. The blue color represents the low-CT number, which corresponds to the CO_2. In each run, there are two images; one shows the horizontal cross section (the upper one) and the other shows the vertical cross section (the lower one).

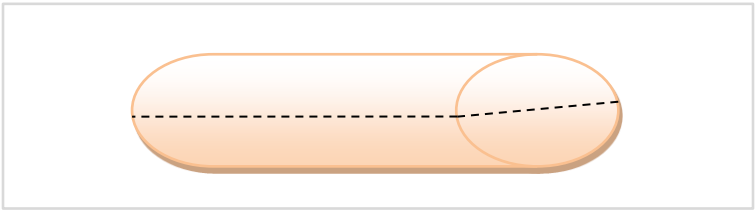

Figure 13. Schematic of fractured Indiana limestone sample

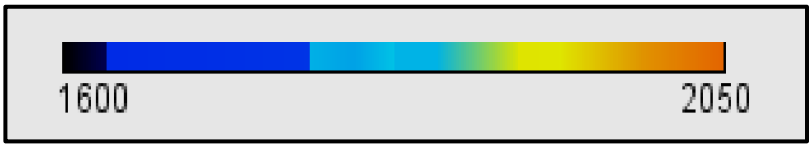

Figure 14. Test 3 CT number scale

To make the comparison between CO_2 and oil easier to investigate for sweep efficiency, images of both CO_2 and oil have been taken when both fluids were 100% saturated in the sample. **Figure 15** shows the sample when it is 100% saturated with CO_2. As is shown in the figure, the inlet shows a slightly higher CT number compared with the other portion of the core sample. This result is attributed to the matrix present in the sample that may have higher density. The vertical slice images for the sample when it is 100% saturated with CO_2 are shown in **Figure 16**. The figure shows the fracture plane having very low-CT number compared with the other portion of the matrix. This result can be explained by the low density of the matrix through the fracture plane.

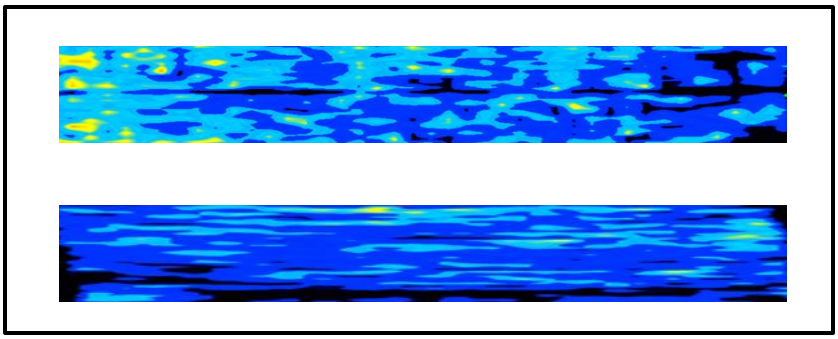

Figure 15. Test 3 core sample 100% saturated withCO_2

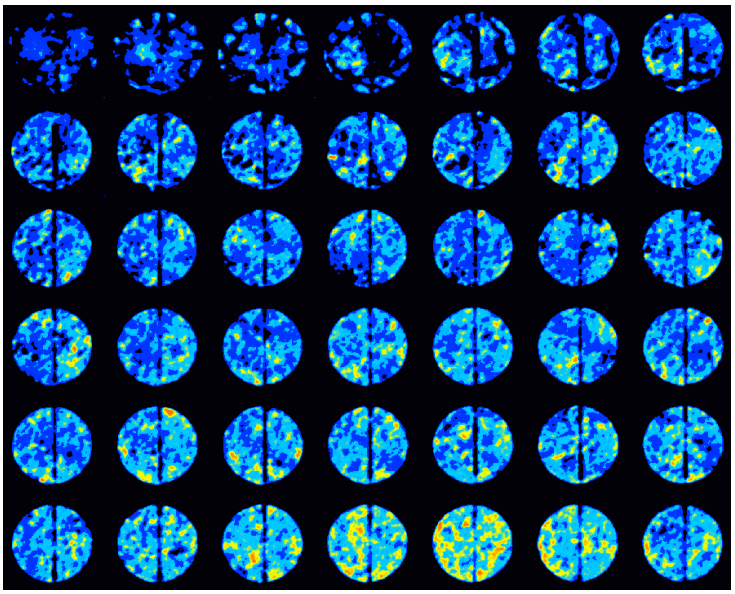

Figure 16. Test 3 vertical slice images 100% saturated with CO_2

Refined oil was then injected into the sample at the rate of 5cc/min. The sample was held at a pressure of 1600 psi for considerable time to make certain that the sample is fully saturated with the refined oil. Also, for more accuracy, 10 PV of refined oil has been injected. The drop in pressure across the core sample was found to be approximately 12 psi. **Figure 17** shows the sample when it is 100% saturated with oil. There are some portions of the rock sample where the blue color appears even though the sample is 100% saturated with oil. The same behavior can be seen in **Figure 15** when the sample was 100% saturated with CO_2. One possibility for this behavior is that the matrix content of the rock has a low-CT number compared with the other portion of the rock sample (high porosity section). The vertical slice images for the sample when it is 100% saturated with oil can be shown in **Figure 18**. The slices showing the low-CT number behavior are highlighted.

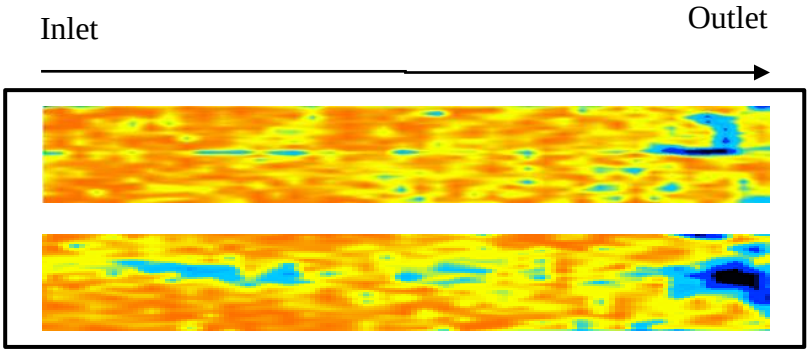

Figure 17. Test 3 rock sample when it is 100% saturated with oil

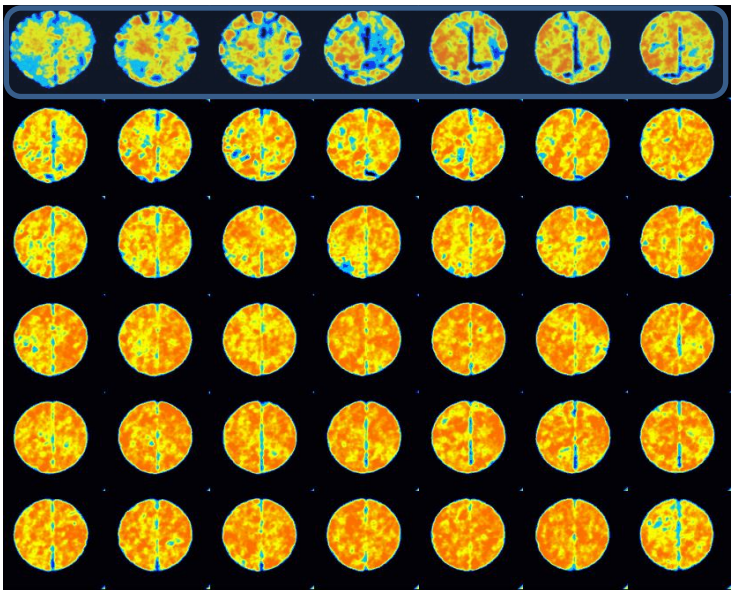

Figure 18. Test 3 vertical slice images the sample is 100% saturated with oil

As described in the experimental procedure, we will go through the injection of the pure CO_2 and then to the viscosified CO_2 using PDMS. The injection of CO_2 in this test will be conducted at 1800 psi. The objective of conducting the test at 1800 psi is to evaluate the performance of the viscosifier at a pressure close to the MMP. Three PVs of neat CO_2 will be injected; i.e., 0.5, 1, 2, and 3. At each injection, the produced oil will be collected and a CT scan will be run to investigate for the sweep efficiency.

Figure 19 shows the images after injection of 0.49 PV of neat CO_2. It can be seen clearly in **Figure 19** how the CO_2 flows inside of the core sample. Most of the CO_2 flows through the fracture, as is shown in the lower image of **Figure 19**, leaving the oil in the rock matrix untouched. This behavior can be seen clearly in **Figure 20** where each

slice shows a low-CT number in the fracture portion of the rock and a higher CT number outside the fracture region. This result is attributed to the poor sweep efficiency of the CO_2 in such heterogeneous media. Generally speaking, the sweep efficiency during the 0.49 PV is very poor; CO_2 does not make a contact with most of the oil in the core sample. The oil recovery after this injection is 15.8%. Also, the CO_2 breakthrough was detected after the injection of 0.33 PV of neat CO_2.

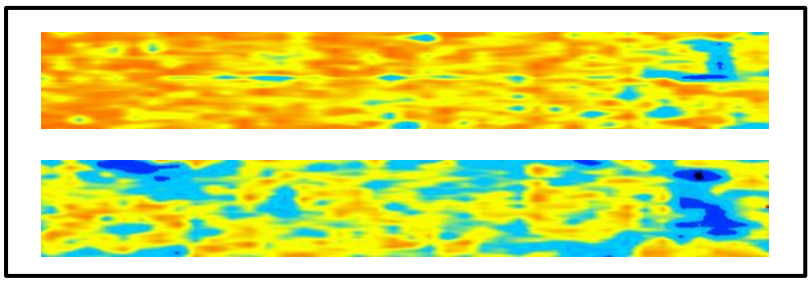

Figure 19. Test 3 rock sample after injecting 0.49 PV of neat CO_2

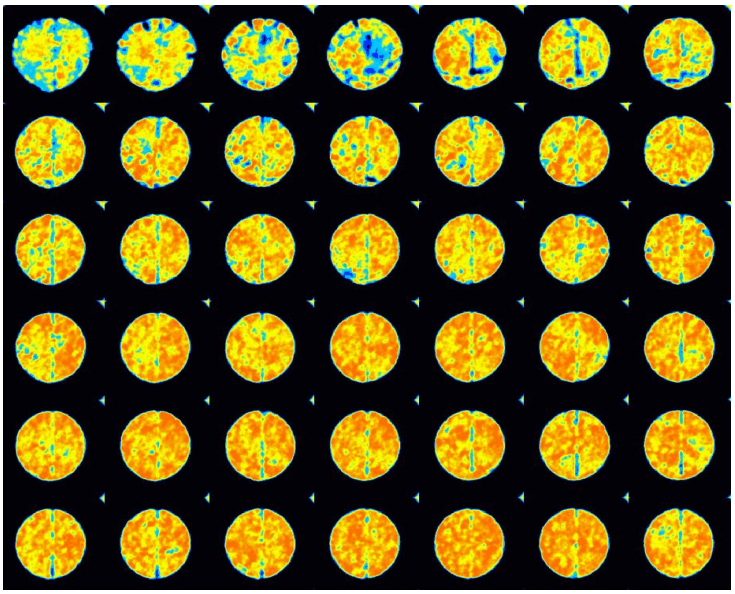

Figure 20. Test 3 vertical slice images after injecting 0.49 PV of neat CO_2

The next step is to inject another 0.5 PV of neat CO_2 at the same pressure, which is 1800 psi. The test was conducted and more oil was recovered. **Figure 21** shows the results after the injection of 1.01 PV of neat CO_2. At this stage, an increase of 24.4% of the original oil in the core sample was achieved. The total recovery at this level reached 40.2%. More oil has been recovered, but still we have a significant amount of oil untouched near the injection point. **Figure 22** shows the fracture and the areas around the fracture dominate the flow of the CO_2. As a result, the sweep efficiency can be considered as a poor sweep.

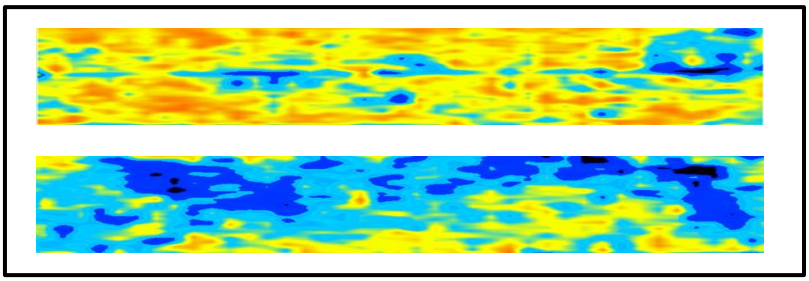

Figure 21. Test 3 rock sample after injecting 1.01 PV of neat CO_2

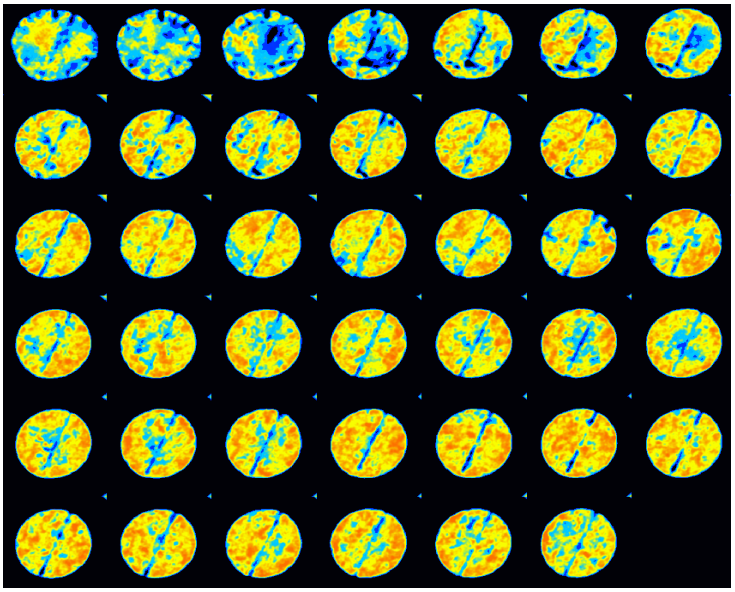

Figure 22. Test 3 vertical slice images after injecting 1.01 PV of neat CO_2

After the first and second injection, still there is about 60% of the original oil in the core sample that needs to be produced. More CO_2 is needed to recover the remaining oil. Another 1.03 PV was injected at the intended pressure. Throughout this stage, more oil has been produced. The total oil recovery after this injection reached 60.79%, which is a 20.59% increase after the second injection. **Figure 23** shows better sweep efficiency of the CO_2 compared with the previous injection. Good sweep can be seen at the inlet and outlet, but at the middle portion of the core sample, quite a lot of oil remains untouched. The vertical slice images in **Figure 24** support this result, which shows how the CO_2 pushed all of the oil at the inlet and outlet, leaving the middle portion untouched. As stated previously, this result is attributed to the poor displacement and sweep efficiency of CO_2 in fractured media.

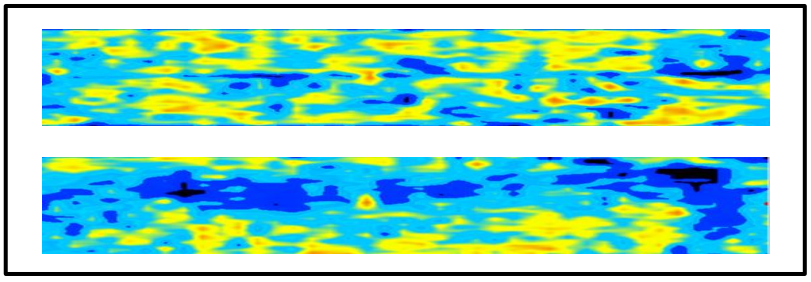

Figure 23. Test 3 rock sample after injecting 2.04 PV of neat CO_2

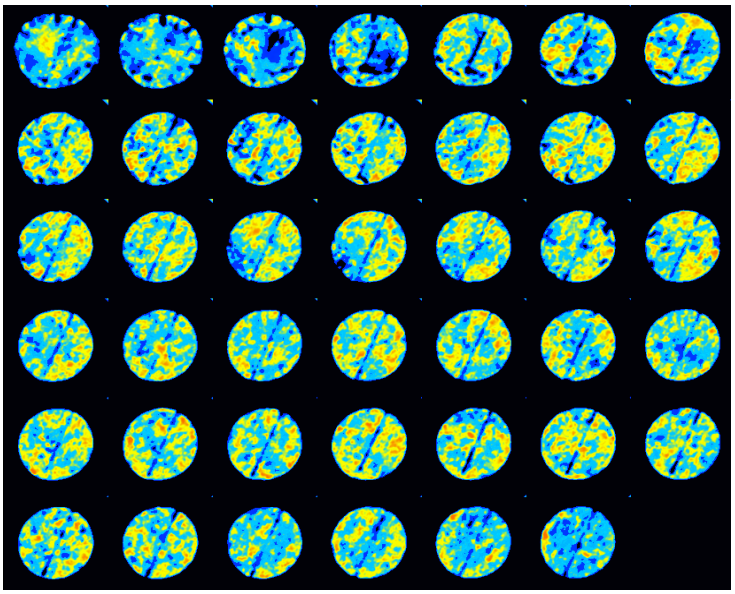

Figure 24. Test 3 vertical slice images after injecting 2.04 PV of neat CO_2

According to the results either from the oil collected or from the CT scan images, we still have about 40% of the oil inside the core sample. Based on that result, another pore volume of CO_2 was injected to recover as much of the original oil in the core sample as possible. With this injection, a total of 2.9 PV of neat CO_2 has been injected. The results show that an additional 4.12% of the original oil in the core sample has been recovered. As a result, the total oil recovery has now reached 64.91%. **Figure 25** shows the result of the CT scan images after the injection of a total of 2.9 PV of neat CO_2, which is very similar to that presented when 2.04 PV was injected. There is no further progress in the overall sweep efficiency as is shown in **Figures 25 and Figure 26**. Most of the injected CO_2 flows inside the fracture plane and the area around the fracture plane,

which leads to a very poor sweep efficiency and low oil recovery. **Table 11** presents the results of the oil recovery after each injection.

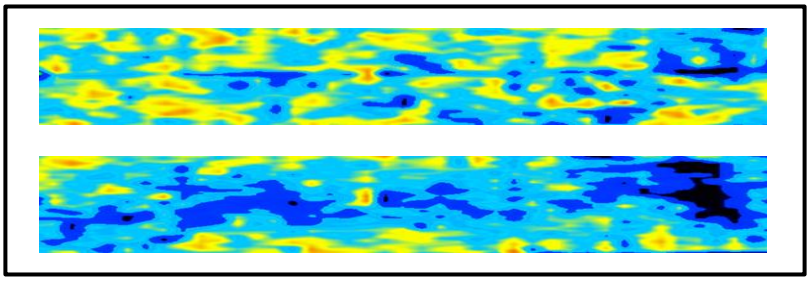

Figure 25. Test 3 rock sample after injecting 2.9 PV of neat CO_2

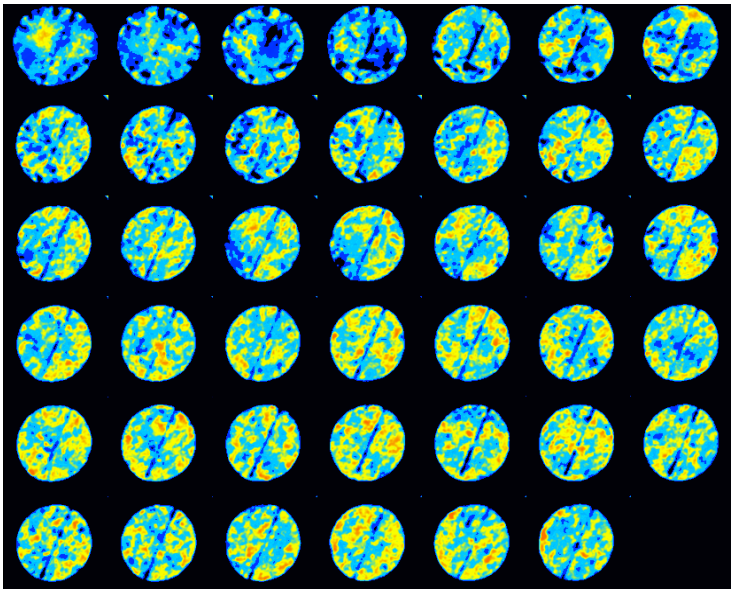

Figure 26. Test 3 vertical slice images after injecting 2.9 PV of neat CO_2

Table 11. Test 3 oil recovery after injecting neat CO_2

PV Injected	Oil Recovery %	Cumulative Oil Recovery %
1.01	40.2	40.2
2.04	20.59	60.79
2.9	4.12	64.91
Total Oil Recovery	**64.91**	

Overall, after injection of 2.9 PV of the neat CO_2 at a pressure of 1800 psi and 130^{o}F, which is above the MMP of oil and at supercritical phase of CO_2, the recovery factor is 64.91%. Also, the sweep efficiency according to the CT images is considered to be poor. **Figure 27** shows how the average CT number across the core sample changes during each injection of neat CO_2. As is shown after 2.9 PV injection of CO_2, the average CT number is still greater than the CO_2 CT number. Also, after the first injection, which is 0.49 PV of neat CO_2, the average CT number is very close to that of the oil, indicating that the CO_2 does not communicate with the oil to change its density and therefore the CT number.

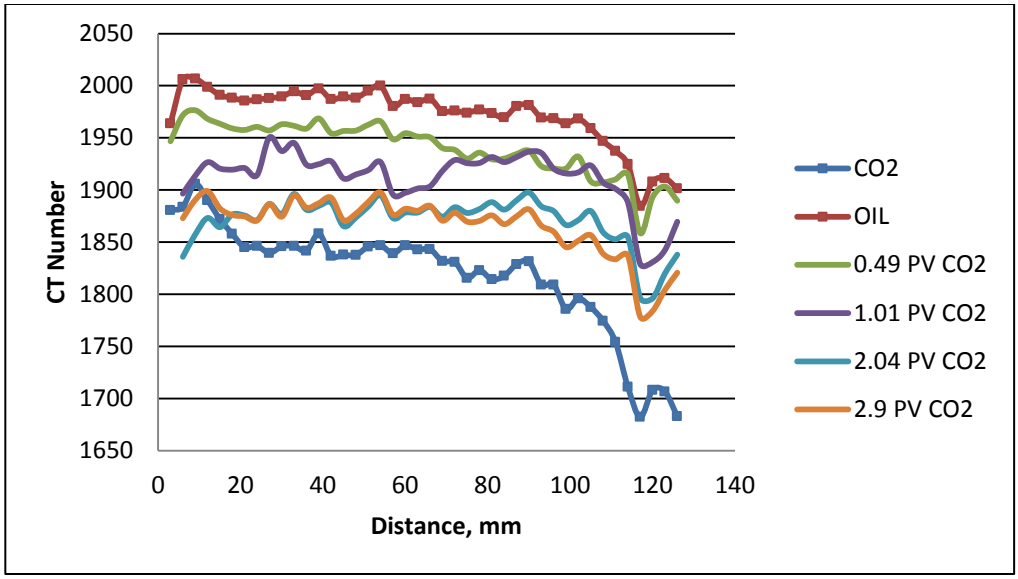

Figure 27. Test 3 average CT number across the sample during neat CO_2 injection

The next step will be injection of viscosified CO_2 to observe the improvement in the oil recovery and sweep efficiency. The PDMS polymer was mixed with CO_2 to increase the viscosity of the CO_2. As illustrated in the procedure of this test, 4 wt% of this polymer and 20 wt% of toluene as a cosolvent were added to CO_2 and pressurized to 2500 psi. The same steps used with the neat CO_2 are applied here. To ensure that the core sample is fully saturated with oil, 10 PV of oil were injected into the core sample and 1600-psi pressure was maintained for a considerable time. The same pore volume injected with neat CO_2 will be injected using viscosified CO_2. Also, the experiment will be conducted at the same pressure and temperature; i.e., 1800 psi and 130^{o}F.

In this test, the first injection was 0.47 PV of viscosified CO_2. **Figure 28** shows the sweep efficiency of oil and CO_2 after 0.47 PV of viscosified CO_2 was injected. Based on the CT images shown in **Figure 28** and compared with 0.49 PV injected using neat CO_2, better sweep efficiency has been developed and observed when 0.47 PV of viscosified CO_2 was injected. Also, compared with neat CO_2 injection at 0.49 PV, viscosified CO_2 covers a larger area and produces a larger volume of oil. The vertical slice images in **Figure 29** also support this behavior. Even though the fracture and the areas around the fracture plane still dominate the flow, viscosified CO_2 has better sweep efficiency than neat CO_2. In addition to the CT images result, the oil recovery, which is 31.22%, also support the finding that the viscosified CO_2 has better performance than neat CO_2. The heterogeneity of the rock sample plays an important factor in the overall sweep efficiency. It is worth to mention that most of the samples used in this study are heterogeneous. The CO_2 breakthrough was observed after the injection of 0.47 PV of viscosified CO_2.

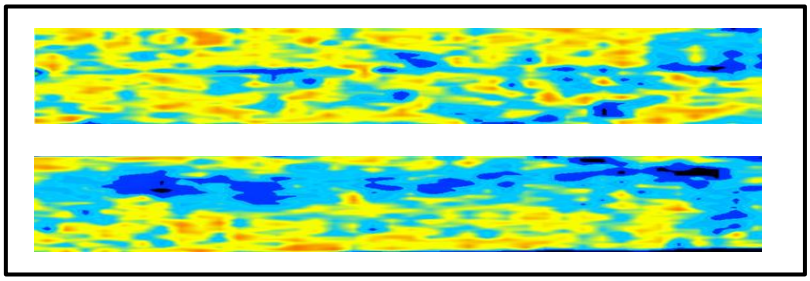

Figure 28. Test 3 rock sample after injecting 0.47 PV of viscosified CO_2

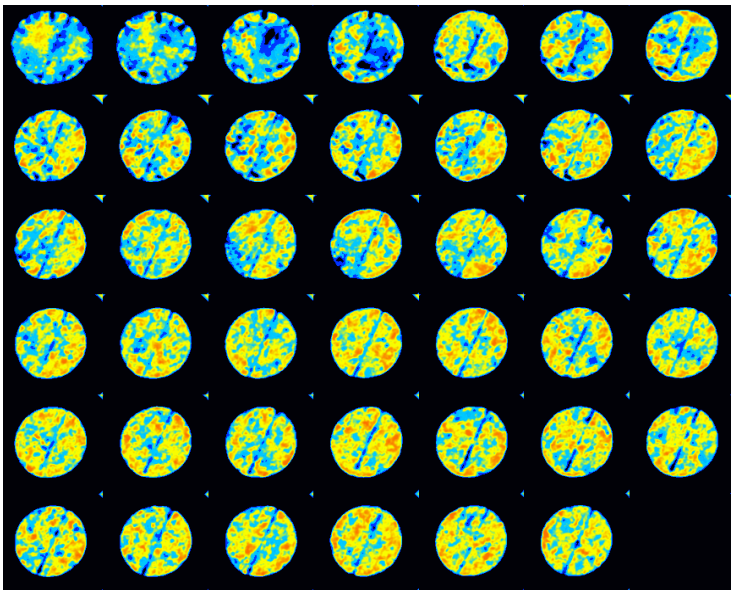

Figure 29. Test 3 vertical slice images after injecting 0.47 PV of viscosified CO_2

Approximately 70 % of the oil in the sample has not yet been produced with the first 0.49 PV injection of the viscosified CO_2. For this reason, an additional 0.43 PV of viscosified CO_2 was injected to make certain that we achieved the maximum oil recovery possible. The results showed that additional 21.23% of the original oil in core sample has been produced. The total oil recovery after this injection now reached 52.45%. **Figure 30** presents the CT scan images of the viscosified CO_2 flood after the 0.9 PV injections. Compared with 0.47 PV injected in the previous step, there is a significant improvement in the sweep efficiency of CO_2. The lower mobility of the viscosified CO_2 compared with that of neat CO_2 results in a better sweep efficiency.

Figure 31 also shows the slice images of the core sample after this injection. Both **Figure 30 and Figure 31** show that most of the oil at the inlet and outlet has been recovered and a small amount of the unproduced oil is concentrated at the upper portion of the core sample. Due to gravity segregation effect, significant sweep efficiency has been achieved in the lower portion of the core sample.

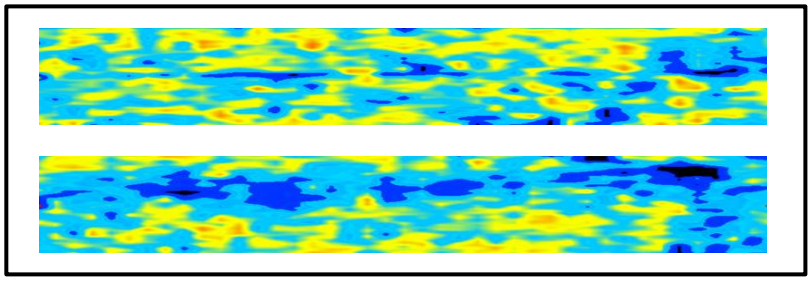

Figure 30. Test 3 rock sample after injecting 0.9 PV of viscosified CO_2

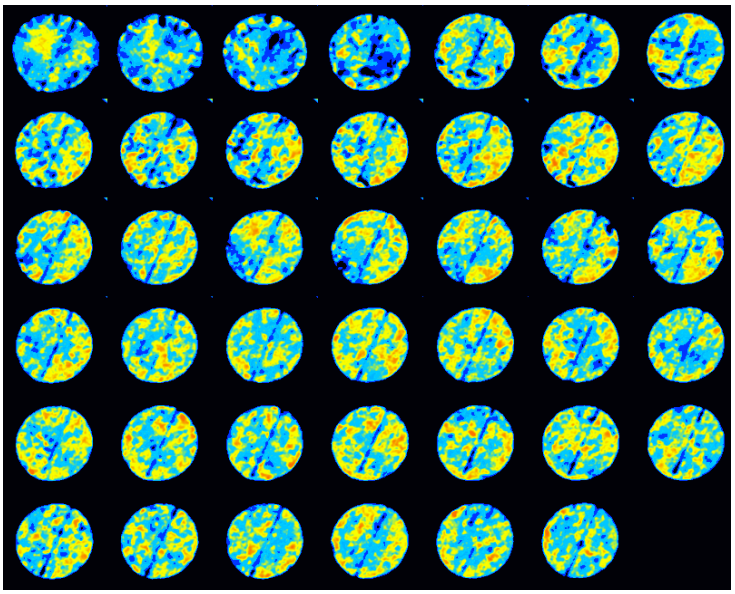

Figure 31. Test 3 vertical slice images after injecting 0.9 PV of viscosified CO_2

It might be possible to produce more oil with additional injection of the viscosified CO_2. Thus, an additional 0.87 PV was injected into the core sample, which has about 45% of the residual oil saturation. The results show that roughly 18.85% of the oil has been recovered, making the total oil recovery up to this level approximately 71.3%. The sweep efficiency of oil and viscosified CO_2 are shown in **Figure 32**. The figure shows that there is a significant improvement in sweep efficiency of the overall flood of CO_2 compared with the previous injection. Also, it can be seen clearly from **Figure 32** that most of the oil in the core sample has been recovered. The vertical slice images in **Figure 33** show that most of the oil in the each slice has been recovered with only a very small portion of the core that has not yet been produced. However, the result

presented here is much better than that presented with the neat CO_2 injection. This conclusion can be supported by two findings: the overall sweep efficiency improvement and the total oil that has been produced.

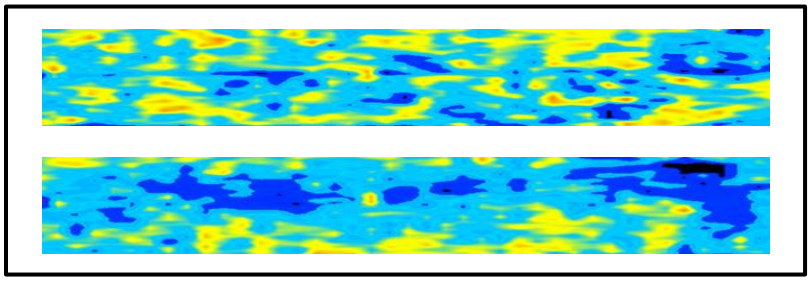

Figure 32. Test 3 rock sample after injecting 1.77 PV of viscosified CO_2

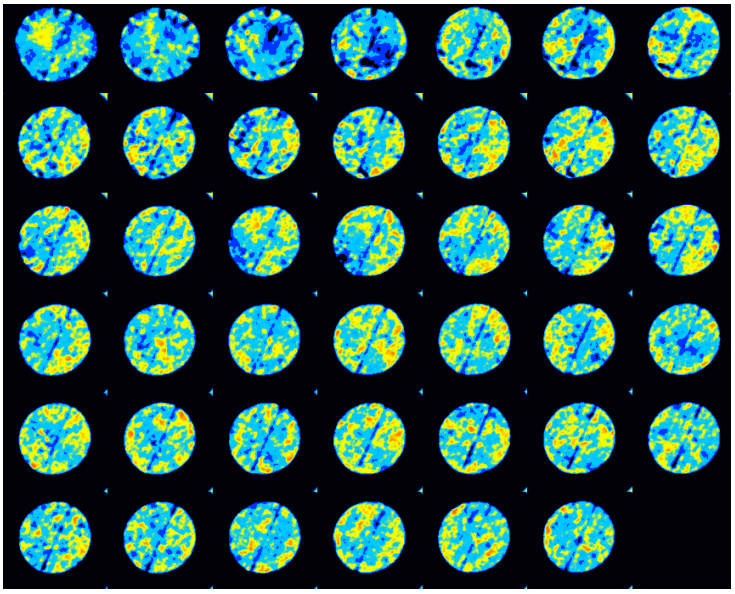

Figure 33. Test 3 vertical slice images after injecting 1.77 PV of viscosified CO_2

Approximately 30% of the OOIP has not been recovered. To make a good comparison with the neat CO_2 injection, an additional 1.01 PV of viscosified CO_2 was injected. As shown in **Figure 34**, most of the oil has been produced. Very little strikes can be shown in the same figure, which indicates the presence of oil in the sample. Also, **Figure 35** presents the vertical slice images that show the ability of the viscosified CO_2 to produce most of the oil and improve the sweep efficiency. In **Figure 35,** there is also a small portion at the inlet that shows a higher CT number, which may indicate the presence of the oil, but this behavior was shown also when the sample was 100% saturated with CO_2. The experimental results showed that about 3.28% of the original oil in core sample was produced after this injection. With that result, the total oil recovery after the injection of 2.78 PV of viscosified CO_2 has reached 74.58%. **Table 12** summarizes the oil recovery at each injection step.

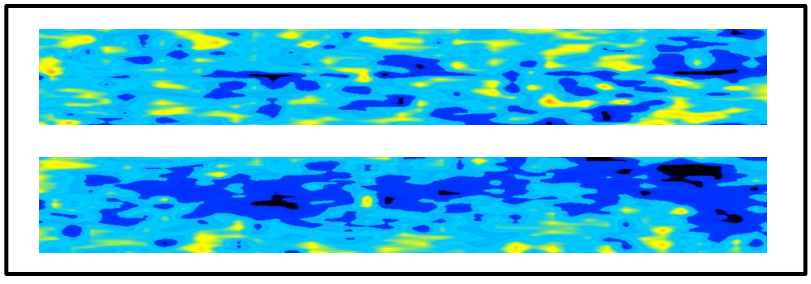

Figure 34. Test 3 rock sample after injecting 2.78 PV of viscosified CO_2

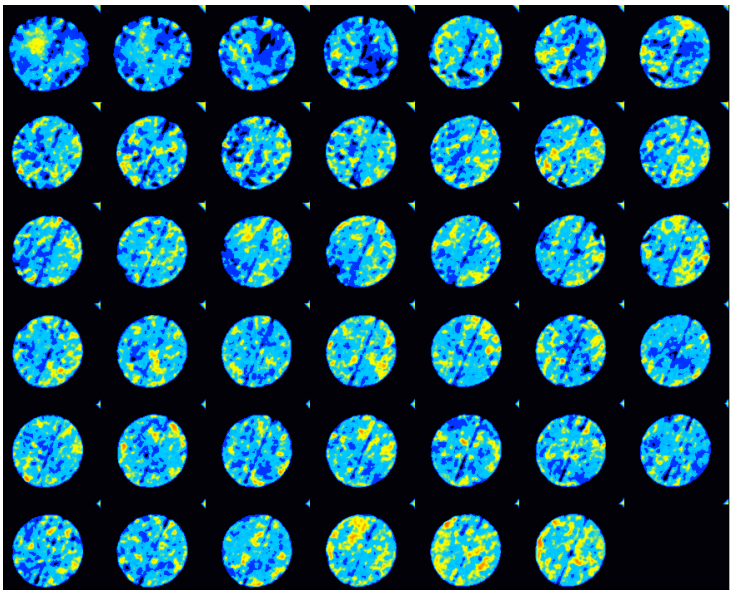

Figure 35. Test 3 vertical slice images after injecting 2.78 PV of viscosified CO_2

Table 12. Test 3 oil recovery after injecting viscosified CO_2

PV Injected	Oil Recovery %	Cumulative Oil Recovery %
0.47	31.22	31.22
0.90	21.23	52.45
1.77	18.85	71.3
2.78	3.28	74.58
Total Oil Recovery	**74.58**	

The final result of this test showed that after injection of 2.78 PV of viscosified CO_2 at a pressure of 1800 psi and 130^oF, which is above the MMP of oil and at the supercritical phase of CO_2, the recovery factor is 74.58%. The oil recovery from both neat and viscosified CO_2 is shown in **Figure 36**. Also, the sweep efficiency according to the CT images is considered to be good compared with that presented in the neat CO_2 injection. **Figure 37** shows how the average CT number across the core sample changes during each injection of viscosified CO_2. As is shown after 2.78 PV injection of viscosified CO_2, the average CT number is very close to that of CO_2. This means that the viscosified CO_2 covers most of the volume and communicates with the large volume of oil inside the core sample.

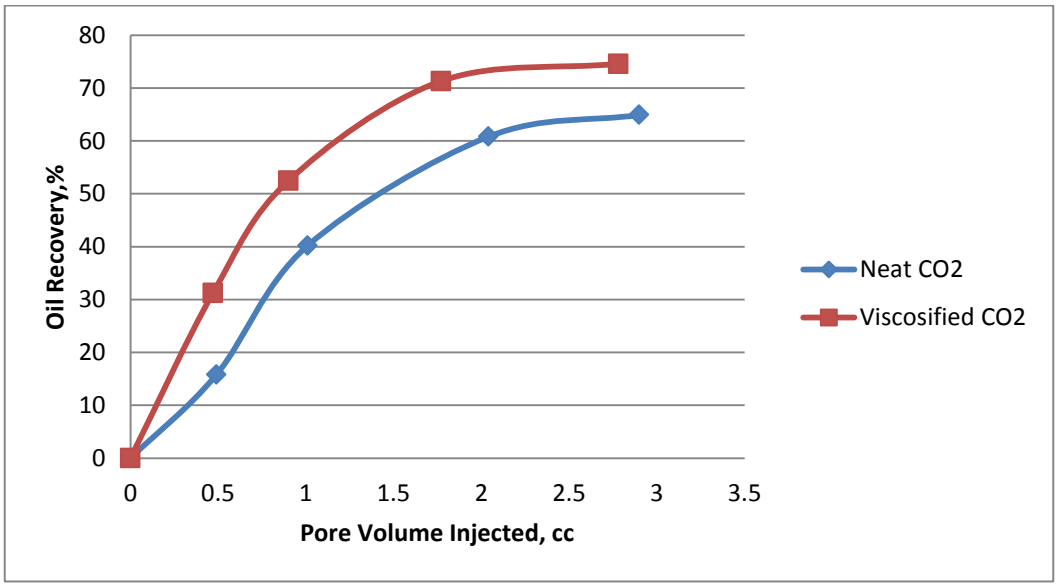

Figure 36. Test 3 Oil recovery from neat and viscosified CO_2

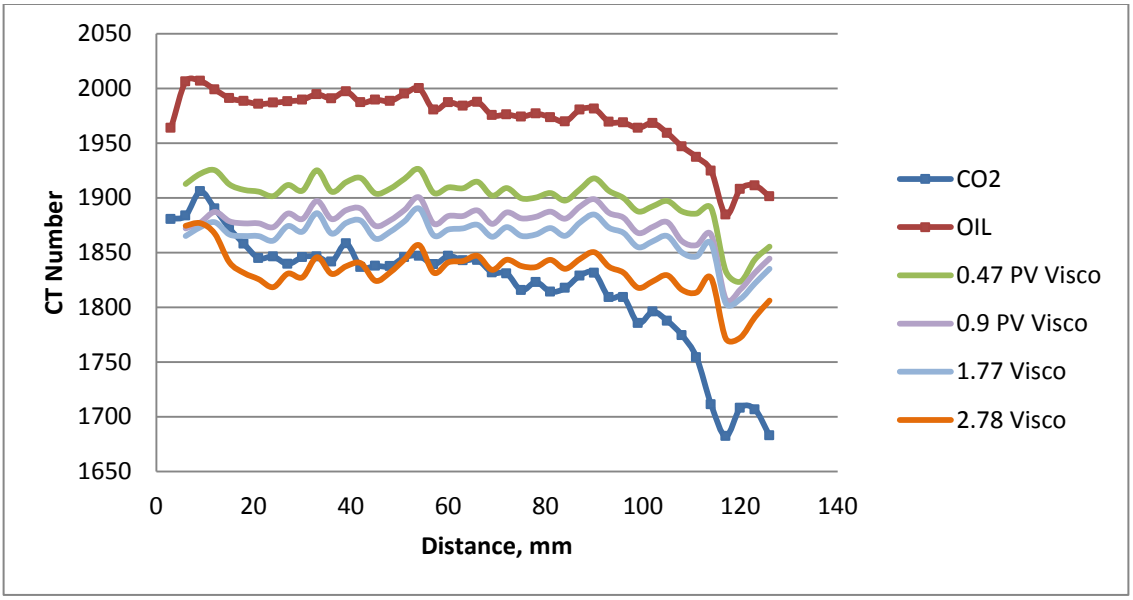

Figure 37. Test 3 average CT number during viscosified CO_2 injection

Overall, the viscosified CO_2 shows better sweep efficiency than the neat CO_2. As presented in **Figure 38**, the average CT number of each viscosified CO_2 injection shows improvement in the CO_2 flood compared with that of the neat CO_2. The lower the CT numbers, the better the sweep efficiency achieved during that injection. **Figure 39** presents the saturation of the CO_2 across the core sample. Higher CO_2 saturation can be seen with the viscosified CO_2 compared with the neat CO_2 at each injection volume.

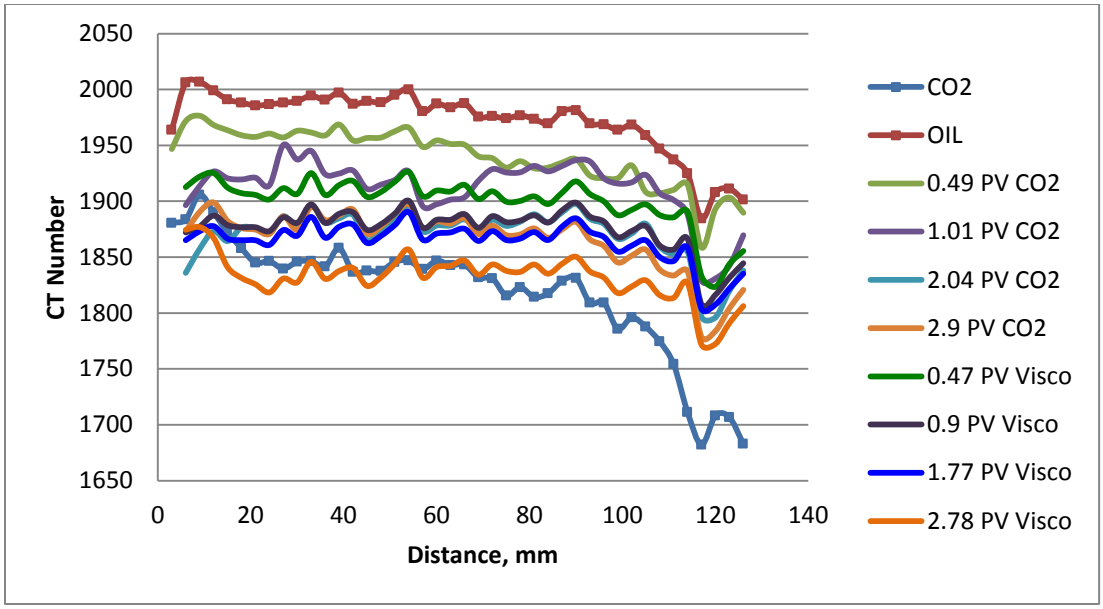

Figure 38. Test 3 average CT number across the sample

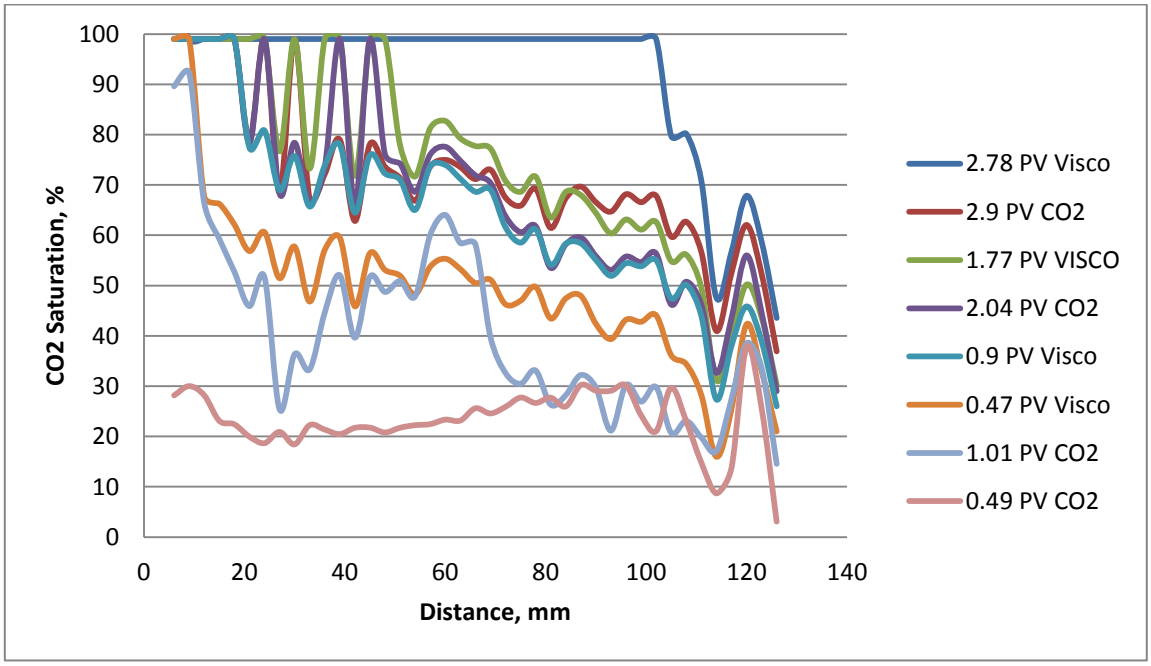

Figure 39. Test 3 CO_2 saturation across the core sample

4.4 Test 4: Injection of CO_2 and Viscosified CO_2 (PDMS) (3)

High-permeability fractured Indiana limestone with 19.44% porosity was used in this test. CO_2 was injected into the sample at the supercritical phase. The objective of this test was to evaluate the ability of the viscosified CO_2 with PDMS to increase the CO_2 viscosity and reduce its mobility and therefore improve the sweep efficiency and enhance the oil recovery in a fractured reservoir at the supercritical phase. Throughout the description of all of the results in this study, the left side in the CT scan images represents the inlet and the right side represents the outlet. For this test, the scale of the CT number is shown in **Figure 40**. The red color represents the high-CT number, which indicates the oil in this study, and the blue color represents the low-CT number, which designates the CO_2. In each run, there are two images; one shows the vertical cross section (the upper one) and the other shows the horizontal cross section (the lower one), which shows the flow across the fracture plane.

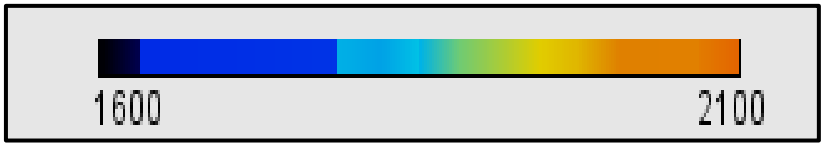

Figure 40. Test 4 CT number scale

As mentioned in the previous test, for the purpose of comparing CO_2 and oil to investigate for sweep efficiency, images of both CO_2 and oil have been taken when both fluids were 100% saturated in the sample. **Figure 41** shows the sample when it is 100% saturated with CO_2. As indicated in the figure, there are some portions of the core sample showing either a moderate CT number or a very low CT number. This behavior can be attributed to the matrix content where it may show high- or low-density contents. The vertical slice images for the sample when it is 100% saturated with CO_2 are shown in **Figure 42**. The figure shows the fracture plane having a very low CT number compared with the other portion of the matrix. This can be explained by the low-density area around the fracture plane (larger pores size).

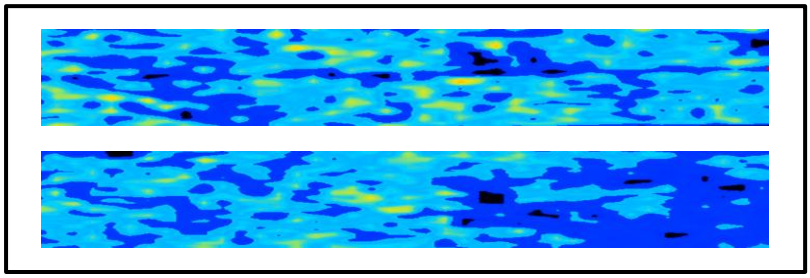

Figure 41. Test 4 rock sample when it is 100% saturated with CO_2

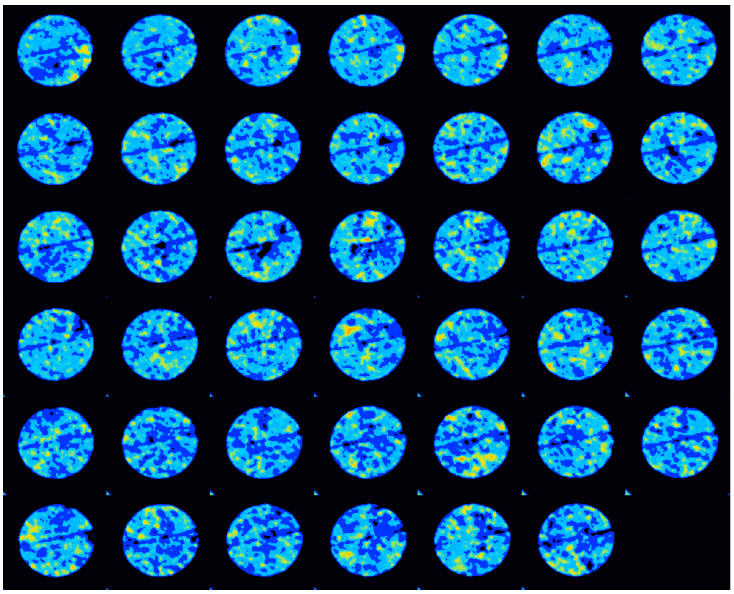

Figure 42. Test 4 vertical slice images the sample is 100% saturated with CO_2

Refined oil was then injected into the sample at the rate of 2cc/min. The sample was held at a pressure of 1600 psi for considerable time to make certain that the sample is fully saturated with the refined oil. Also, for improved accuracy, 10 PV of refined oil was injected. The pressure drop across the core sample was found to be on the order of 5 psi. **Figure 43** shows the sample when it is 100% saturated with oil. There are some portions of the rock sample, very close to the fracture plane, where the blue color appears even though the sample is 100% saturated with oil. The same behavior can be seen in Figure 41 when the sample was 100% saturated with CO_2. One explanation for this behavior is that the matrix content of the rock has a low CT number compared with the other portion of the rock sample and most likely, it is a high-porosity section where

the density is very low. The vertical slice images for the sample when it is 100% saturated with CO_2 are shown in **Figure 44**.

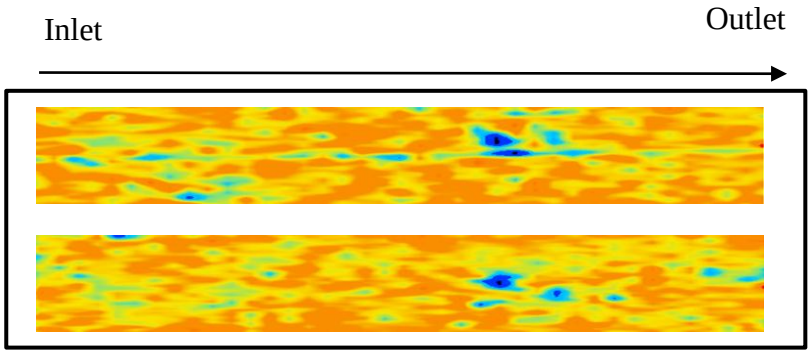

Figure 43. Test 4 rock sample when 100% saturated with oil

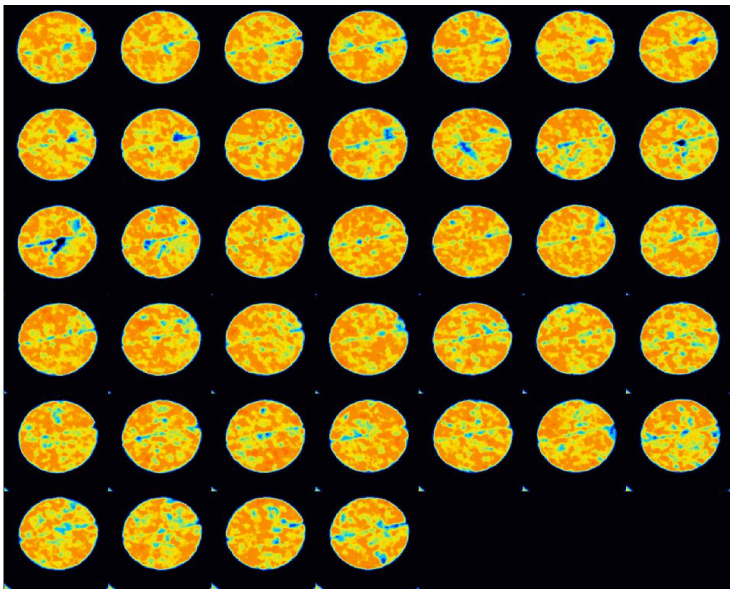

Figure 44. Test 4 vertical slice images of the sample 100% saturated with oil

As was described in the experiment procedure section, we will go through the injection of neat CO_2 and then the viscosified CO_2 using PDMS. The test will be conducted at 2000 psi and 130^{o}F. The difference between this test and the previous test is that the previous one was conducted at a pressure very close to the MMP, and this test will be conducted at a pressure very close to the MSP of PDMS in CO_2. Three PVs of neat CO_2 will be injected; 0.5, 1, 2, and 3. At each injection, the produced oil will be collected and the CT scan will be run to investigate the sweep efficiency.

After injecting 0.44 PV of neat CO_2, it can be seen clearly from **Figure 45** how the CO_2 flows inside the core sample. Most of the CO_2 flows through the fracture plane and the area close to the fracture, leaving the oil in the rock matrix untouched. This behavior can be observed clearly in **Figure 46** where each slice shows a low CT number in the fracture portion of the rock and higher CT number in the matrix portion. In such heterogeneous media, the high mobility of neat CO_2 compared with the oil results in the poor sweep efficiency and low-displacement efficiency. The oil recovery after this injection was 28.48%.

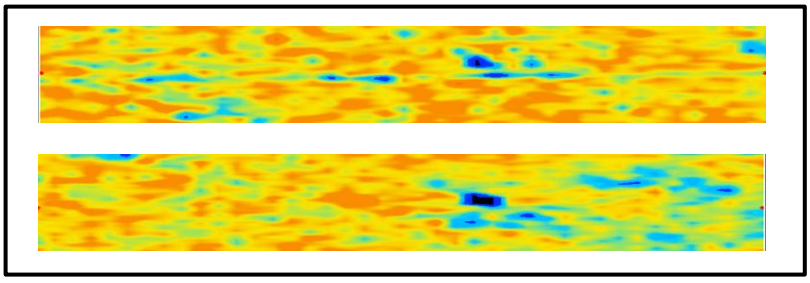

Figure 45. Test 4 rock sample after injecting 0.44 PV of neat CO_2

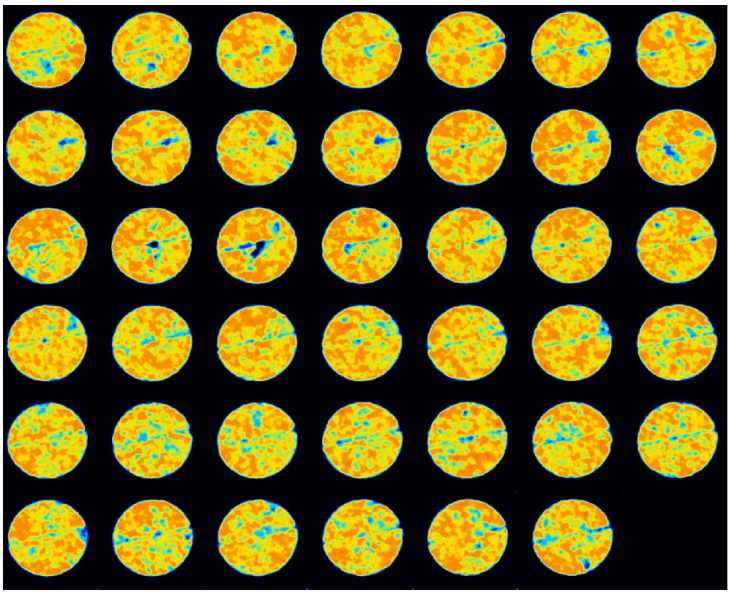

Figure 46. Test 4 vertical slice images after injecting 0.44 PV of neat CO_2

The next injection will be another 0.5 PV of neat CO_2 at the same pressure, which is 2000 psi. The test was conducted and more oil was collected. An increase of 31.11% of the original oil in core sample was recovered. The total recovery up to this level is now 59.59%. **Figure 47 and Figure 48** show the results after the injection of 0.98 PV of neat CO_2 with good sweep being observed at the inlet portion of the core sample. The fracture and the areas around the fracture dominate the flow of the CO_2, especially at the outlet portion. As a result, the sweep efficiency can be evaluated as being moderate to low.

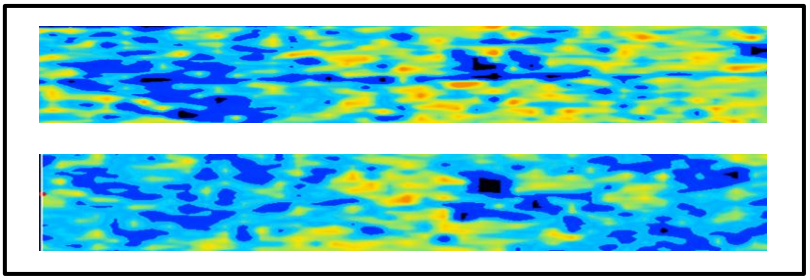

Figure 47. Test 4 rock sample after injecting 0.98 PV of neat CO_2

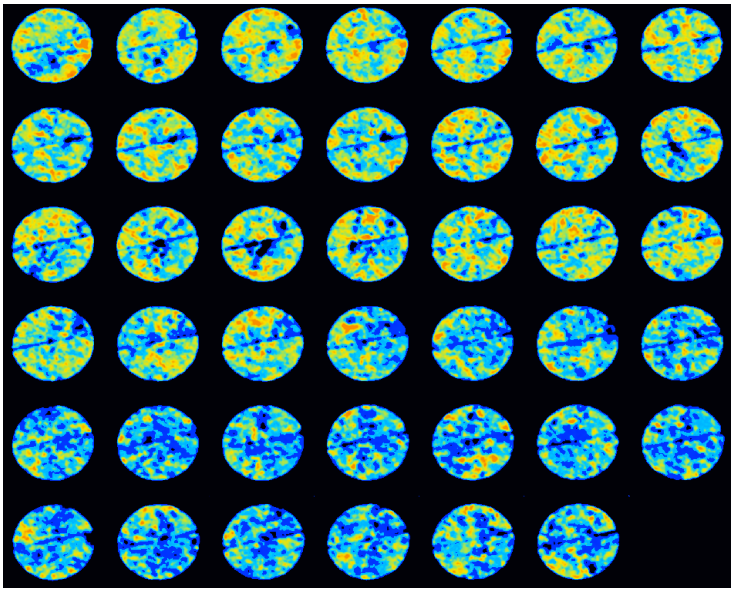

Figure 48. Test 4 vertical slice images after injecting 0.98 PV of neat CO_2

After the first and second injection, roughly 40% of the original oil in the core still needs to be recovered. More CO_2 is needed to recover the remaining oil. Another 1.02 PV was injected at the planned pressure. Throughout this stage, more oil was produced. The total oil recovery after this injection reached 68.72%, which is a 9.13% increase after the second injection. **Figure 49** shows better sweep efficiency of the CO_2 compared with the previous injection. Good sweep can be seen at the inlet section, but at the middle and outlet portions of the core sample, quite a lot of oil remains to be untouched. **Figure 49** gives an indication that most of the oil in the core sample has been recovered. This is not correct because the image shown in **Figure 49** represents the average CT number of each slice and it does not show more details about how much oil has been produced and where the CO_2 is concentrated in each slice. However, the vertical slice images in **Figure 50** give more details about the sweep efficiency in each slice after 2 PV were injected and where the CO_2 is concentrated. From **Figure 50**, it can be seen clearly how the CO_2 pushed most of the oil at the inlet, leaving quite a lot of the oil at the middle and outlet portions untouched. As stated previously, this result is attributed to the poor displacement and sweep efficiency of CO_2 in fractured media.

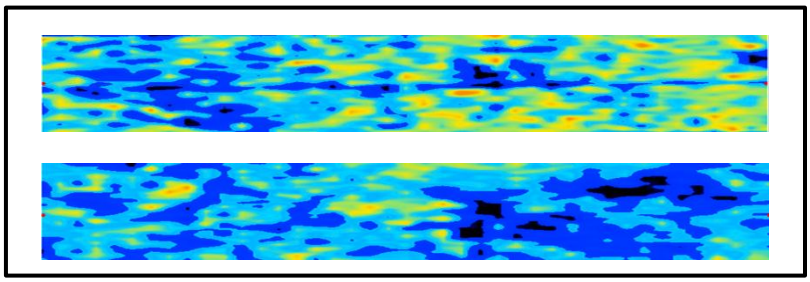

Figure 49. Test 4 rock sample after injecting 2 PV of neat CO_2

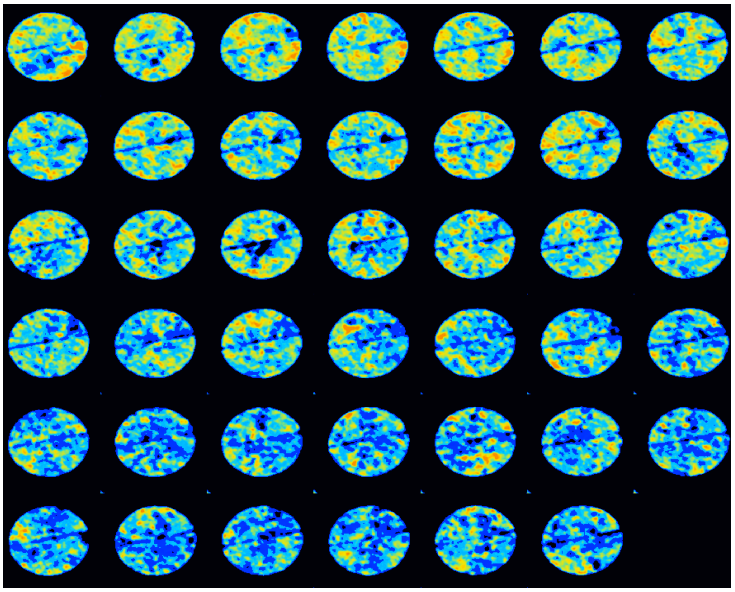

Figure 50. Test 4 vertical slice images after injecting 2 PV of neat CO_2

The results either from the oil collected or from the CT scan images show that there is still roughly 32% of the residual oil inside the core sample. According to that

result, another 0.21PV of neat CO_2 was injected to recover as much of the original oil in the core sample as possible. The result shows that there is no oil has been produced during this injection. Up to this level, a total of 2.21 PV of pure CO_2 was injected and the total oil recovery reached 68.72%. **Figure 51** shows the result of the CT scan images after the injection of a total of 2.21 PV of neat CO_2, which is very similar to that presented at 2 PV injections. There is no more progress in the overall sweep efficiency as shown in **Figures 51 and 52**. Most of the CO_2 injected is flowing inside the fracture and the area around the fracture, which leads to a very poor sweep efficiency and low oil recovery. One thing can be observed either from **Figure 51 or Figure 52** that there is a small portion of the inlet side showing higher CT numbers even though in the previous injection, it was not shown. This result may be attributed to the increase of density of the CO_2 at the supercritical phase which will results in a very close CT number to that of oil. **Table 13** summarizes the results of the oil recovery after each injection.

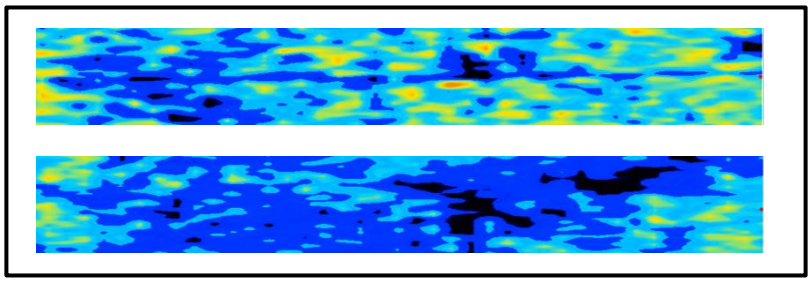

Figure 51. Test 4 rock sample after injecting 2.21 PV of neat CO_2

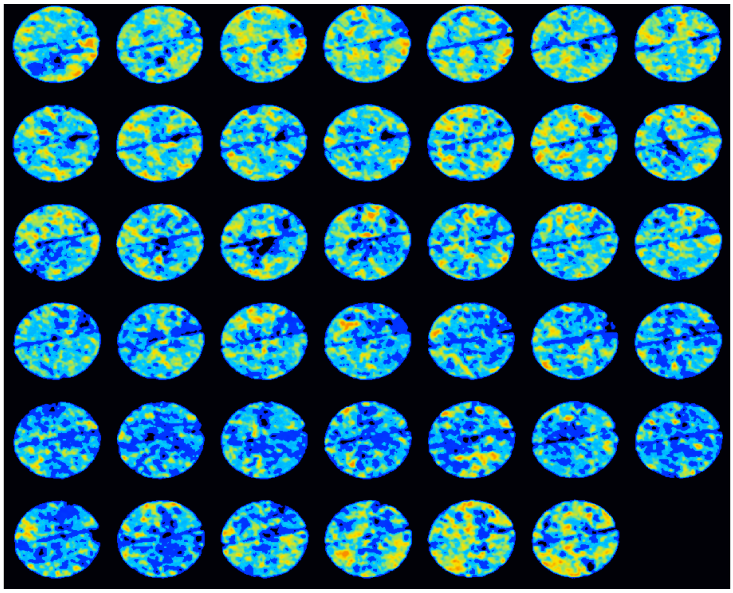

Figure 52. Test 4 vertical slice images after injecting 2.21 PV of neat CO_2

Table 13. Test 4 oil recovery after injecting neat CO_2

PV Injected	Oil Recovery %	Cumulative Oil Recovery%
0.44	28.48	28.48
0.98	31.11	59.59
2	9.13	68.72
2.21	0	68.72
Total Oil Recovery	**68.72**	

The final results of this test show that after injection of 2.21 PV of neat CO_2 at a pressure of 2000 psi and 130°F, which is above the MMP of oil, and at the supercritical phase of CO_2, the recovery factor is 68.72%. Also, the sweep efficiency according to the CT images is considered to be moderate to poor. **Figure 53** shows how the average CT number across the core sample changes during each injection of neat CO_2. As shown after 2.21 PV injection of CO_2, the average CT number is still greater than the CO_2 CT number. Also, the average CT number at the last injection, 2.21 PV, shows higher values at the inlet compared with the same location at the previous injection, 2PV.

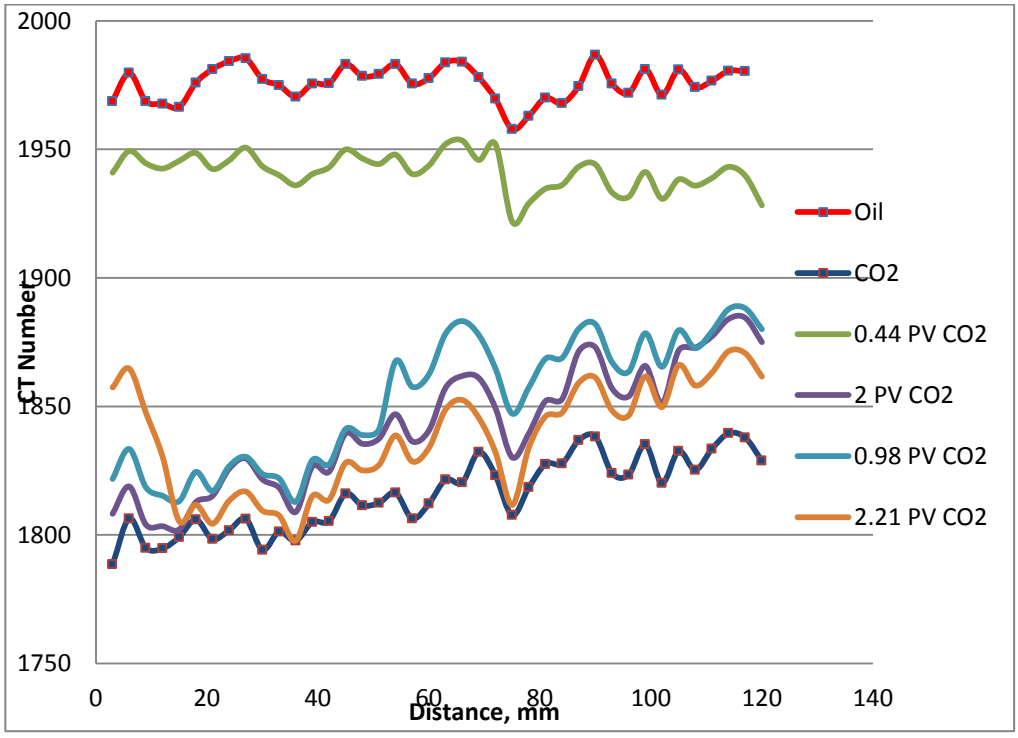

Figure 53. Test 4 average CT number across the sample during neat CO_2 injection

The test with the neat CO_2 is completed with a total recovery of 68.72%. Another test is to show how the viscosified CO_2 will improve the sweep efficiency and enhance the oil recovery when the test is conducted above the MMP of CO_2 and at the supercritical phase. The PDMS polymer was mixed with CO_2 to increase the viscosity of the CO_2 and the same steps used with the neat CO_2 test are applied here. To ensure that the core is fully saturated with oil, 10 PV of oil were injected into the core sample and kept for half a day at a pressure of 1600 psi. The same pore volume injected with the pure CO_2 test will be injected using viscosified CO_2.

In this test, the first injection was 0.43 PV of viscosified CO_2. **Figure 54** shows the sweep efficiency of oil and CO_2 after 0.43PV of viscosified CO_2 has been injected. Based on the CT images shown in **Figure 54** and compared with 0.44 PV injected using neat CO_2, better sweep efficiency has been developed and observed when 0.43 PV of viscosified CO_2 was injected. Also, compared with the 0.44 PV injection of neat CO_2, viscosified CO_2 flows in larger areas and covers more volume of oil. The increase in the CO_2 viscosity and therefore the reduction in its mobility help develop better sweep efficiency than that with the neat CO_2 injection. The vertical slice images in **Figure 55** also support this behavior. Even though the fracture and the areas around the fracture dominate the flow, viscosified CO_2 has better sweep efficiency than neat CO_2. The oil recovery after this injection is about 33.71%. The random sweep of CO_2 can give an indication about the degree of heterogeneity present in the rock sample used in this test.

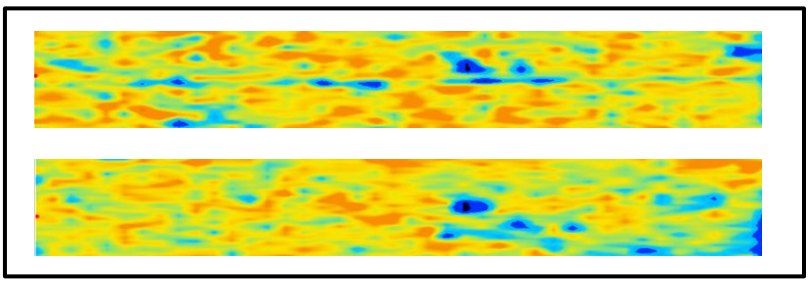

Figure 54. Test 4 rock sample after injecting 0.43 PV of viscosified CO_2

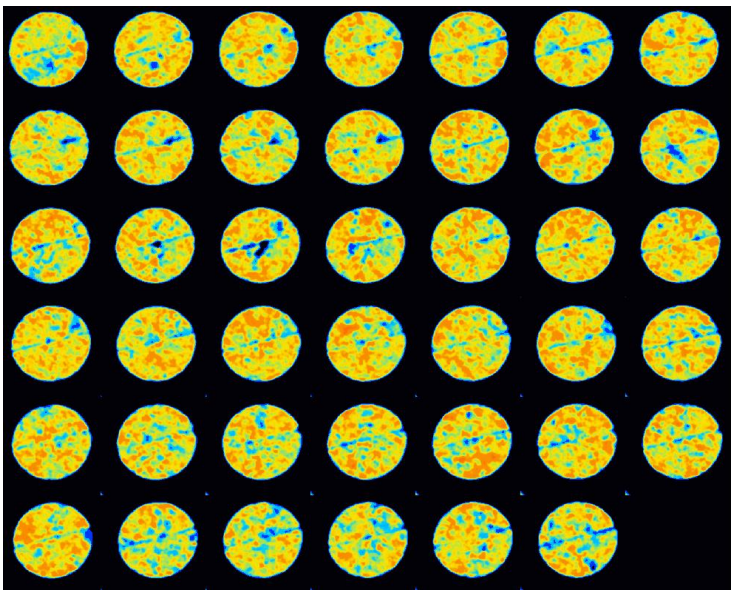

Figure 55. Test 4 vertical slice images after injecting 0.43 PV of viscosified CO_2

The residual oil saturation up to this level is approximately 67%. The next step will be to inject 0.56 PV of viscosified CO_2. The results showed that an additional 32.12% of the original oil in the rock sample has been produced. The total oil recovery after this injection reached 65.83%. **Figure 56** shows the CT scan images of the viscosified CO_2 flood after 0.99 PV was injected. Compared with 0.43 PV injected in the previous step, there is a significant improvement in the sweep efficiency of CO_2. Also, **Figure 57** shows the slice images of the core after this injection. Both **Figure 56 and Figure 57** show that most of the oil at the inlet has been produced. Due to gravity segregation effect, significant sweep efficiency has been achieved in the lower portion of the core sample as shown in **Figure 57**. Compared with the images shown in the neat CO_2 injection test at the 0.98 PV, the images shown in this test show better CO_2 sweep efficiency occurs across the rock sample.

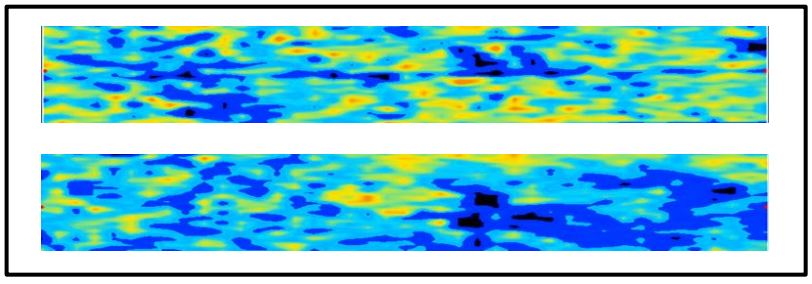

Figure 56. Test 4 rock sample after injecting 0.99 PV of viscosified CO_2

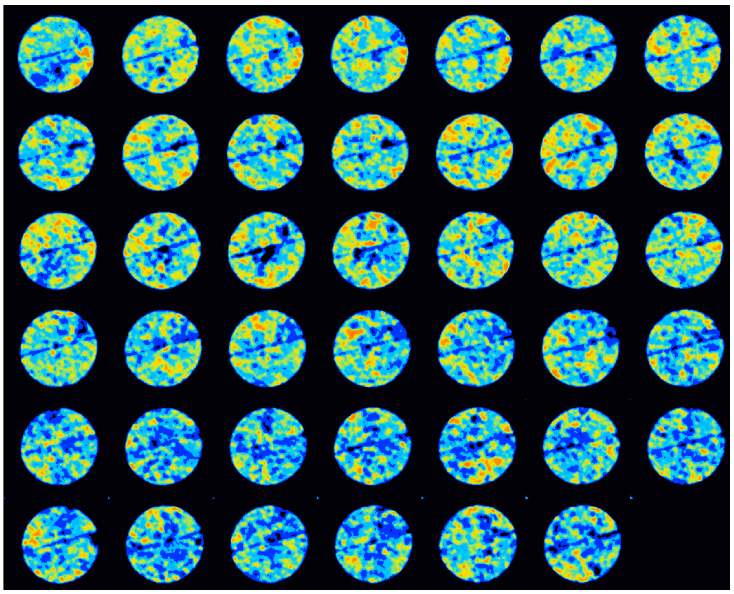

Figure 57. Test 4 vertical slice images after injecting 0.99 PV of viscosified CO_2

There might be a possibility for producing more oil by injecting more of the viscosified CO_2. Therefore, an additional 1.01 PV was injected into the core sample, which has about 35% of the residual oil saturation. The result showed that about 10.14% of the oil was recovered, which makes the total oil recovery up to this level approximately 75.97%. The sweep efficiency of oil and viscosified CO_2 are shown in **Figure 58**. The figure shows that there is a significant improvement in sweep efficiency of the overall flood of CO_2 compared with the previous injection. Also, it can be seen clearly from **Figure 59** that most of the oil in the core sample has been recovered. The vertical slice images in **Figure 59** also show that most of the oil in the each slice has

been recovered with only very small portion of the core that has not yet been produced. However, the result presented here is much better than that presented in the neat CO_2 injection. The same behavior was observed with the previous injection where the CT number increases with this injection. The first slices presented in **Figure 59** show higher CT numbers than the previous injection procedure and this can be explained by the high density of the viscosified CO_2, which seems to be very close to that of the oil used in this study. As a result, the CT will give a higher number.

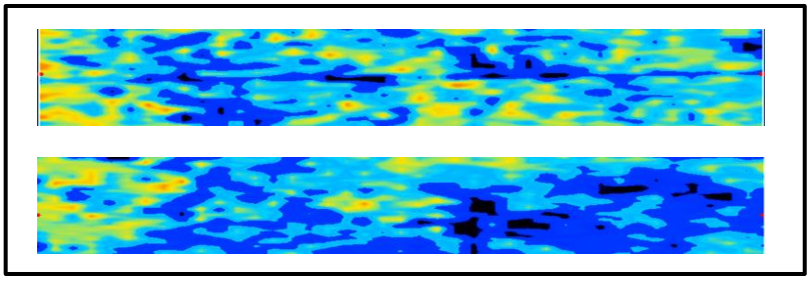

Figure 58. Test 4 rock sample after injecting 2 PV of viscosified CO_2

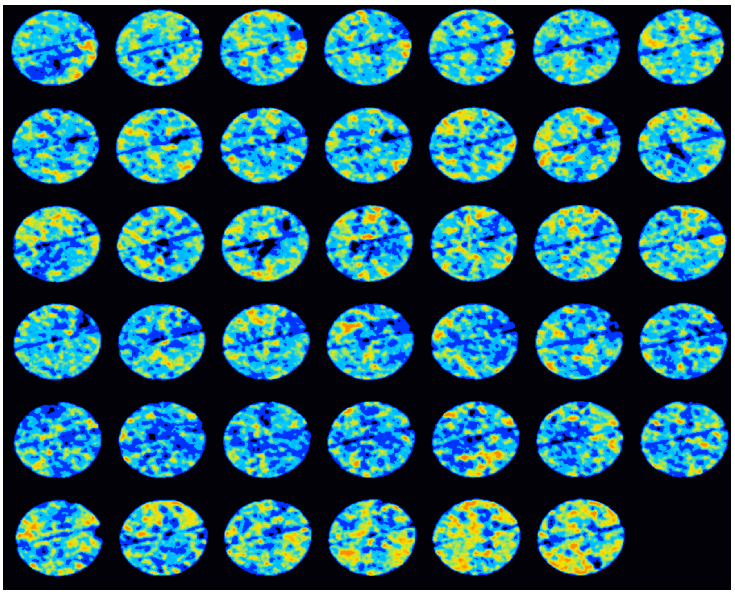

Figure 59. Test 4 vertical slice images after injecting 2 PV of viscosified CO_2

There is still roughly 25% of the OOIP that has not been recovered. To make a good comparison with the neat CO_2 injection and to achieve the maximum oil recovery, an additional 0.33 PV of viscosified CO_2 was injected. As is shown in **Figure 60**, most of the oil has been produced. Very few strikes can be shown in the same figure, indicating the presence of the oil in the sample. Also, **Figure 61** presents the vertical slice images that show the ability of the viscosified CO_2 to produce most of the oil and improve the sweep efficiency. The oil recovery from this injection was found to be 1.65% and the total oil recovery after 2.33 PV injection of viscosified CO_2 was 77.62%. It appears that there are some difficulties in determining whether the high CT number shown with the viscosified CO_2 is due to the poor sweep efficiency and therefore the

presence of oil or is caused by the high density of the new mixture of viscosifier and CO_2. This result is possibly caused by the density increase of the viscosified CO_2. The higher recovery achieved with the viscosified CO_2 compared with that of the neat CO_2 can prove this finding. **Table 14** summarizes the oil recovery at each injection step.

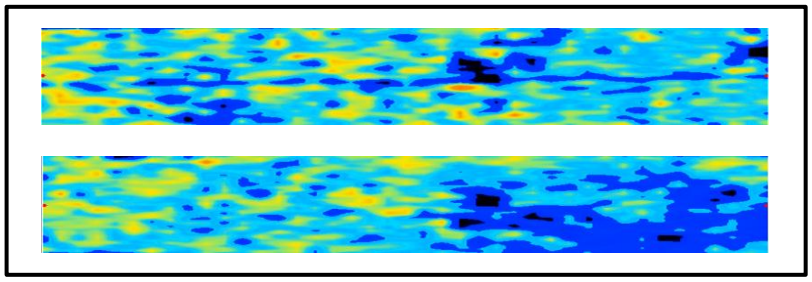

Figure 60. Test 4 rock sample after injecting 2.33 PV of viscosified CO_2

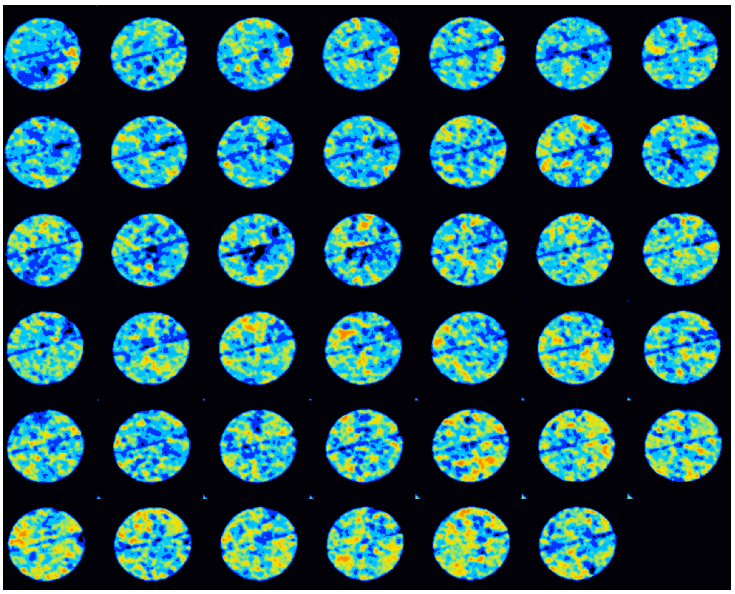

Figure 61. Test 4 vertical slice images after injecting 2.33 PV of viscosified CO_2

Table 14. Test 4 oil recovery after injecting viscosified CO_2

PV Injected	Oil Recovery %	Cumulative Oil Recovery %
0.43	33.71	33.71
0.99	32.12	65.83
2	10.14	75.97
2.33	1.65	77.62
Total Oil Recovery	**77.62**	

The final result of this test shows that after a 2.33 PV injection of viscosified CO_2 at a pressure of 2000 psi and 130^{o}F, which is above the MMP of oil and at the supercritical phase of CO_2, the recovery factor was 77.62%. The oil recovery from both neat and viscosified CO_2 are shown in **Figure 62**. Also, the sweep efficiency according to the CT images is considered to be good comparison with that presented for the neat CO_2 injection. **Figure 63** shows how the average CT number across the core sample changes during each injection of viscosified CO_2. The high CT number shown with the 2- and 2.33-PV injection of viscosified CO_2 has been discussed previously. The results shown in **Figure 63** are only for comparison purposes.

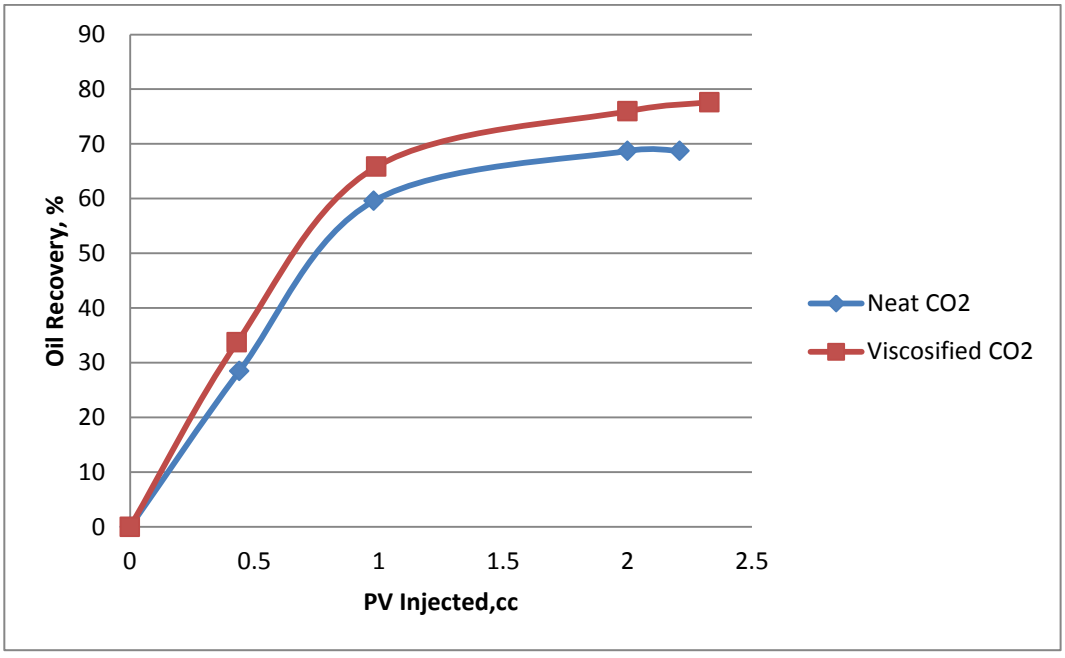

Figure 62. Test 4 oil recovery from neat and viscosified CO_2

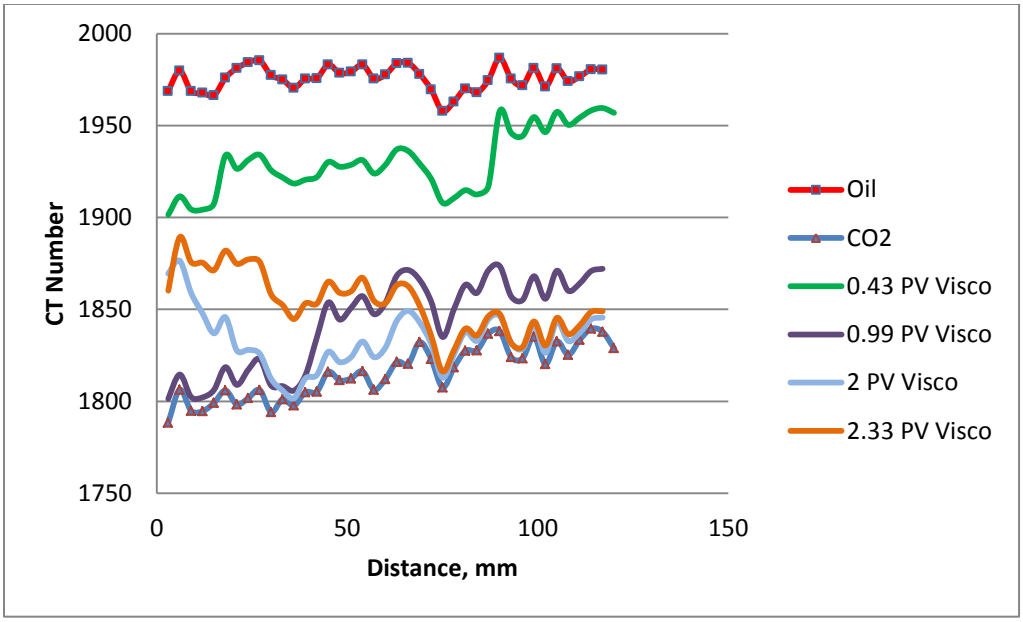

Figure 63. Test 4 average CT number during viscosified CO_2 injection

Overall, the viscosified CO_2 shows better sweep efficiency than neat CO_2. As is shown in **Figure 64**, the average CT number after each injection of viscosified CO_2 shows improvement in the CO_2 flood compared with that of neat CO_2. The lower the CT numbers, the better the sweep efficiency achieved during that injection. Also, **Figure 65** presents the saturation of the CO_2 across the core sample. Higher CO_2 saturation can be seen with the viscosified CO_2 compared with the pure CO_2 at each injection volume. The high CT number may indicate the presence of the oil in the rock sample and therefore affect the CO_2 saturation calculation that has already been explained and clarified previously.

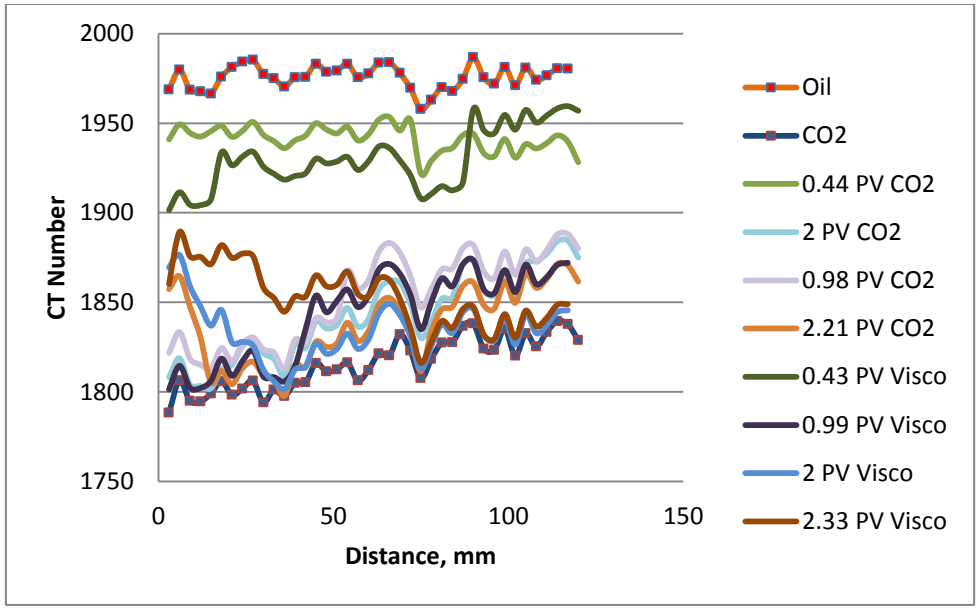

Figure 64. Test 4 average CT number across the rock sample

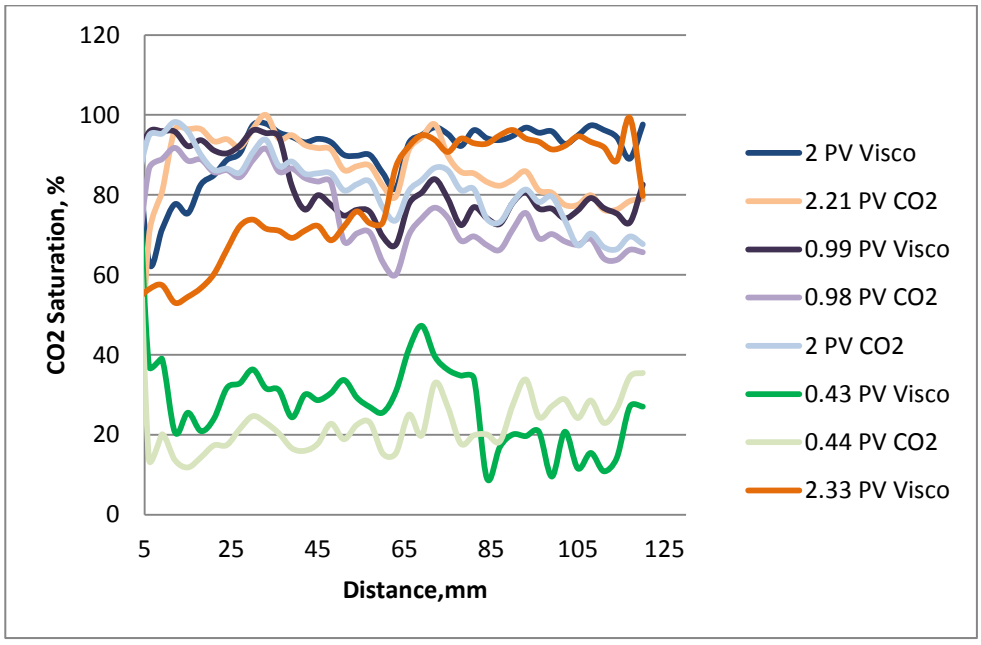

Figure 65. Test 4 CO_2 saturation across the rock sample

4.5 Test 5: Injection of CO_2 and Viscosified CO_2 (PVEE) (1)

High-permeability fractured Indiana limestone with 18.04% porosity was used in this test. The objective of this test was to evaluate the ability of the viscosified CO_2 using PVEE to increase the CO_2 viscosity, reduce its mobility, and therefore improve the sweep efficiency and enhance the oil recovery in a fractured reservoir. The scale of the CT number used for this test is shown in **Figure 66**. As stated previously, the red color represents the high CT number, which indicates the oil in this study, and the blue represents the low CT number, which designates the CO_2 phase. In each run, there are two images; one shows the vertical cross section (the upper one) and the other shows the horizontal cross section (the lower one).

Figure 66. Test 5 CT number scale

To simplify the comparison between CO_2 and oil and investigate sweep efficiency, images of both CO_2 and oil have been taken when both fluids were 100% saturated in the sample. **Figure 67** shows the sample when it is 100% saturated with

CO_2. The vertical slice images for the sample when it is 100% saturated with CO_2 are shown in **Figure 68**. The figure shows the fracture plane having very low CT number compared with the other portion of the rock matrix that results from the low density across the fracture plane.

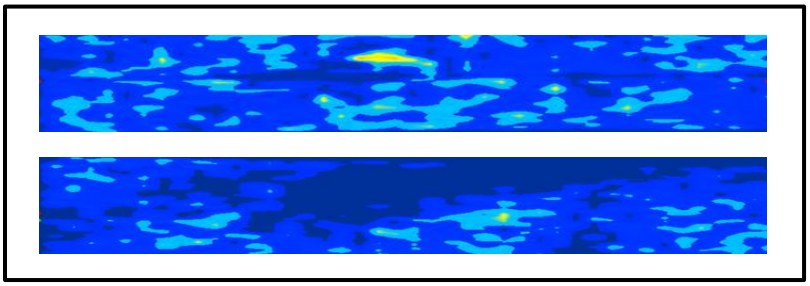

Figure 67.Test 5 rock sample when it is 100% saturated with CO_2

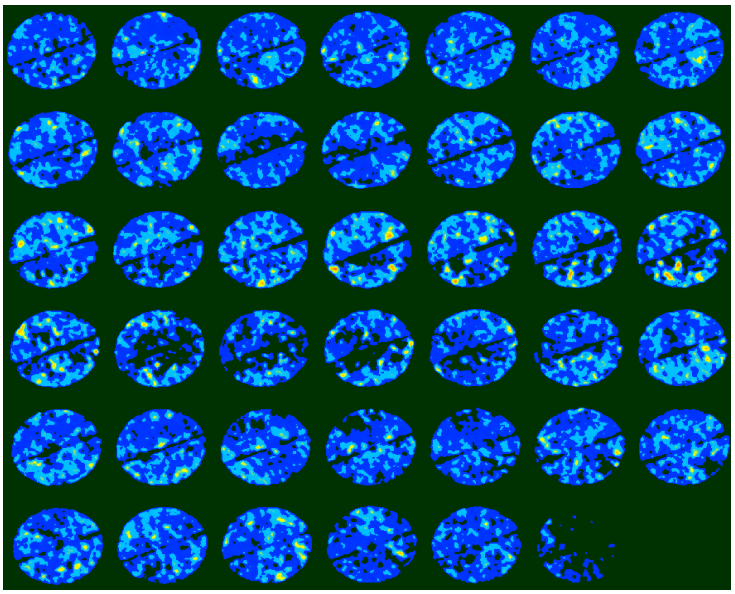

Figure 68. Test 5 vertical slice images the sample is 100% saturated with CO_2

Refined oil was then injected into the sample at a rate of 2cc/min. The sample was held at 1600-psi pressure for a considerable time to make certain that the sample was fully saturated with the refined oil. Also, to improve the measurement accuracy, 10 PV of refined oil was injected into the sample. The pressure drop across the core sample was found to be roughly 5 psi. **Figure 69** shows the sample when it is 100% saturated with oil. There are some portions of the rock sample where the blue color appears even though the sample is 100% saturated with oil. This condition can be explained by the low density caused by the larger pores that exist in the rock sample. Such behavior may give an indication of how heterogeneous is the rock sample used in this test. The vertical

slice images for the sample when it is 100% saturated with CO_2 are shown in **Figure 70**. The slices showing the low CT number behavior are highlighted.

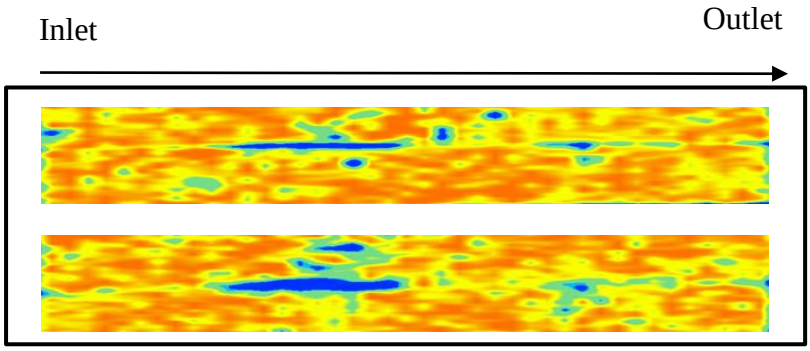

Figure 69. Test 5 rock sample when it is 100% saturated with oil

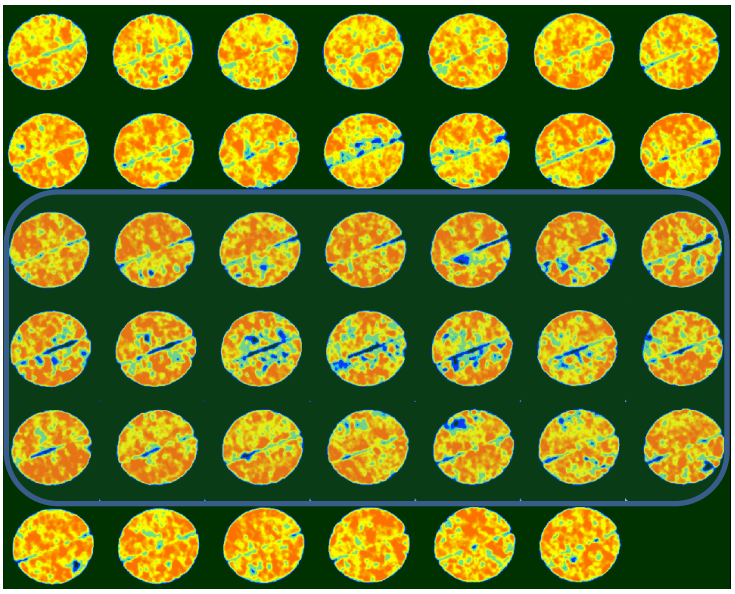

Figure 70. Test 5 vertical slice images when the sample is 100% saturated with oil

As with the previous tests, two runs were conducted to assess the ability of the viscosifiere to enhance the oil recovery and improve the sweep efficiency. The first run was conducted using the neat CO_2 and the second run will be conducted using the PVEE polymer with CO_2. The injection of CO_2, as mentioned in the procedure of this study, was conducted at 2000 psi and at the rate of (2.5 to 3cc/min). Three PVs of neat CO_2 will be injected; 0.5, 1, 2, and 3. At each injection, the produced oil will be collected and static images of the rock sample will be taken using CT scans to investigate the sweep efficiency.

The first injection of neat CO_2 was conducted at 0.48 PV. As shown in **Figure 71**, CO_2 flows through the fracture plane, leaving most of the oil in the rock matrix untouched. Only a small portion of the rock matrix was touched by the CO_2. This behavior can be seen clearly in **Figure 72** where each slice shows a low CT number in the fracture portion of the rock and a higher CT number outside the fracture region, even at the inlet side. This result is attributed to the poor sweep efficiency of the CO_2 in such heterogeneous media. The oil recovery after injecting 0.48PV of neat CO_2 is 27.01%. Also, the CO_2 breakthrough was observed after this injection.

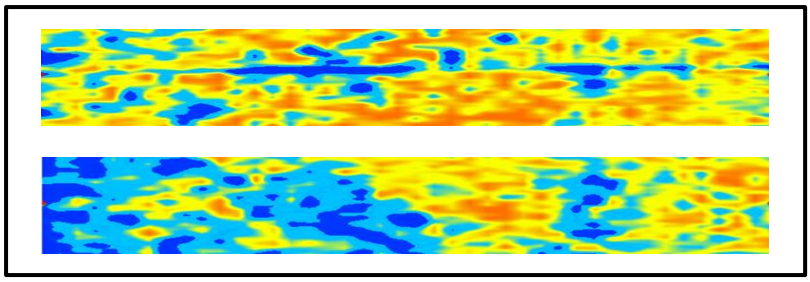

Figure 71. Test 5 rock sample after injecting 0.48 PV of neat CO_2

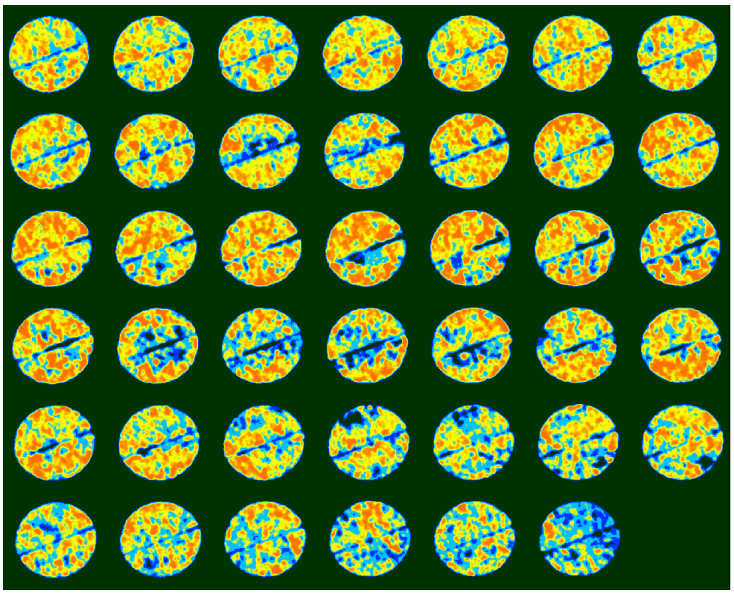

Figure 72. Test 5 vertical slice images after injecting 0.48 PV of neat CO_2

Most of the oil in the rock sample had not been touched with the first 0.48 PV injected. The next step called for injecting another 0.55 PV of neat CO_2 at the same

pressure, which was 2000 psi. The test was conducted and more oil was recovered. **Figure 73** shows the results after the injection of 1.03 PV of neat CO_2. At the end of this step, an increase of 24.4% of the original oil in the rock sample was achieved. The total recovery at this level reached 51.57%. Even though some oil has been produced after this injection, roughly half of the oil in the rock sample has not been produced after the 1.03 PV injections. As shown in **Figure 74**, the fracture and the areas around the fracture plane dominate the flow of the CO_2, leaving a significant amount of oil untouched in the rock matrix. As a result, the sweep efficiency can be referred to as a very poor sweep. Also, compared with the inlet and outlet side, the middle portion of the core sample shows very poor sweep efficiency. This behavior can be explained by the degree of heterogeneity existing within the rock sample.

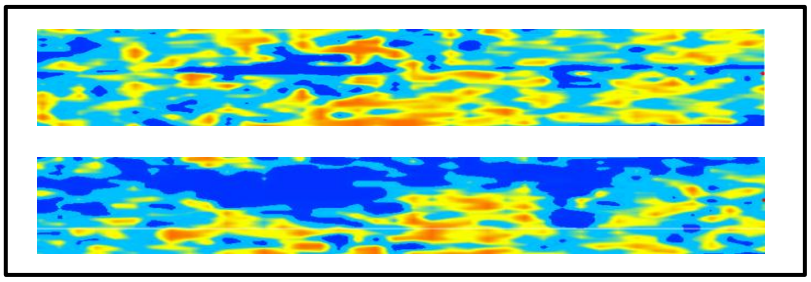

Figure 73. Test 5 rock sample after injecting 1.03 PV of neat CO_2

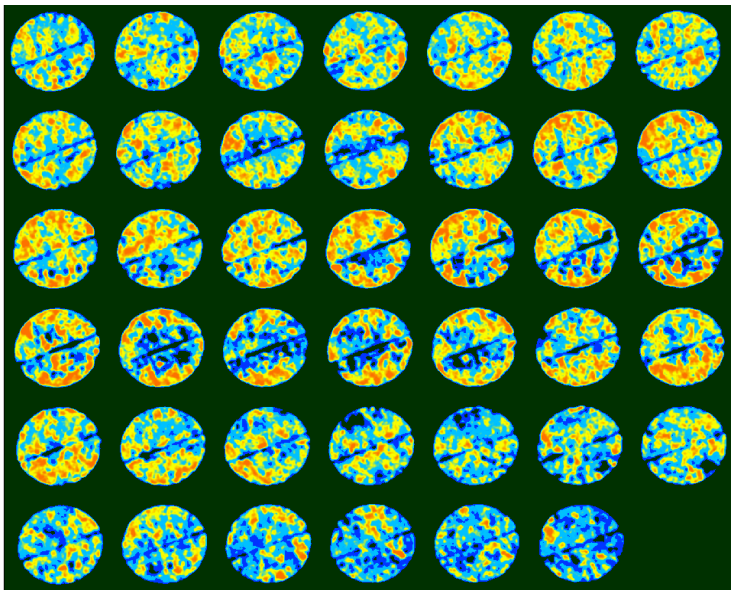

Figure 74. Test 5 vertical slice images after injecting 1.03 PV of neat CO_2

There is approximately 49% of the original oil in the rock sample that needs to be recovered, and more CO_2 is needed to recover the remaining oil. Another 1.04 PV of neat CO_2 was injected under the test conditions. The total oil recovery after this injection reached 62.96%, which is an 11.39% increase after the second injection. As shown in **Figure 75**, the slices that were highlighted previously with low CT number show very good sweep efficiency compared to the other slices. This condition can be explained based on the tendency of the CO_2 to flow through the larger pores that supposedly have higher permeability and leave the other pores with low permeability untouched. Compared with the previous injection, more oil has been produced and a better sweep was observed. Good sweep can be seen at the inlet and outlet compared with the middle

portion of the rock sample where there is quite a lot of oil untouched. The vertical slice images in **Figure 76** support this result and show how the CO_2 pushed all the oil at the inlet and outlet, leaving most of the oil in the middle portion untouched.

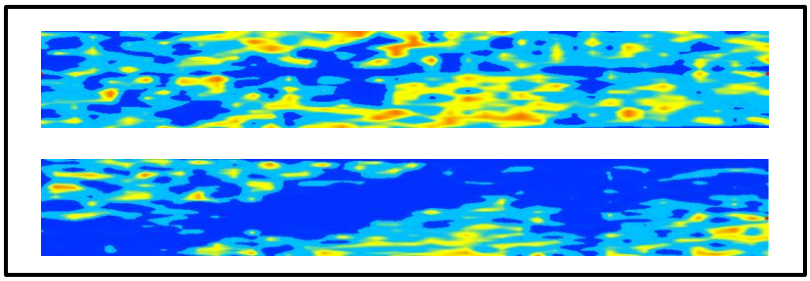

Figure 75. Test 5 rock sample after injecting 2.07 PV of neat CO_2

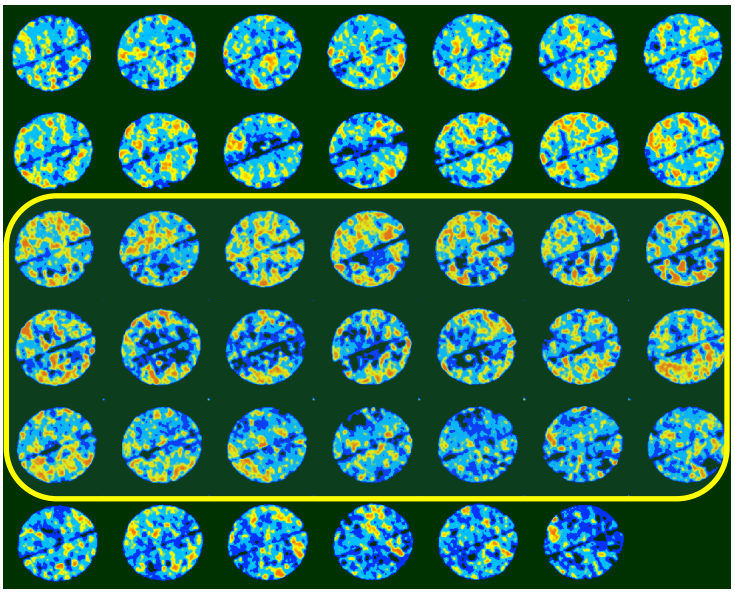

Figure 76. Test 5 vertical slice images after injecting 2.07 PV of neat CO_2

According to the results from the oil collected and the CT scan images, approximately 37% of remaining oil is still in the rock sample. Because of that, another 1.08PV of CO_2 was injected. With this injection, a total of 3.15 PV of neat CO_2 has been injected. The results showed that a very small volume of the oil has been produced, and that only 0.1% of the original oil in the core sample was recovered. As a result, the total oil recovery reached 63.06%. **Figure 77** shows the result of the CT scan images after injecting a total of 3.15 PV of neat CO_2, which is similar to that one presented at the 2.07 PV injections. There is no further progress in the overall sweep efficiency as shown in **Figure 77 and Figure 78**. Most of the CO_2 injected is flowing inside the fracture and the area around the fracture plane, which leads to a very poor sweep efficiency and low oil recovery. **Table 15** presents the results of the oil recovery after each injection.

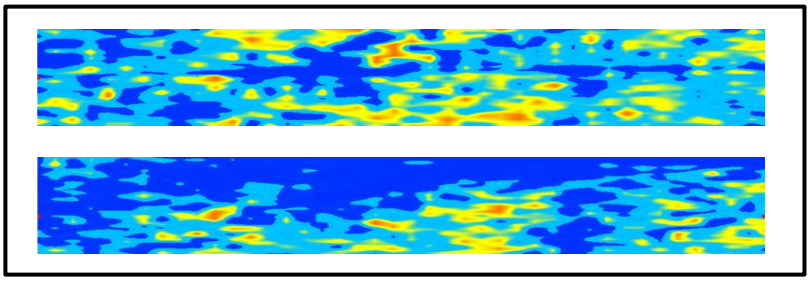

Figure 77. Test 5 rock sample after injecting 3.15 PV of neat CO_2

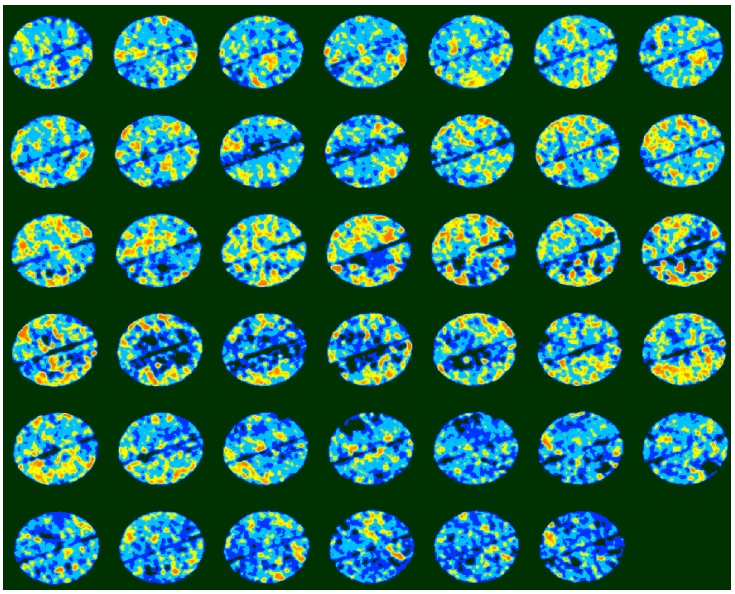

Figure 78. Test 5 vertical slice images after injecting 3.15 PV of neat CO_2

Table 15. Test 5 oil recovery after injecting neat CO_2

PV Injected	Oil Recovery %	Cumulative Oil Recovery %
0.48	27.01	27.01
1.03	24.56	51.57
2.07	11.39	62.96
3.15	0.1	63.06
Total Oil Recovery	**63.06**	

The final results of this test show that after injecting 3.15 PV of the neat CO_2 at a pressure of 2000 psi and at 130^{o}F, which is above the MMP of oil and the supercritical phase of CO_2, the recovery factor is 63.06%. Also, the sweep efficiency according to the CT images is considered to be poor. **Figure 79** shows how the average CT number across the core sample changes during each injection of neat CO_2. As is shown in this figure, the changes in the CT number occur steadily at each injection, which is attributed to the poor sweep efficiency of the CO_2. Also, there is no difference between the third and fourth injection, 2.07 and 3.15 PV respectively, which support the results that show a very small volume produced by the last injection.

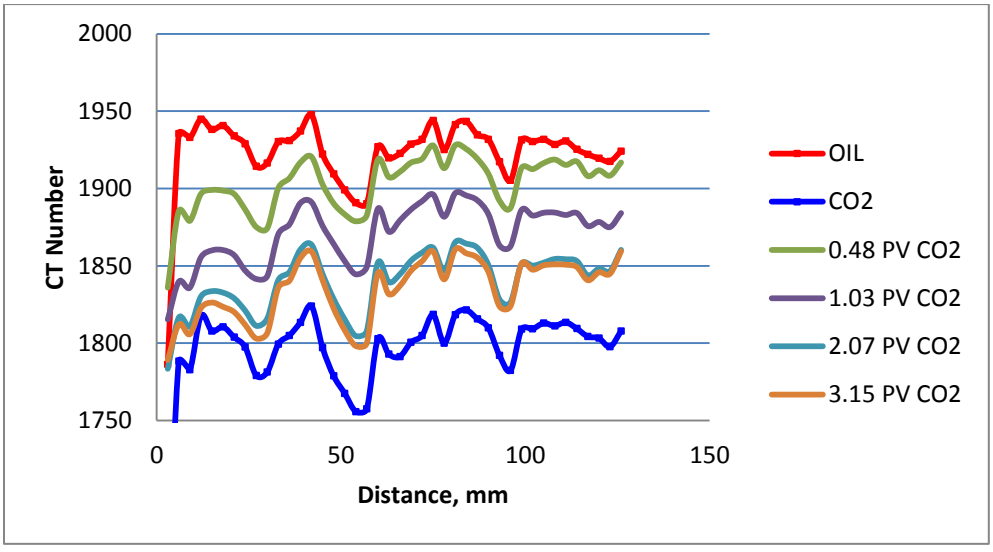

Figure 79.Test 5 average CT number during neat CO_2 injection

The results just presented show how poor sweep efficiency of CO_2 can occur when it is injected into a fractured reservoir. Better controlling of the CO_2 mobility may result in better sweep efficiency. The next step will be injection of viscosified CO_2 and observe the improvement in the oil recovery and sweep efficiency. The PVEE polymer was mixed with CO_2 to increase the viscosity of the CO_2. As described in the procedure of this test, 0.8 wt% of this polymer was added to CO_2 and pressurized to 2843 psi. The same steps followed with the neat CO_2 were applied here. To ensure that the core is fully saturated with oil, 10 PV of oil were injected into the core sample and 1600-psi pressure was maintained for a considerable length of time. The same pore volume injected with neat CO_2 was injected using viscosified CO_2. Also, the experimental conditions, 2000-psi pressure and 130^{o}F temperature, will be used once again.

Throughout this test, we will try to inject the same volume of CO_2 to make certain that we have a good base of comparison. In this test, the first injection was 0.49 PV of viscosified CO_2. **Figure 80** shows the sweep efficiency of oil and viscosified CO_2 after 0.49 PV of viscosified CO_2 was injected. Based on the CT images shown in **Figure 80** and compared with 0.48 PV injected using neat CO_2, the same oil volume was collected, but better sweep efficiency has been developed and observed when neat CO_2 was injected. One important effect worth mentioning is that no dopant was used with oil during this experiment. As mentioned earlier, the dopant plays a major role in contrasting between the oil phase and the CO_2 phase. The density of the oil used in this study is 0.76 g/cc and the density of the viscosified CO_2 is about 0.968 g/cc. Adding

dopant with oil will increase the density of the oil and therefore will enhance the CT number and result in a good contrast between the oil phase and the viscosified CO_2 phase. Because there is no dopant added with the oil, having the same recovery from both neat CO_2 and viscosified CO_2 but with different CT scan images is caused by the effect of density of both the oil phase and viscosified CO_2 phase, which are very similar in this case. In this test, we may not achieve a good contrast between the oil phase and viscosified CO_2 phase due to the reasons just mentioned. **Figure 81** shows how the viscosified CO_2 flows through the fracture plane, leaving most of the oil in rock matrix untouched. Only a small portion of the rock matrix was touched by the CO_2 but most of the regions around the fracture plane have not been touched. The same behavior was observed with the neat CO_2 after 0.48 PV had been injected. This means that even with the viscosified CO_2, there is not much difference between the neat and viscosified CO_2 in terms of enhancing the oil recovery and improving the sweep efficiency. The oil recovery after this injection was 27.01%, which is same as the produced with the neat CO_2 injection. Also, the CO_2 breakthrough was observed after this injection.

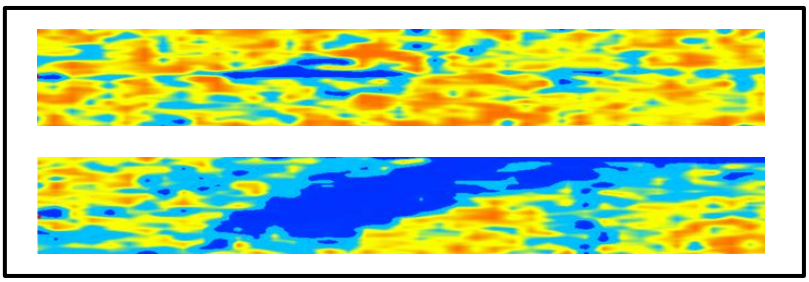

Figure 80. Test 5 rock sample after injecting 0.49 PV of viscosified CO_2

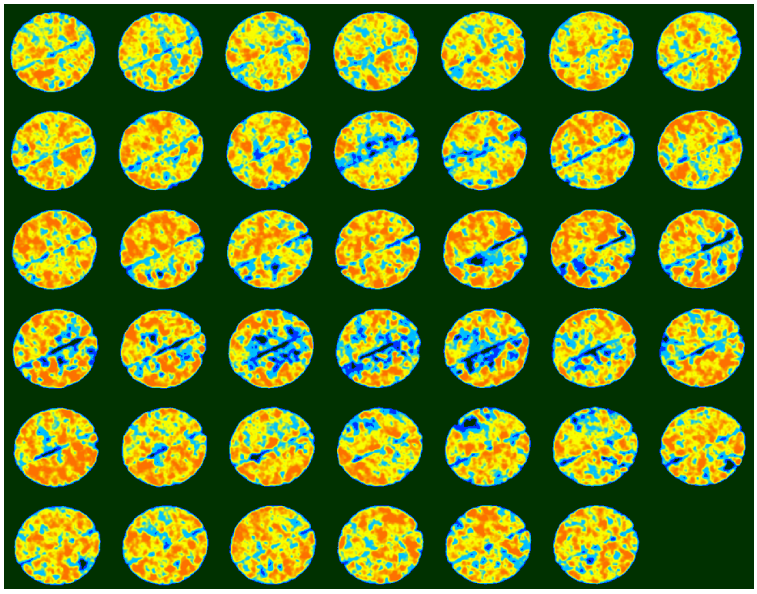

Figure 81. Test 5 vertical slice after injecting 0.49 PV of viscosified CO_2

Approximately 73% of the original oil in the rock sample has not yet been produced following the first 0.49 PV injection of the viscosified CO_2. To recover more oil, an additional 0.52 PV of viscosified CO_2 was injected. The results show that the total oil recovery after 1.01 PV injected is 51.67%, which is almost the same as that produced by the neat CO_2 after the 1.03 PV injections. **Figure 82** presents the CT scan images of the viscosified CO_2 flood after the 1.01 PV injections. Compared with the previous injection, there is a significant improvement in the sweep efficiency of CO_2. However,

compared with the 1.03 PV injection of neat CO_2, the sweep efficiency of CO_2 and oil is almost the same with a better contrast shown with the neat CO_2 injection due to the absence of the dopant in the oil phase. Up to this level and compared with neat CO_2 injection, there is no improvement in the sweep efficiency and the total oil recovery. **Figure 83** shows the slice images of the core sample after this injection. Both **Figure 82 and Figure 83** show that most of the oil at the inlet and outlet has been produced. However, most of the oil at the middle portion of the core sample has not been touched. The sweep efficiency up to this level can be rated as a poor sweep.

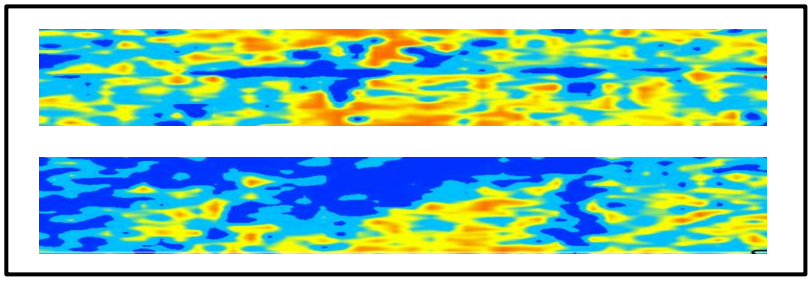

Figure 82. Test 5 rock sample after injecting 1.01 PV of viscosified CO_2

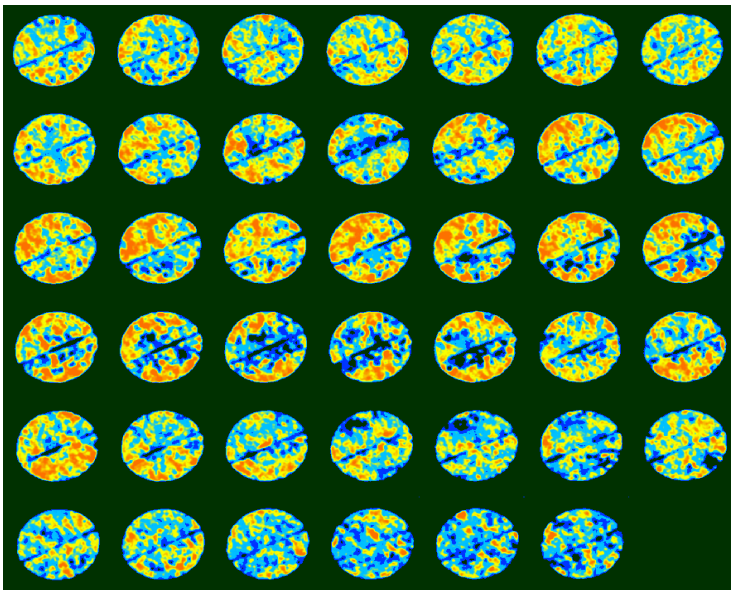

Figure 83. Test 5 vertical slice images after injecting 1.01 PV of viscosified CO_2

With the first and second injection, only half of the OOIP has been produced. This means that there is about half of the oil that has not been produced after the 1.01 PV injection of viscosified CO_2. It might be a possible to produce more oil with additional injections of the viscosified CO_2. For that reason, an additional 0.9 PV of viscosified CO_2 was injected into the core sample that has about 50% of the residual oil saturation. The result showed that about 13.17% of the oil has now been recovered, which made the total oil recovery up to this level approximately 64.84%. The sweep efficiency of oil and viscosified CO_2 are shown in **Figure 84**. The figure shows that there is a significant improvement in sweep efficiency of the overall flood of CO_2 compared with the previous injection, especially in the middle portion of the rock sample. Also, it can be seen clearly from **Figure 85** that most of the oil in the core sample has been recovered.

The vertical slice images in **Figure 85** show that most of the oil in each slice has been recovered; only some portions of the core sample have not yet been produced. Because the same rock sample used with the neat CO_2 injection is also being used in this test, the same behavior was observed in which there are some portions of the rock sample showing lower CT number values than other portions. As explained previously, this condition is caused by the large pore sizes available in these regions compared with the other regions. As a result, the permeability in these large pore sizes regions is expected to be high. The regions where the high permeability is expected are highlighted in **Figure 85**. One point that supports the finding is that the contrast between the oil phase and the viscosified CO_2 phase is not ideal can be proven in this section. If we compare the sweep efficiency of the neat CO_2 after 2.07 PV injection with the 1.91 PV injection of viscosified CO_2, the former shows better sweep efficiency. However, the oil recovery of the viscosified CO_2 is higher than that of neat CO_2 even with less pore volume injected of viscosified CO_2. This result means that the sweep efficiency image presented in the viscosified CO_2 case does not represent the actual sweep efficiency.

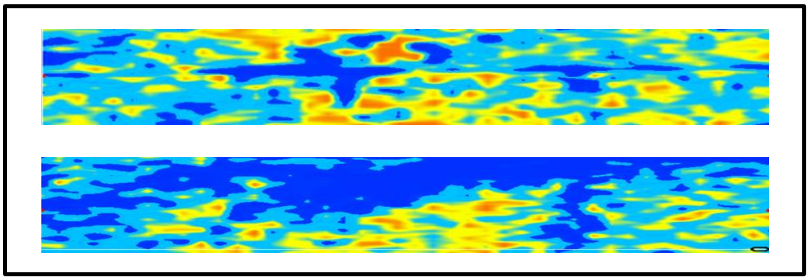

Figure 84. Test 5 rock sample after injecting 1.91 PV of viscosified CO_2

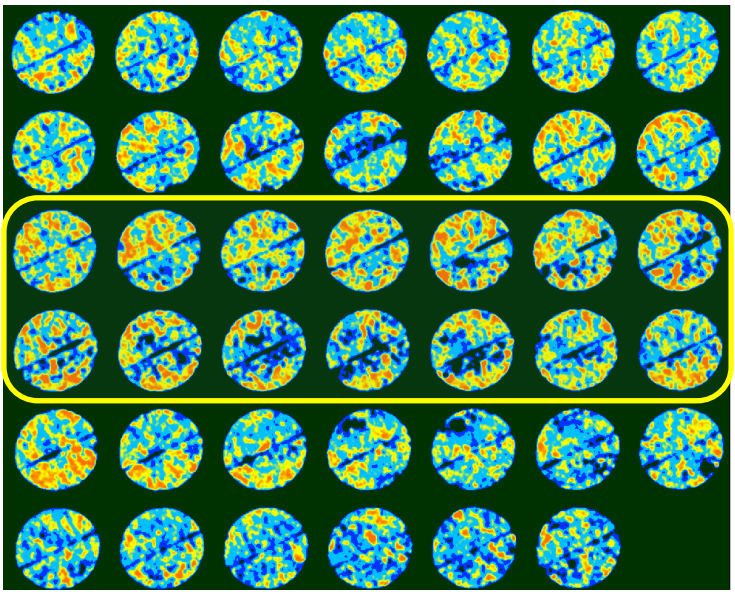

Figure 85. Test 5 vertical slice images after injecting 1.91 PV of viscosified CO_2

At this point, approximately 35% of the OOIP has not been recovered. To make a good comparison with the neat CO_2 injection, an additional 0.91 PV of viscosified CO_2 was injected. As shown in **Figure 86**, most of the oil has been produced, and most of the oil that has not been produced is concentrated in the middle portion of the rock sample. The heterogeneity of the rock sample plays an important factor in the overall sweep efficiency process. Also, **Figure 87** shows the vertical slice images, which shows the ability of the viscosified CO_2 to produce most of the oil and improve the sweep efficiency except for the portion where the high heterogeneity exists. The experimental

result showed that about 5.75% of the original oil in core was produced after this injection. With that in mind, the total oil recovery after the injection of 2.82 PV of viscosified CO_2 is now 70.59%. **Table 16** summarizes the oil recovery at each injection step.

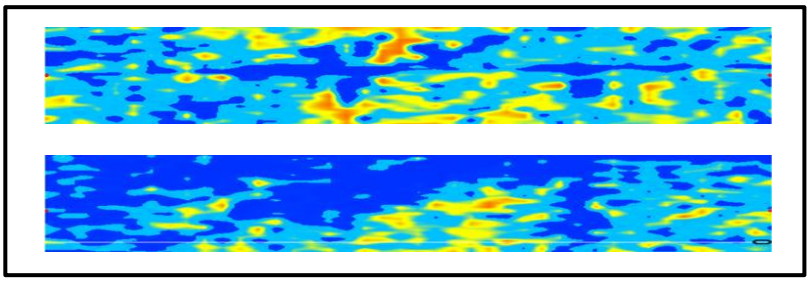

Figure 86. Test 5 rock sample after injecting 2.82 PV of viscosified CO_2

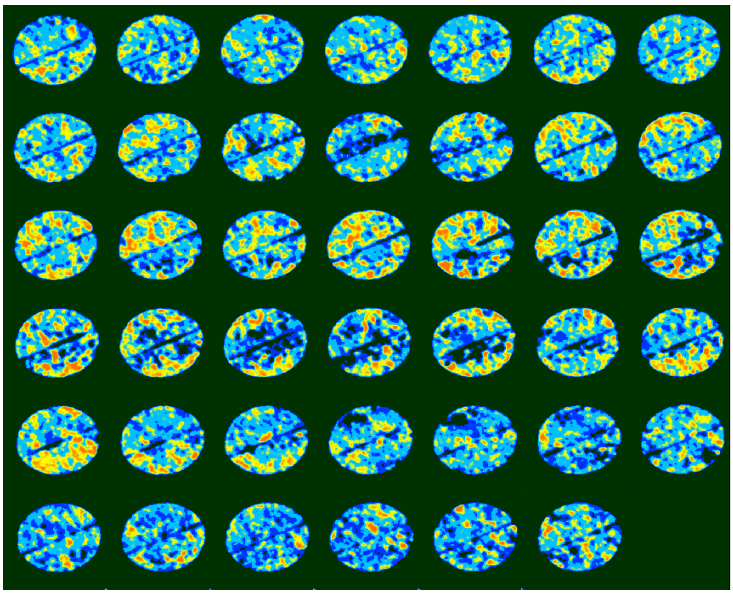

Figure 87. Test 5 vertical slice images after injecting 2.82 PV of viscosified CO_2

Table 16. Test 5 oil recovery after injecting viscosified CO_2

PV Injected	Oil Recovery %	Cumulative Oil Recovery %
0.49	27.01	27.01
1.01	24.66	51.67
1.91	13.17	64.84
2.82	5.75	70.59
Total Oil Recovery	**70.59**	

The final result of this test shows that after injecting 2.82 PV of viscosified CO_2 at a pressure of 2000 psi and 130°F, which is above the MMP of oil and at the supercritical phase of CO_2, the recovery factor is 70.59%. The oil recovery from both neat and viscosified CO_2 shown in **Figure 88**. **Figure 89** indicate how the average CT number across the core sample changes during each injection of viscosified CO_2. According to the results presented in **Figure 89** and based on the CT number contrast, it will be difficult to compare the CT number in both neat CO_2 and viscosified CO_2 and make a final conclusion based on the numbers. The oil recovery results presented in **Figure 88** may support the conclusion that the viscosified CO_2 should show better sweep efficiency than that presented with neat CO_2.

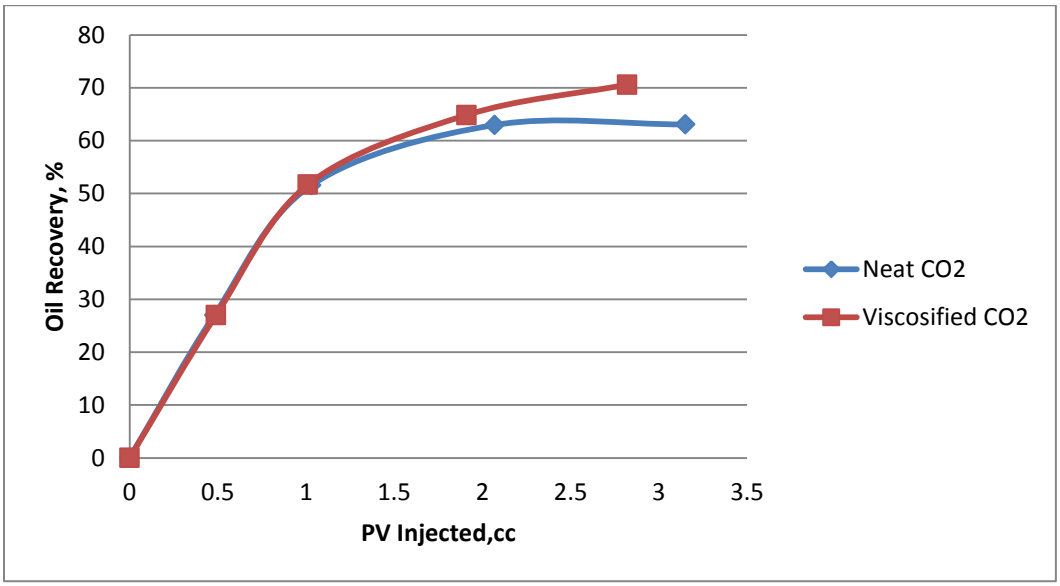

Figure 88. Test 5 oil recovery for neat and viscosified CO_2

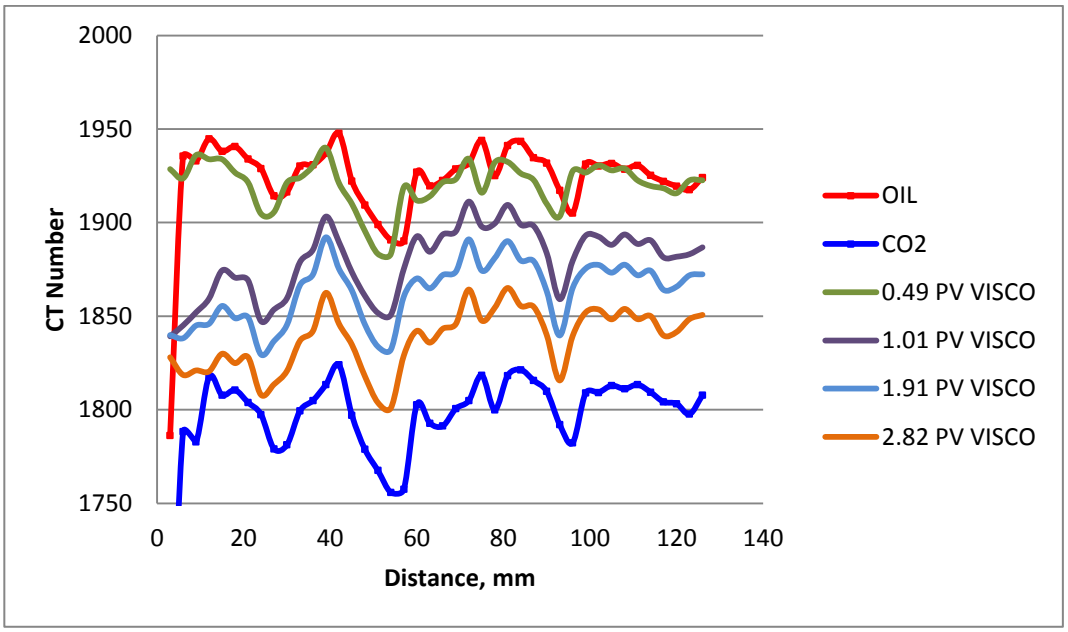

Figure 89. Test 5 average CT number during viscosified CO_2 injection

Overall, the viscosified CO_2 shows higher oil recovery than neat CO_2 injection. Again, it will be difficult to make a conclusion based on the average CT numbers of both neat and viscosified CO_2, which are shown in **Figure 90**. **Figure 91** presents the saturation of the CO_2 across the core sample. The highest CO_2 saturation can be seen at 3.15 PV injection of neat CO_2. This conclusion is not correct though because the calculation of the saturation is based on the average CT numbers, which do not reflect the correct average CT numbers in the viscosified CO_2 case.

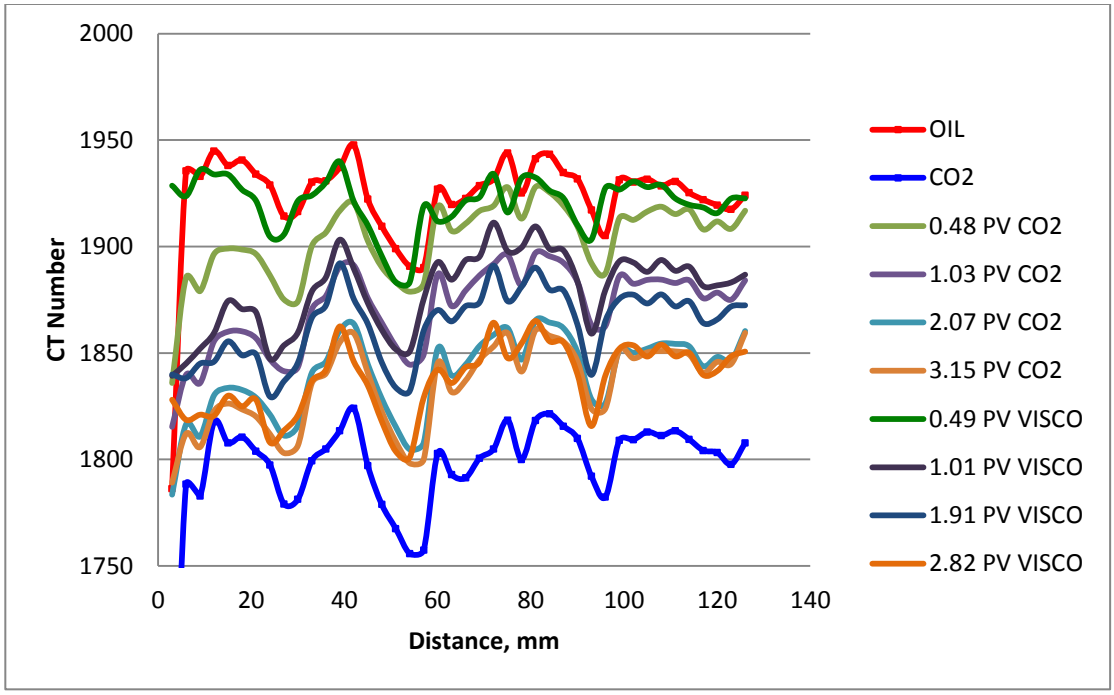

Figure 90. Test 5 average CT number across the sample

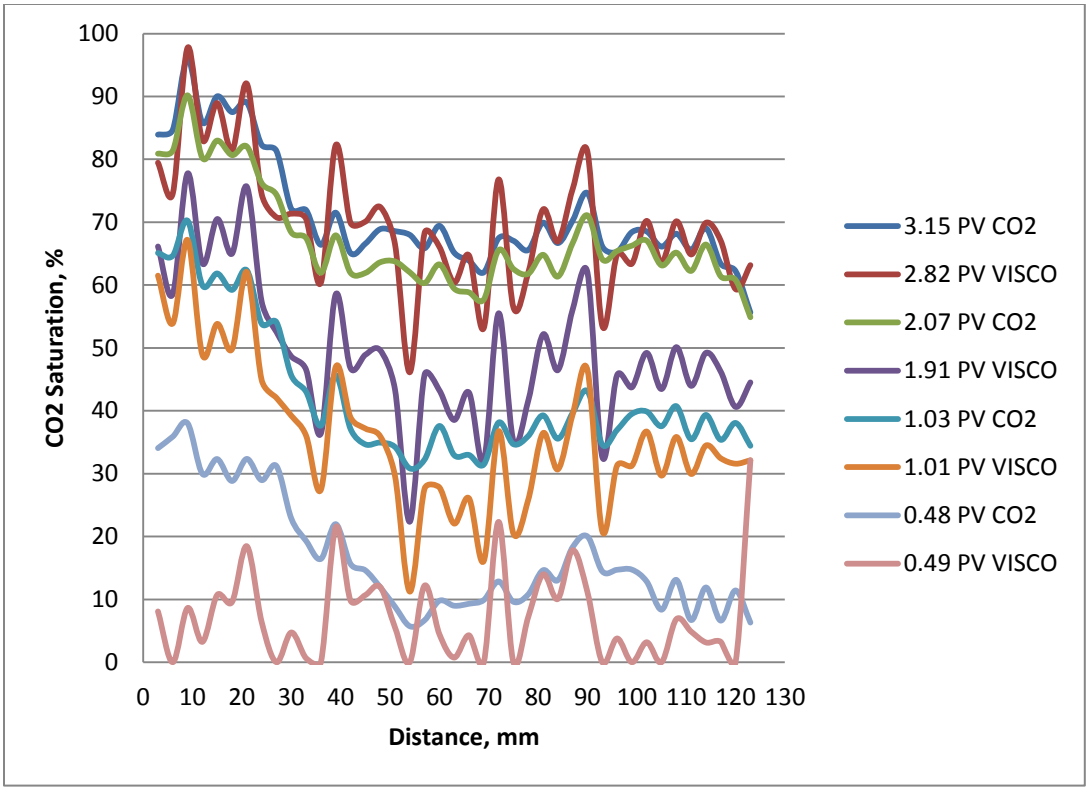

Figure 91. Test 5 CO_2 saturation across the core sample

4.6 Test 6: Injection of CO_2 and Viscosified CO_2 (PVEE) (2)

High-permeability Indiana limestone with 17.47% porosity and 12.9 cc PV was 100% saturated with refined oil (Soltrol 130 Isoparaffin). The refined oil was injected into the sample at a rate of 2cc/min., and the pressure drop across the core sample was found to be 7 psi.

The objective of this test is to evaluate the ability of the viscosified CO_2 with PVEE to improve the oil recovery compared with that produced by the neat CO_2 at a pressure above the MMP and at the supercritical phase of CO_2. The difference between this test and the previous test is that this test is conducted at an injection rate of 2.5 to 2.6 cc/min. First, we will inject the neat CO_2 and then the viscosified CO_2 using PVEE. The injection of CO_2, as mentioned in the procedure for this study, will be conducted at 2000 psi, which is above the MMP of the oil used in this study. Three PVs of neat CO_2 will be injected; 0.5, 1, 2, and 3. At each injection, the produced oil will be collected and the CO_2 breakthrough will be observed to investigate for any improvement of oil recovery and sweep efficiency.

Due to the close value of pressure drop presented in test 1 of both neat CO_2 and viscosified CO_2 with PVEE, this test must be run carefully and precisely. If there is an improvement in the overall oil recovery of both neat and viscosified CO_2, it will be very small, especially because the core sample that was used in this test is very small (1-in. diameter and 5 in. in length). It is clear that the fracture dominates the flow of the CO_2 inside the core sample. This behavior of CO_2 early breakthrough is attributed to the high mobility of CO_2 that is function of its viscosity and relative permeability as explained in

the mobility ratio section. The high permeability, which is about 200 md, and heterogeneity of the sample are major factors in developing a nonuniform floodfront during CO_2 injection. The oil recovery after injecting 0.54 PV was 34.08%.

Moving to the next step, another 0.57 PV of neat CO_2 at the same pressure was injected. With this injection, a total of 1.11 PV of neat CO_2 has been injected. The test was conducted and more oil was recovered. During this injection, an increase of 18.03% of the original oil in the core was recovered. The total recovery at this level reaches 52.11%. Based on this result, there is a significant amount of oil untouched inside the core sample. Approximately half of the oil has been produced after a full PV injection of neat CO_2. As mentioned previously, this is due to the poor sweep efficiency that is caused by the high mobility of CO_2. Also, the injection rate of the CO_2 has a huge effect in the displacement and the sweep efficiency processes. Lowering the rate may result in better displacement and sweep efficiency.

Roughly 48% of the original oil in the core has not been recovered; therefore, additional CO_2 is needed to recover the remaining oil. Another 1.16 PV of neat CO_2 was injected at the stated conditions. The total oil recovery after this injection reached 62.39%, which is a 10.28% increase after the second injection. With this injection, a total of 2.27 PV of neat CO_2 has been injected but quite a lot of oil remains to be unproduced and is not communicating with CO_2 at all.

The last step is to inject another PV of neat CO_2. After this injection, the total PV of neat CO_2 injected is 3.47. The purpose of doing that is to recover as much oil as possible and also to evaluate the performance of the CO_2 injection after several PV

injections. The result of this injection shows that there is a small improvement in the overall oil recovery. An increase of 6.46% of the OOIP was achieved after this injection. The cumulative oil produced at the end of the test reached 68.85% of the OOIP. **Table 17** shows the oil recovery for each PV injection.

Table 17. Test 6 oil recovery after injecting neat CO_2

PV Injected	Oil Recovery %	Cumulative Oil Recovery %
0.54	34.08	34.08
1.11	18.03	52.11
2.27	10.28	62.39
3.47	6.46	68.85
Total Oil Recovery	**68.85**	

Overall, after injecting 3.47 PV of the neat CO_2 at a pressure of 2000 psi and 130^{o}F, which is above the MMP of oil, and at the supercritical phase of CO_2, and at rate of 2.6 cc/min the oil recovery was 68.85%.

The next step will be injection of viscosified CO_2 to evaluate the improvement in the oil recovery and sweep efficiency. In this test, the PVEE polymer was mixed with CO_2 to increase its viscosity and reduce its mobility. As stated in the previous test, 0.8

wt% of this polymer were added to CO_2 and pressurized to 2843 psi to reach the minimum solubility pressure. The same steps followed with the neat CO_2 were applied here.

In this test, the first injection was 0.48 PV of viscosified CO_2, and the oil recovery was found to be 34.08% of the OOIP. Compared with the 0.54 PV injection of neat CO_2, viscosified CO_2 shows the same recovery with less PV injected. It would be better if we had the same PV injected for both the neat and viscosified CO_2 to have had a good base for comparison.

Approximately 65% of the oil was not yet been produced after the first 0.48 PV injection of the viscosified CO_2. Because of that, an additional 0.62 PV was injected to make sure we achieved the maximum oil recovery that can be obtained. The results show that an additional 27.7% of the original oil in the core has been produced, and the total oil recovery at this level reaches 61.78%. Compared with 1.11 PV of neat CO_2, viscosified CO_2 shows better improvement in the oil recovery that is attributed to the better sweep efficiency of viscosified CO_2 compared with the neat CO_2 injection. With 1.11 PV of neat CO_2, the total oil recovery was 52.11% and with the viscosified CO_2, the oil recovery after 1.1 PV injected is 61.78% of the OOIP.

There is still some oil inside the core sample that needs to be recovered. For that reason, an additional 1.09 PV was injected into the core sample that contains about 38% of the residual oil saturation. The results show that approximately 6.44% of the oil has been recovered, which makes the total oil recovery on the order of 68.22%. Compared with the previous injection, there is a small improvement in the oil produced. Also, the

2.19 PV of viscosified CO_2 shows almost the same recovery that had been produced with the neat CO_2 after a 3.47 PV injection. This result is attributed to the good sweep efficiency that has been achieved during the viscosified CO_2 injection test.

With the decline in the recovery, it might be difficult to produce more oil. However, to make a good comparison with the neat CO_2 injection and to confirm that it is possible to recover more oil, an additional 1.1 PV of viscosified CO_2 was injected. The experimental result showed that about 4.5% of the original oil in core was produced; thus, the total oil recovery is now 72.72%. Also, the viscosified CO_2 with PVEE showed late breakthrough during the first injection, unlike the neat CO_2, where the breakthrough was observed earlier during the first PV injection. **Table 18** shows the oil recovery at each injection, and the final results of this test are summarized in **Table 19**.

Table 18. Test 6 oil recovery after injecting viscosified CO_2

PV Injected	Oil Recovery %	Cumulative Oil Recovery %
0.48	34.08	34.08
1.1	27.7	61.78
2.2	6.44	68.22
3.3	4.5	72.72
Total Oil Recovery	**72.72**	

Table 19. Test 6 summary

Parameter	Neat CO_2	Viscosified CO_2 (PVEE)
Sample	Fractured Indiana Limestone	Fractured Indiana Limestone
Injection Status	Above MMP	Above MMP
Oil Recovery	68.85%	72.72%

The overall results show that the viscosified CO_2 has higher oil recovery compared with the neat CO_2 injection. These results are attributed to the lower mobility in the former case, and as a result, better sweep efficiency has been achieved using the viscosified CO_2. The late breakthrough of CO_2 and the higher oil recovery with the viscosified CO_2 prove the ability of the viscosifier to increase the CO_2 viscosity and therefore reduce its mobility. **Figure 92** shows a comparison of the oil recovery versus the PV injected for both neat CO_2 and viscosified CO_2.

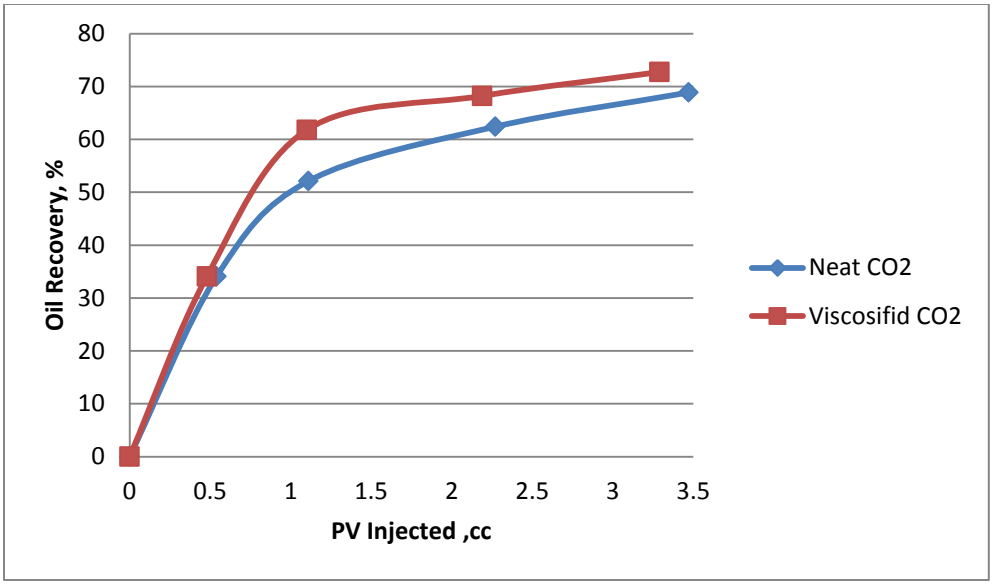

Figure 92. Test 6 Oil recovery with PV injections of neat and viscosified CO_2

CHAPTER V

CONCLUSIONS AND RECOMMENDATIONS

5.1 Conclusions

In our study, coreflood experiments were conducted to investigate possible improvements in CO_2 sweep efficiency and EOR. A number of tests were conducted with various objectives to assess the ability of the CO_2 thickening agents (viscosifiers) to achieve the goals of this study. Based on the results that have been collected:

1. CO_2 thickening agents (viscosifiers) prove their ability to delay the CO_2 breakthrough and EOR.
2. A drop in pressure test was conducted to evaluate the viscosifier's ability to increase CO_2 viscosity and therefore reduce its mobility. The results of this test showed that the PDMS polymer (higher molecular weight polymer) has the greatest effect on increasing the CO_2 viscosity and reducing its mobility. Also, the PVEE polymer (lower molecular weight polymer) has lower mobility than that of neat CO_2.
3. Based on the coreflood experiments, injection of viscosified CO_2 using PDMS showed the highest oil recovery among the other injection tests that were conducted. Also, the laboratory tests showed that the injection of viscosified CO_2 using PVEE lead to a higher oil recovery than from the neat CO_2 injection.

4. The results from both viscosified CO_2 using PDMS and PVEE showed a delay in CO_2 breakthrough. This result supports the finding that the viscosified CO_2 improved the overall sweep efficiency during the coreflood experiments.
5. Most of the coreflood experiments were conducted at a pressure of 2000 psi. To investigate the effect of the pressure change in the overall processes, some tests were conducted at a pressure of 1400 psi and 1800 psi. The results showed that the injection of the viscosified CO_2 at a pressure of 2000 psi, which were very close to the MSP, showed better results in terms of delaying the CO_2 breakthrough and EOR.
6. The rate of CO_2 injection has enormous effects on the overall processes. The lower the injection rate, the better are the results.
7. The high oil recovery obtained with neat CO_2 and viscosified CO_2 injections in fractured rock samples is attributed to the high permeability of the rock samples and the high confining pressure applied during the tests. The confining pressure applied was 3000 psi. Figure 93 shows the oil recovery of all of the tests conducted during this study.

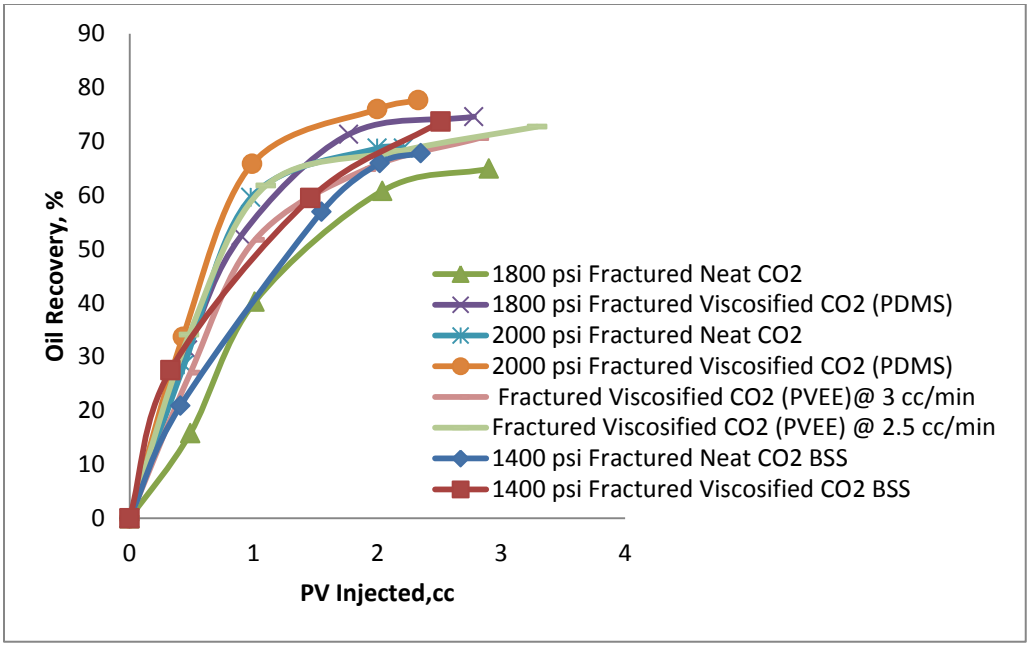

Figure 93. Oil recovery versus PV injections of CO_2

5.2 Recommendations

1. In this study, the rock samples used had a 1-in. diameter and a 5-in. length. A larger core sample would result in obtaining more accurate and representative results. An aluminum or titanium core holder with a larger diameter would also be required for future work with the CT scan.
2. Oil used in this study was refined oil. It would be advisable to conduct future studies using crude oil.
3. Additional searches for industrial suppliers of polymers are required to identify the best CO_2 thickening agent that could be used in future field trials.
4. Conduct a study to assess the effect of the polymers on the rock and fluid properties.
5. Model the laboratory results using simulator programs to forecast the future work of viscosified CO_2 injection.

REFERENCES

Ahmed, T. 2000. Minimum Miscibility Pressure from EOS. Canadian International Petroleum Conference, Calgary, Alberta. PETSOC 2000-001.

Ahmed, T. 2010. *Reservoir Engineering Handbook*. Amsterdam, The Netherlands: Elsevier. Fourth edition. ISBN 978-1-85617-803-7.

Alvarado, V. and Manrique, E. 2010. Enhanced Oil Recovery: An Update Review. *Energies* (3). DOI: 10.3390/en3091529

Bae, J.H. 1995. Viscosified CO_2 Process: Chemical Transport and Other Issues. SPE International Symposium on Oilfield Chemistry, San Antonio, Texas. SPE 28950-MS.

Bae, J.H. and Irani, C.A. 1993. A Laboratory Investigation of Viscosified CO_2 Process. *SPE Advanced Technology Series* (04). DOI: 10.2118/20467-pa

Bank, G.C., Riestenberg, D.E., and Koperna, G.J. 2007. CO_2-Enhanced Oil Recovery Potential of the Appalachian Basin. Eastern Regional Meeting, Lexington, Kentucky USA. SPE 111282-MS.

Cheek, R.E. and Menzie, D.E. 1955. Fluid Mapper Model Studies of Mobility Ratio. *Petroleum Transaction, AIME*: p. 278-281. DOI: 432-G

Cronquist, C. 1978. Carbon Dioxide Dynamic Displacement with Light Reservoir Oils. U.S. DOE Annual Symposium, Tulsa, USA.

Dawe, R.A. 2004. Miscible Displacement in Heterogeneous Porous Media. *The Sixth Caribbean Congress of Fluid Dynamics*, The University of the West Indies, St Augustine, Trinidad.

Desimone, J.M., Maury, E.E., Menceloglu, Y.Z. et al. 1994. Dispersion Polymerizations in Supercritical Carbon Dioxide. *American Association for the Advancement of Science*: p. 356-359. DOI: 10.1126/science.265.5170.356

Dong, M., Huang, S., and Srivastava, R. 2000. Effect of Solution Gas in Oil on CO_2 Minimum Miscibility Pressure. *SPE Petroleum Society of Canad* (11). DOI: 10.2118/00-11-05

Enick, R.M. 1998. *A Literature Review of Attempts to Increase the Viscosity of Dense Carbon Dioxide.* University of Pittsburgh, Pittsburgh, Pennsylvania.

Enick, R.M., Beckman, E.J., and Johnson, J.K. 2010. Synthesis and Evaluation of CO_2 Thickeners Designed with Molecular Modeling. *National Energy Technology Laboratory*.

Espie, T. 2005. A New Dawn for CO_2 EOR. International Petroleum Technology Conference, Doha, Qatar. PTC10935-MS.

Farajzadeh, R., Andrianov, A., and Zitha, P.L.J. 2009. Foam Assisted Enhanced Oil Recovery at Miscible and Immiscible Conditions. Kuwait International Petroleum Conference and Exhibition, Kuwait City, Kuwait. SPE-126410-MS.

Gharbi, R.B., Peters, E.J., Elkamel, A. et al. 1997. The Effect of Heterogeneity on the Performance of EOR Processes with Horizontal Wells. SPE Western Regional Meeting, Long Beach, California. SPE 38320-MS.

Ghedan, S.G. 2009. Global Laboratory Experience of CO_2-EOR Flooding. SPE/EAGE Reservoir Characterization and Simulation Conference, Abu Dhabi, UAE. SPE 125581-MS.

Grigg, R.B. and Schechter, D.S. 1997. State of the Industry in CO_2 Floods. SPE Annual Technical Conference and Exhibition, San Antonio, Texas. SPE 38849-MS.

Gullapalli, P., Tsau, J.-S., and Heller, J.P. 1995. Gelling Behavior of 12-Hydroxystearic Acid in Organic Fluids and Dense CO_2. SPE International Symposium on Oilfield Chemistry, San Antonio, Texas. SPE 28979-MS.

Heller, J.P., Dandge, D.K., Card, R.J. et al. 1985. Direct Thickeners for Mobility Control of CO_2 Floods. *SPE Journal (10)*. DOI: 10.2118/11789-pa

Holm, L.W. and Josendal, V.A. 1974. Mechanisms of Oil Displacement by Carbon Dioxide. *SPE Journal of Petroleum Technology* (12). DOI: 10.2118/4736-pa

Huang, Z., Shi, C., Xu, J. et al. 2000. Enhancement of the Viscosity of Carbon Dioxide Using Styrene/Fluoroacrylate Copolymers. *Macromolecules* **33** (15): p. 5437-5442. DOI: 10.1021/ma992043+

Johns, R.T., Ahmadi, K., Zhou, D. et al. 2009. A Practical Method for Minimum Miscibility Pressure Estimation of Contaminated Gas Mixtures. SPE Annual Technical Conference and Exhibition, New Orleans, Louisiana. SPE 124906-MS.

Liave, F.M., Chung, F.T.-H., and Burchfield, T.E. 1990. Use of Entrainers in Improving Mobility Control of Supercritical CO_2. *SPE Reservoir Engineering* (02). DOI: 10.2118/17344-pa

Manrique, E.J., Thomas, C.P., Ravikiran, R. et al. 2010. EOR: Current Status and Opportunities. SPE Improved Oil Recovery Symposium, Tulsa, Oklahoma, USA. SPE 130113-MS.

Murray, M.D., Frailey, S.M., and Lawal, A.S. 2001. New Approach to CO_2 Flood: Soak Alternating Gas. SPE Permian Basin Oil and Gas Recovery Conference, Midland, Texas. SPE 70023-MS.

NETL. 2010. Report Titled: Carbon Dioxide Enhanced Oil Recovery- Untapped Domestic Energy Supply and Long Term Carbon Storage Solution.

Oil and Gas Journal. 2010. Special Report:EOR/Heavy Oil Survey.

Rao, D.N., Ayirala, S.C., Kulkarni, M.M. et al. 2004. Development of Gas Assisted Gravity Drainage (GAGD) Process for Improved Light Oil Recovery. SPE/DOE Symposium on Improved Oil Recovery, Tulsa, Oklahoma. SPE 89357-MS.

Rindfleisch, F., DiNoia, T.P., and McHugh, M.A. 1996. Solubility of Polymers and Copolymers in Supercritical CO_2. *The Journal of Physical Chemistry* **100** (38): 15581-15587. DOI: 10.1021/jp9615823

Sahimi, M. 1995. *Flow and Transport in Porous Media and Fractured Rock: from Classical Methods to Modern Approaches.* Weinheim, Germany: VCH. Original edition. ISBN 3-527-29260-8.

Sandrea, I. and Sandrea, R. 2007. Global Oil Reserves - Recovery Factors Leaves Vast Target for EOR Technologies. *Oil & Gas Journal***105**(41): 1-8.

Stalkup Jr., F.I. 1983. Status of Miscible Displacement. *SPE Journal of Petroleum Technology* **35** (04). DOI: 10.2118/9992-pa

Stalkup Jr., F.I. 1984. Miscible Displacement. *SPE Monograph* **8**.

Sweatman, R.E., Crookshank, S., and Edman, S. 2011. Outlook and Technologies for Offshore CO_2 EOR/CCS Projects. Offshore Technology Conference, Houston, Texas. OTC 21984-MS.

Terry, R.E., Zaid, A., Angelos, C. et al. 1987. Polymerization in Supercritical CO_2 to Improve CO_2/Oil Mobility Ratios. SPE International Symposium on Oilfield Chemistry, San Antonio, Texas. SPE 16270-MS.

Wu, X., Ogbe, D.O., Zhu, T. et al. 2004. Critical Design Factors and Evaluation of Recovery Performance of Miscible Displacement and WAG Process. Canadian International Petroleum Conference, Calgary, Alberta. PETSOC 2004-192.

Yongmao, H., Zenggui, W., Binshan, J. et al. 2004. Laboratory Investigation of CO_2 Flooding. Nigeria Annual International Conference and Exhibition, Abuja, Nigeria. SPE 88883-MS.

Yuan, H. and Johns, R.T. 2005. Simplified Method for Calculation of Minimum Miscibility Pressure or Enrichment. *SPE Journal* **10** (4): 416-425. DOI: 10.2118/77381-pa

Zhang, S., She, Y., and Gu, Y. 2011. Evaluation of Polymers as Direct Thickeners for CO_2 Enhanced Oil Recovery. *Journal of Chemical & Engineering Data* **56** (4): 1069-1079. DOI: 10.1021/je1010449

VITA

Name: Zuhair Ali A Al Yousef

Address: Saudi Aramco Oil Company, Dhahran, Saudi Arabia

Email Address: zuhairco11@hotmail.com

Education: B.S., Petroleum Engineering, King Fahd University of Petroleum and Minerals, 2008

M.S., Petroleum Engineering, Texas A&M University, 2012